Structural and functional analysis of cyanobacterial IscA protein homologues
- a scaffold protein involved in iron-sulfur cluster biosynthesis -

藍色細菌由来 IscA 蛋白質の構造と機能の解析
-鉄硫黄クラスター生合成における「足場蛋白質」としての視点から-

A Doctoral Thesis

Kozo Morimoto

Department of Biology
Graduate School of Science

Division of Enzymology
Institute for Protein Research
Osaka University

Japan
2005

CONTENTS

ABBREVIATIONS ---------- 3

ABSTRACT (Japanese) ---------- 4

GENERAL INTRODUCTION ---------- 7

CHAPTER1; A HEAT-repeats containing protein, IaiH, stabilizes the iron-sulfur cluster bound to the cyanobacterial IscA homologue, IscA2. ---------- 12

ABSTRACT ---------- 13

INTRODUCTION ---------- 14

MATERIALS AND METHODS ---------- 16

RESULTS ---------- 18

DISCUSSION ---------- 23

CHAPTER2; Partially exposed [2Fe-2S] cluster bound by asymmetric IscA homodimer suggests the structural basis for its scaffold function in iron-sulfur cluster biosynthesis. ---------- 25

ABSTRACT ---------- 26

INTRODUCTION ---------- 27

MATERIALS AND METHODS ---------- 29

RESULTS AND DISCUSSION ---------- 35

REFERENCES ---------- 46

ACKNOWLEDGMENTS ---------- 53

ABBREVIATIONS

3-AT	3-aminotriazole
3D	three dimension(al)
AMS	4-acetamido-4'-maleimidylstilbene-2,2'-disulfonic acid, disodium salt
BSA	bovine serum albumin
Cys	cysteine
DTT	dithiothreitol
E. coli	*Escherichia coli*
EDTA	ethylenediaminetetraacetic acid
Fd	ferredoxin
HEAT	huntingtin-elongation-A subunit-TOR
IPTG	isopropyl-β-D(-)-thiogalactopyranoside
MAD	multiwavelength anomalous dispersion
PAGE	polyacrylamide gel electrophoresis
PCR	polymerase chain reactions
SDS	sodium dodecyl sulfate
TCEP-HCl	Tris(2-carboxyethyl)phosphine hydrochloride
T. elongatus	*Thermosynechococcus elongatus*
TFA	trifluoroacetic acid
Tris	tris(hydroxymetyl)aminomethane

ABSTRACT (Japanese)

Structural and functional analysis of the cyanobacterial IscA protein - a scaffold protein involved in iron-sulfur cluster biosynthesis -

藍色細菌由来 IscA 蛋白質の構造と機能の解析

-鉄硫黄クラスター生合成における「足場蛋白質」としての視点から-

蛋白質研究所　酵素反応学部門　　森本耕造

(背景と目的)

鉄硫黄クラスターは様々な鉄硫黄蛋白質のコファクターとして、電子伝達反応・触媒反応・遺伝子発現調節等の働きに関与している。鉄硫黄クラスター生合成において、中心的役割を担っているのが足場蛋白質である。すなわち、足場蛋白質上で鉄硫黄クラスターが一過的に形成され、その鉄硫黄クラスターがさまざまなアポ型鉄硫黄蛋白質へ受け渡される。IscA 蛋白質は、CXnCXC という進化的に保存された 3 つのシステイン残基を含む配列をもつ可溶性蛋白質で、ホモダイマー間に[2Fe-2S]型鉄硫黄クラスターを一つ持ちうることが報告されている。この鉄硫黄クラスターはアポ型鉄硫黄蛋白質へ転移する事が示されており、現在 IscA は鉄硫黄クラスター生合成における足場蛋白質の一つと考えられている。

一過的に形成された鉄硫黄クラスターが効率よくアポ型鉄硫黄蛋白質へ転移する、という IscA の足場蛋白質としての機能はどのような構造的基盤に基づいているのであろうか。現在までに、大腸菌由来 IscA のアポ型の結晶構造が報告されている。しかし、保存された２つのシステイン残基を含む C 末付近の構造が見えておらず、IscA がどのように鉄硫黄クラスターを保持するかについての構造的知見は得られていない。

藍色細菌 *Synechocystis* sp. PCC6803 には IscA 蛋白質ホモログとして IscA1 と IscA2 が存在する。われわれはこれまでの研究で、IscA2 が細胞内で機能未知蛋白質 IaiH と複合体として存在することを見出した [1]。IscA2/IaiH 複合体の[2Fe-2S]クラスターは還元剤ジチオナイトの添加に影響を受けないのに対し、IscA2 の[2Fe-2S]クラスターはジチオナイト添加により容易に壊れた [2]。他生物種由来 IscA の鉄硫黄クラスターも還元に不安定であることが知られており、藍色細菌由来 IscA2 のホロ型は一般的な IscA 蛋白質のホロ型と同様な構造的特徴を持つと考えられる。

本研究では、好熱性藍色細菌 *Thermosynechococcus elongatus* BP-1 由来 IscA2 蛋白質のホロ型の立体構造を X 線結晶解析により決定することにより、IscA が足場蛋白質として働くための構造的基盤を明らかにすることを目指した。

（結果と考察）

T. elongatus 由来 IscA2 は[2Fe-2S]型鉄硫黄クラスターを持った状態で精製され、結晶化条件の検討を行ったところ、高塩濃度条件下で結晶化した。結晶に X 線を照射することにより得た約 2.3Åの回折点よりホロ型 IscA2 の構造を決定した。

1結晶格子あたりには4分子の IscA2 と2つの[2Fe-2S]クラスターが含まれていた。[2Fe-2S]クラスターは A 分子（C 分子）からの3つのシステイン残基と B 分子（D 分子）からの1つのシステイン残基により非対称に保持されていた。A 分子と C 分子がグロビュールな構造をしているのに対し、B 分子と D 分子はドメインスワッピングを起こしていた。ドメインスワッピングとは、隣接する分子間で相同部分が置き換わる現象のことある。現在までに 100 以上の蛋白質結晶構造がドメインスワッピングした状態で報告されているが、その多くは結晶化条件下に何らかの原因によりドメインスワッピングが生じたものと考えられている。今回結晶化に用いた IscA2 のホロ型蛋白質は生化学的解析から、生理的塩濃度条件下においてダイマーとして存在することが強く示唆された。したがって、今回用いた結晶化条件下では2組の IscA2 のホロ型のダイマーがドメインスワッピングを起こし、テトラマーを形成したものと結論した。そこで生化学的データおよび今回決定した立体構造データに基づき、生理塩濃度溶液中のホロ型 IscA2 の立体構造をダイマーとしてモデルを構築した。

ホロ型 IscA2 のダイマー構造モデル中で最も特徴的なところは、ダイマーを形成する2つのモノマー分子の立体構造が、全体構造は似ているものの非対称であるという点である。その非対称性は特にシステイン残基を含む構造部分に見られる。すなわち Cys37 は A 分子では配位子として鉄硫黄クラスターに近い位置にあるが、B'分子ではクラスターとは離れた位置にある。また2つのシステイン残基を含む C 末端がそれぞれ異なるコンフォメーションをとっている。A 分子では、C 末端は急激に折れ曲がった構造をしており、2つのシステイン残基 A__Cys101 と A__Cys103 が鉄硫黄クラスターに配位している(A 分子の A__Cys37 も鉄硫黄クラスターに配位)。一方、B'分子の C 末端は伸びた構造をしており、1つのシステイン残基 B'__Cys103 がクラスターに配位している。様々な生物種で C 末端の CXC 付近の配列には小さな側鎖を持つアミノ酸残基がよく保存されており、このことがフレキシブルな C 末端構造を可能にしていると考えられる。また、小さな側鎖は他の蛋白質との相互作用を邪魔せず、鉄硫黄クラスターの構築・転移反応に都合がよいと考えられる。

他の鉄硫黄蛋白質の鉄硫黄クラスターとは異なり、IscA2 の鉄硫黄クラスターは一部が溶媒に露出している。また、鉄硫黄クラスターに配位する4つの硫黄原子のうち2つ（B'__Cys103 と A__Cys37 由来）は溶媒に露出し、さらにこれらが同一の鉄原子に配位している一方、残り2つの硫黄原子（A__Cys101 と A__Cys103 由来）は蛋白質内部に埋もれている。鉄硫黄クラスタ

ーが他のアポ型鉄硫黄蛋白質に転移するときには、まず溶媒に露出した硫黄原子がアポ型鉄硫黄蛋白質の配位原子と置き換わり、最後に埋もれた硫黄原子が置き換わると考えられる。

A 分子は３つのシステイン残基で鉄硫黄クラスターに配位するために C 末構造も含めて鉄硫黄クラスターの保持に適した立体構造に安定化されているのに対して、B' 分子は１つのシステイン残基しか鉄硫黄クラスターに配位していないため構造的に不安定であることが示唆された。この非対称性が鉄硫黄クラスターの転移を容易にする一因であると考えられる。すなわち、アポ型鉄硫黄蛋白質は不安定な B' 分子を押しやるようにして、ホロ型 IscA から鉄硫黄クラスターを受け取るのではないかと考えられる。

（まとめ）

本研究より、*T. elongatus* 由来ホロ型 IscA2 は鉄硫黄クラスターをダイマー間に非対称に保持することが明らかとなった。鉄硫黄クラスターの一部が溶媒に露出していることや、片方の分子が構造的に不安定であることなどが、IscA が足場蛋白質として効率よく働くために重要ではないかと考えられる。

（発表論文）

1) Morimoto K, Nishio K, Nakai M. (2002) *FEBS Lett.* **519**, 123-127.
Identification of a novel prokaryotic HEAT-repeats-containing protein which interacts with a cyanobacterial IscA homolog.

2) Morimoto K, Sato S, Tabata S, Nakai M. (2003) *J Biochem.* **134**, 211-217.
A HEAT-repeats containing protein, IaiH, stabilizes the iron-sulfur cluster bound to the cyanobacterial IscA homologue, IscA2.

GENERAL INTRODUCTION

The iron-sulfur cluster biosynthesis requires complex protein machinery.

Iron-sulfur proteins are distributed among various organisms and are known to play important physiological roles not only in electron transfer or metabolic reactions but also in gene regulation (Beinert et al., 1997, 2000). At least 120 distinct types of iron-sulfur proteins have been identified. [2Fe-2S], [3Fe-4S] and [4Fe-4S] iron-sulfur clusters are most common structural motifs found in these iron-sulfur proteins (Fig. 0-1). While iron-sulfur proteins have been the focus of extensive genetic, biochemical, or biophysical characterization, detailed information on the complex process of iron-sulfur cluster biosynthesis has only recently begun to emerge. It requires complex protein machinery that is only now becoming identified and characterized (Fig. 0-2). Much of what is currently known stems from investigations on the function of some *nif* (*ni*trogen *f*ixiation) gene products involved in nitrogenase assembly in *Azotobacter vinelandii*. Especially, two gene products, NifS and NifU, were found to be essential for optimal assembly of iron-sulfur clusters in the nitrogenase proteins (Jacobson et al., 1989; Dean et al., 1993). Subsequent studies revealed that NifS was a homodimeric, pyridoxal phosphate-dependent L-cysteine desulfurase that catalyzed the conversion of cysteine to alanine and sulfane sulfur *via* a protein-bound cysteine persulfide intermediate (Zheng et al., 1993, 1994). NifU was shown to be a homodimeric protein containing a stable redox-active $[2Fe\text{-}2S]^{2+,+}$ cluster in each subunit (Fu et al., 1994) and an additional site that serves as a scaffold for NifS-directed assembly of a transient iron-sulfur cluster (Yuvaniyama et al., 2000).

Homologues of *nifU* and *nifS*, termed *iscU* and *iscS*, respectively, were subsequently identified in *A. vinelandii* and *Escherichia coli* as a part of a widely conserved prokaryotic operon (called *isc* operon) possibly involved in general iron-sulfur cluster biosynthesis (Zheng et al., 1998). IscS was shown to have the cysteine desulfurase activity and to be highly homologous to NifS. IscU is a truncated version of NifU, containing only the N-terminal transient cluster-binding domain identified in the originally identified *A. vinelandii* NifU. Recent *in vitro* studies have demonstrated that IscU also can provide a scaffold for sequential, IscS-directed assembly of $[2Fe\text{-}2S]^{2+}$ and $[4Fe\text{-}4S]^{2+}$ clusters (Agar et al., 2000; Smith et al., 2001).

Although IscU proteins are highly conserved during evolution and seem to play a

central role in iron-sulfur cluster biosynthesis, some bacteria have been found to possess no *iscU* gene in their entire genomes. One of such bacteria, the cyanobacterium *Synechocystis* PCC6803 contains another *nifU*-like gene, which we call *cnfU*, instead of *iscU* gene. The translated product of this *cnfU* gene corresponds to the C-terminal one third of *A. vinelandii* NifU and was demonstrated to assemble itself a labile [2Fe-2S]-type iron-sulfur cluster. Moreover Nishio and Nakai showed that the cyanobacterial CnfU protein has the ability to deliver its [2Fe-2S] cluster to an apoferredoxin protein indicating that the CnfU protein also functions as an intermediate site/scaffold for the iron-sulfur cluster assembly and delivery (Nishio et al., 2000).

In addition to IscU and IscS, the above mentioned *isc* operons usually contain genes encoding two molecular chaperones, (HscA and HscB), a stable [2Fe-2S] cluster-containing ferredoxin (Fdx), a transcription factor for the regulation of *isc* operon (IscR) (Schwartz et al., 2001), and IscA (Zheng et al., 1998). A number of homologues of these bacterial Isc proteins and the cyanobacterial CnfU protein have also been identified in several archaebacteria and also in various eukaryotes (Lill et al., 2000), indicating that the process of iron-sulfur cluster biosynthesis has been highly conserved during evolution of life, from ancient bacteria to higher eukaryotes.

Early works about IscA protein; IscA is involved in the iron-sulfur cluster biosynthesis as a molecular scaffold.

IscA is about 110 amino acid residues in length and contains three revolutionary conserved cystein residues.

Gene disruption studies of IscA protein homologues in *E. coli* (Takahashi et al., 1999; Tokumoto et al., 2001) and *Saccharomyces cerevisiae* (Jensen et al., 2000; Pelzer et al., 2000; Kaut et al., 2000) have demonstrated an important, albeit nonessential role for IscA-type proteins in iron-sulfur cluster biosynthesis. Point mutations in each of three conserved cysteine residues (Fig. 0-3) of the yeast IscA protein yielded the same phenotypes as the gene knockouts (Jensen et al., 2000; Kaut et al., 2000) , which suggests essentiality of these cysteine residues for the function of IscA probably for binding of either iron and/or an iron-sulfur cluster.

Subsequently, *E. coli* IscA was shown to assemble an air-sensitive [2Fe-2S] cluster, and this cluster was able to serve as a source of [2Fe-2S] cluster to be reconstituted into apo ferredoxin *in vitro* (Ollagnier-de-Choudens et al., 2001, 2004). A homologous ^{nif}*iscA*

(previously termed *orf6*) is present in the *nif* regulon of *A. vinelandii*, immediately upstream of *nifU*, and the role of this ^{Nif}IscA as an alternate scaffold protein in iron-sulfur cluster biosynthesis has also been proposed, based on its NifS-directed assembly of a labile [4Fe-4S] cluster *via* a transient [2Fe-2S] cluster (Krebs et al., 2001). Eukaryotic IscA homologue of *Schizosachar pombe*, Isa1, was reported to be a multimeric protein carrying the $[2Fe\text{-}2S]^{2+}$ cluster and formed a complex with a redox-active ferredoxin (Wu et al., 2002), which also suggests eukaryotic IscA as an alternate scaffold protein in iron-sulfur cluster biosynthesis.

The [2Fe-2S] cluster transfer reaction from holo IscA to apo substrate protein proceeds in two observable steps *in vitro*: a first fast one leading to a protein-protein complex between the holo IscA protein and apo substrate protein, and a slow one consisting of cluster transfer leading to the apo form of the scaffold protein and the holo form of the target protein (Wu et al., 2003; Ollagnier-de-Choudens et al., 2004).

Cyanobacterial two IscA protein homologues, IscA1 and IscA2.

It has been well known that several organisms including both prokaryotes and eukaryotes possess a plural copies of *iscA* genes in their genomes. However it is not clear whether these homologous IscA proteins perform either overlapped/complemental or distinct differentiated functions in the cell.

The entire genome of the cyanobacterium *Synechocystis* PCC6803 has been already determined (Nakamura et al., 1998) and found to contain two genes, *iscA1* (*slr1417*) and *iscA2* (*slr1565*), whose translated products are similar to IscA. Predicted amino acid sequences of IscA1 and IscA2 show 39.3% sequence identity to each other and 37.4% and 37.7% to *A. vinelandii* ^{Nif}IscA protein, respectively.

In our previous work (Morimoto et al., 2002), we analyzed molecular status of IscA1 and IscA2 in the cyanobacterial cell extracts and performed a molecular characterization of their recombinant proteins that were expressed in and purified from *E. coli* to elucidate detailed functions of the two cyanobacterial IscA homologues. Although both IscA1 and IscA2 proteins were localized in the soluble fraction of the cyanobacterial cell and represented about 0.01% of the cellular soluble proteins, their molecular status in the cell extracts were remarkably different to each other; IscA1 resides in the cell most likely as a homodimer whereas IscA2 exists as a complex with a HEAT-repeats containing protein, IaiH (protein product of *slr1098*), whose function has

not yet been elucidated (Fig. 0-4). These findings suggested different cellular roles for two cyanobacterial IscA protein homologues. When IscA2 and IaiH were co-expressed in *E. coli*, two proteins form rather stable complex at 1:1 stoichiomety and exhibit a characteristic UV-visible spectra typical for [2Fe-2S] cluster-containing iron-sulfur proteins (Fig. 0-5, Lower panel blue line).

Wollenberg et al also reported about IscA1 protein from cyanobacterium *Synechocystis* PCC6803. The [2Fe-2S] cluster was chemically constructed on recombinant IscA1 (Wollenberg et al, 2003). Although they speculated that the [2Fe-2S] cluster is located between the two protomers of the IscA1 dimer and ligated probably by Cys110 and Cys112 of both protomers, further structural investigations are necessary to confirm their speculation. The [2Fe-2S] cluster of IscA1 could be transferred to apo ferredoxin (Wollenberg et al, 2003).

CHAPTER1; A HEAT-repeats containing protein, IaiH, stabilizes the iron-sulfur cluster bound to the cyanobacterial IscA homologue, IscA2.

The absorption spectrum of purified recombinant cyanobacteiral IscA2 or the IscA2/IaiH complex is typical of [2fe-2S]-cluster-containing proteins. The rather stable retention of [2Fe-2S] cluster in IacA2 or the IscA2/IaiH complex is quite contrastive to extreme labile property of iron-sulfur cluster reconstituted into IscA from *E. coli* or *A. vinelandii*. Taking advantage of this stable property of iron-sulfur cluster assembled in the cyanobacterial IscA, we carried out various biochemical characterizations against the purified IscA2 and IscA2/IaiH complex.

CHAPTER2; Partially exposed [2Fe-2S] cluster bound by asymmetric IscA homodimer suggests the structural basis for its scaffold function in iron-sulfur cluster biosynthesis.

In recently reported X-ray crystal structure, *E. coli* IscA existed as a homotetramer (Bilder et al., 2004; Cupp-Vickery et al., 2004) (Fig. 0-6). Cys35, one of three evolutionally conserved cysteine residues, was located in a central cavity formed at the tetramer interface. However, the crystal structure of the *E. coli* IscA lacked the electron density map of the C-terminal region that contains two conserved cysteine residues,

Cys99 and Cys101. Moreover a crystal structure of the holo protein form of IscA has not been reported. Thus, it still remains unclear how iron-sulfur cluster is coordinated in IscA.

In our previous work, we purified recombinant cyanobacterial IacA2 as holo form. The rather stable retention of [2Fe-2S] cluster in IacA2 is quite contrastive to extremely labile property of iron-sulfur cluster reconstituted into IscA from *E. coli* or *A. vinelandii*. The [2Fe-2S] cluster of IscA2 became reductively labile upon the addition of sodium dithionite in the presence of dithiothreitol (Morimoto et al., 2003; Fig 0-5, middle panel, compare blue and pink line). The iron-sulfur clusters of IscA protein from other organisms are also known to be reductively labile. Therefore, although IscA2 can retain rather stable iron-sulfur cluster, the holo protein was expected to have structural similarity to holo IscA from other organisms. Taking advantage of this stable property of assembled iron-sulfur cluster, we tried to determine the crystal structure of cyanobacterial IscA2 as holo form.

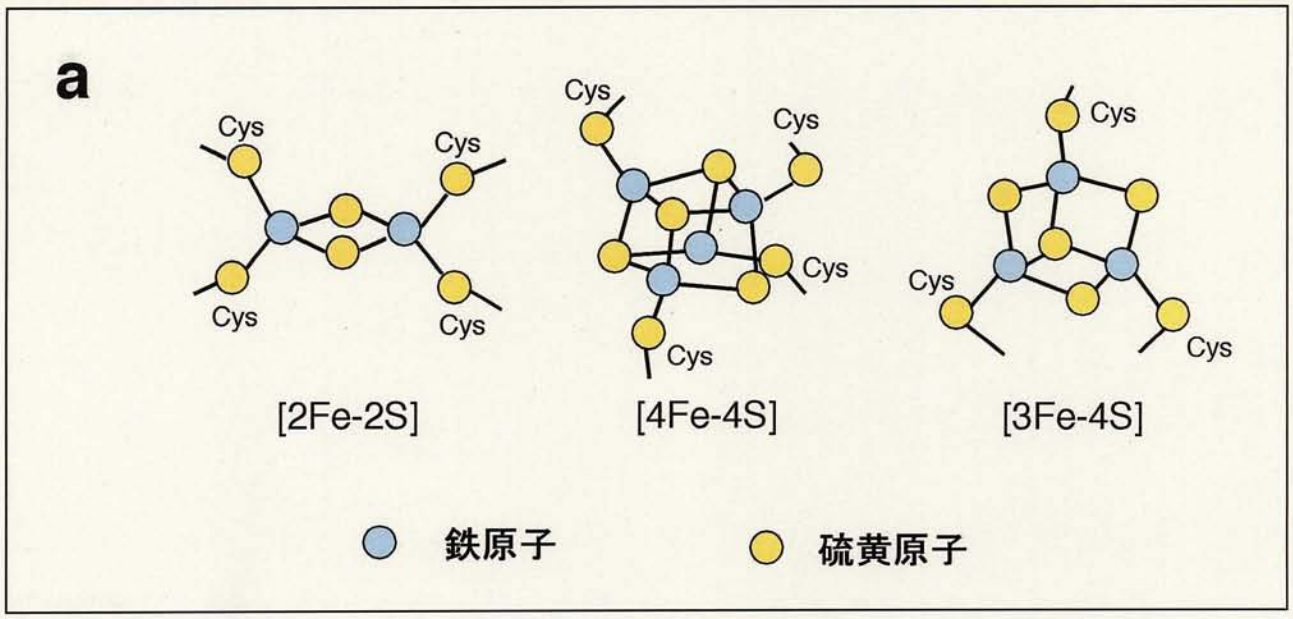

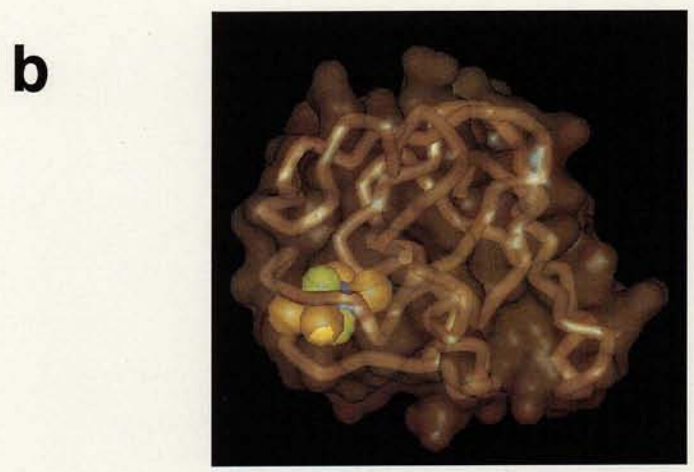

***Spirulina* ferredoxin**

Fig. 0-1. Typical types of the iron-sulfur clusters and iron-sulfur protein.
(a) [2Fe-2S], [3Fe-4S] and [4Fe-4S] iron-sulfur clusters are most common structural motifs. Iron-sulfur cluster exhibit a wide range in geometry, oxidation state, and chemical reactivity. In most cases, the iron-sulfur cluster is covalently bound to cysteine residues in the protein. Atoms are colored cyan (iron) or yellow (sulfur).
(b) *Spirulina* ferredoxin with the [2Fe-2S] iron-sulfur cluster.
Atoms are colored yellow (inorganic sulfur), orange (cysteine sulfur), or cyan (iron).

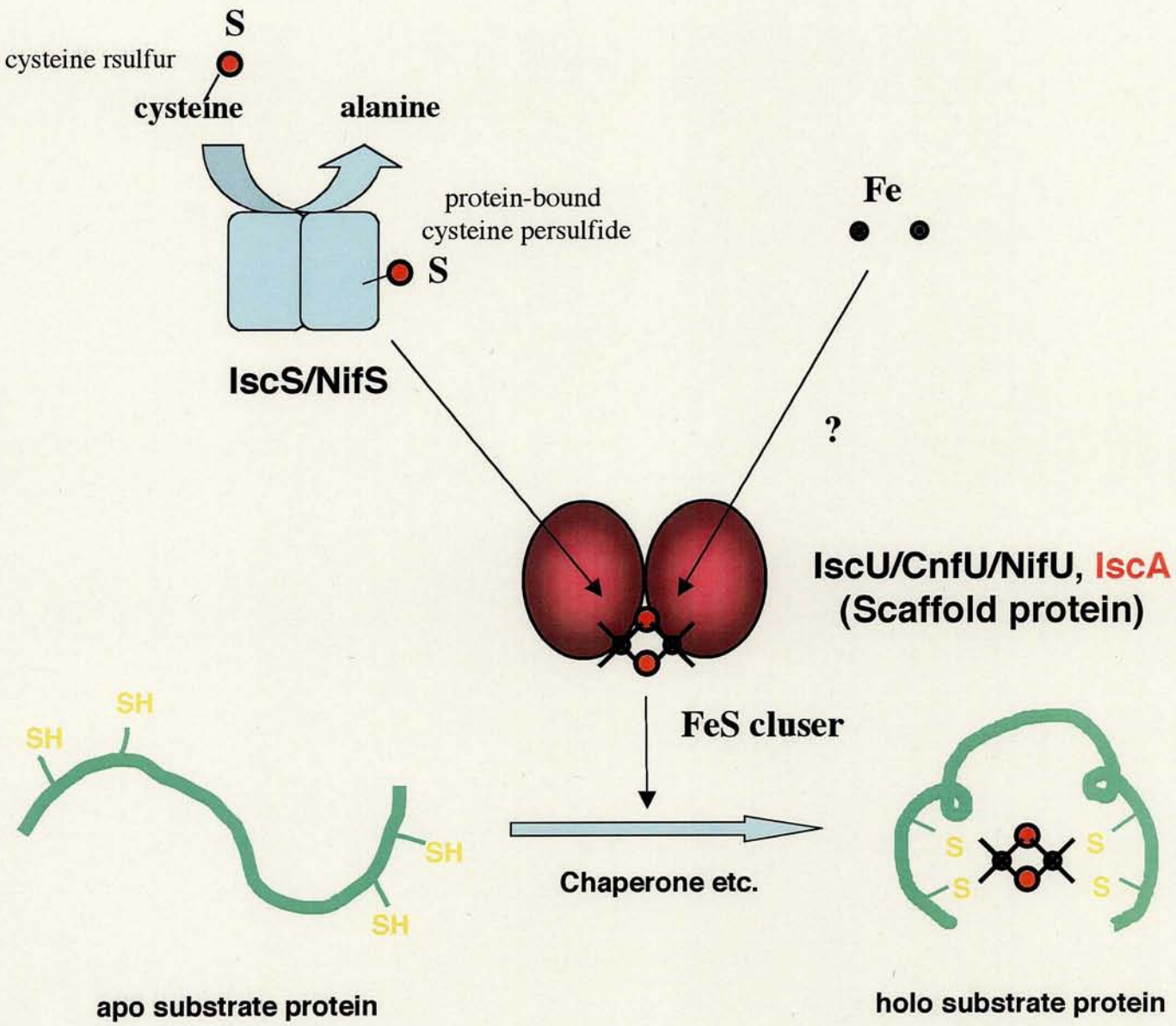

Fig. 0-2 The process of scaffold protein-assisted iron-sulfur cluster biosynthesis.
Please refer to the context about how the iron-sulfur cluster is biosynthesized in the cell.

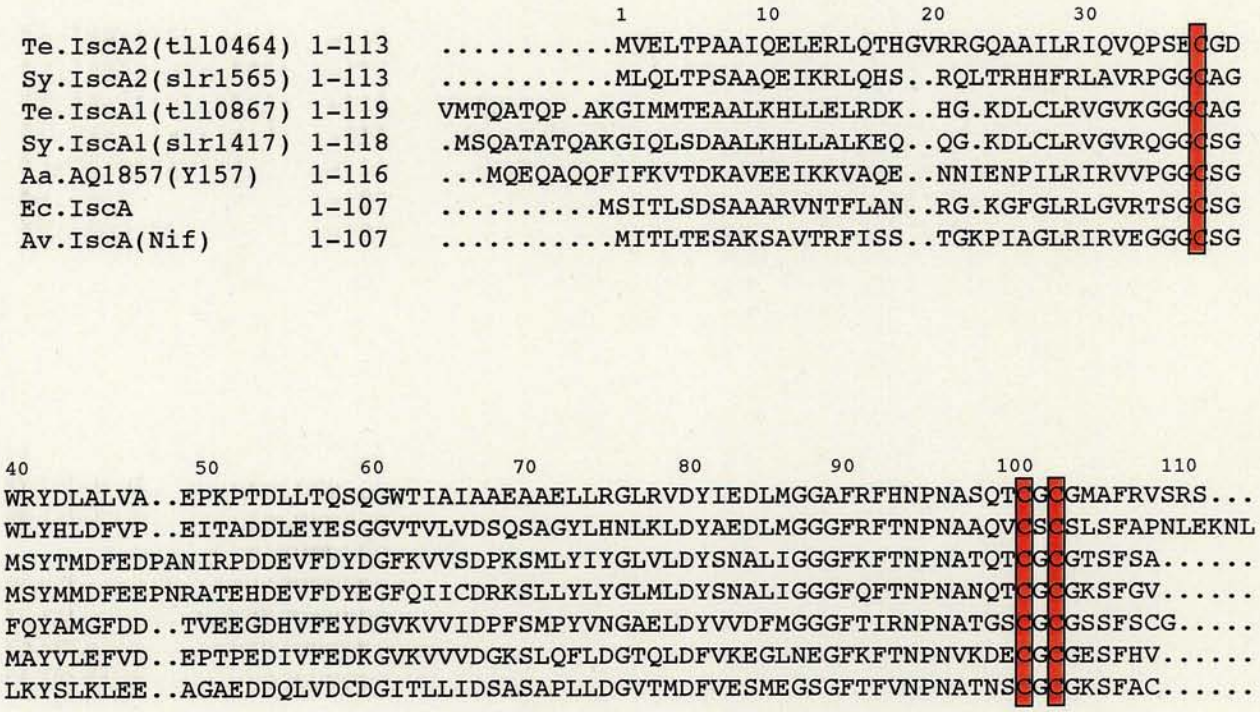

Fig. 0-3 Sequence alignment of IscA homologues from various bacteria.
Red shading indicates three evolutionally conserved cysteine residues.

Te, *Thermosynechococcus elongatus*; Sy, *Synechocystis* sp. PCC6803; Aa, *Aquifex aeolicus;* Ec, *Escherichia coli*; Av, *Azotobacter vinelandii.*
The alignment was generated using the Multalin program (Corpet, 2001).

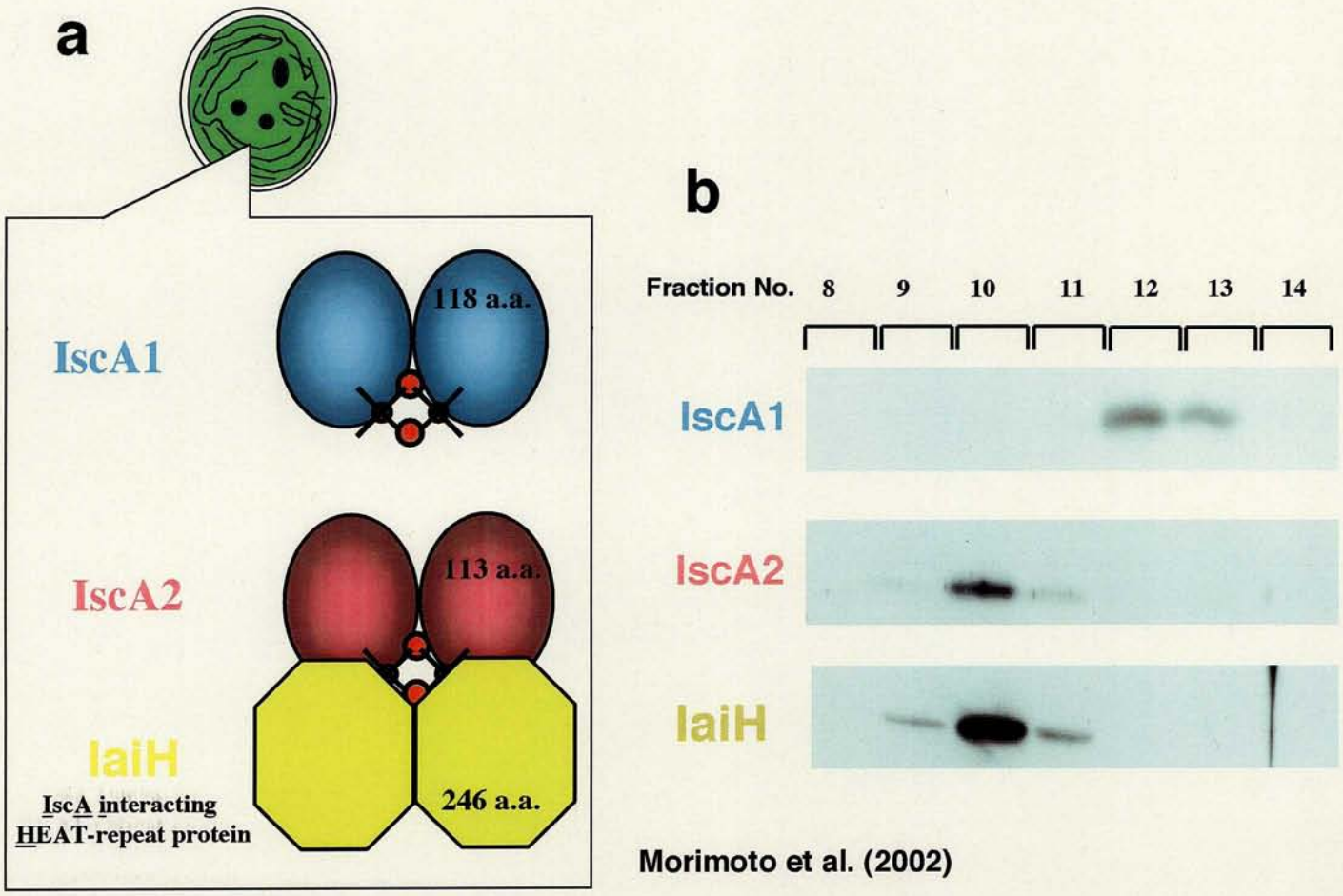

Fig. 0-4 Two IscA protein homologues in cyanobacterium *Synechocystis* sp. PCC6803.
(a) There are two IscA protein homologues, IscA1 and IscA2 in cyanobacterium *Synechocystis* PCC6803. IscA1 resides in the cell most likely as a homodimer whereas IscA2 exists as a complex with a HEAT-repeats containing protein, IaiH (protein product of *slr1098*), whose function has not yet been elucidated.
(b) Gel filtration analysis. When the cyanobacterial cell extract is loaded on the gel filtration column, the IscA2/IaiH complex elutes faster than IscA1 protein.

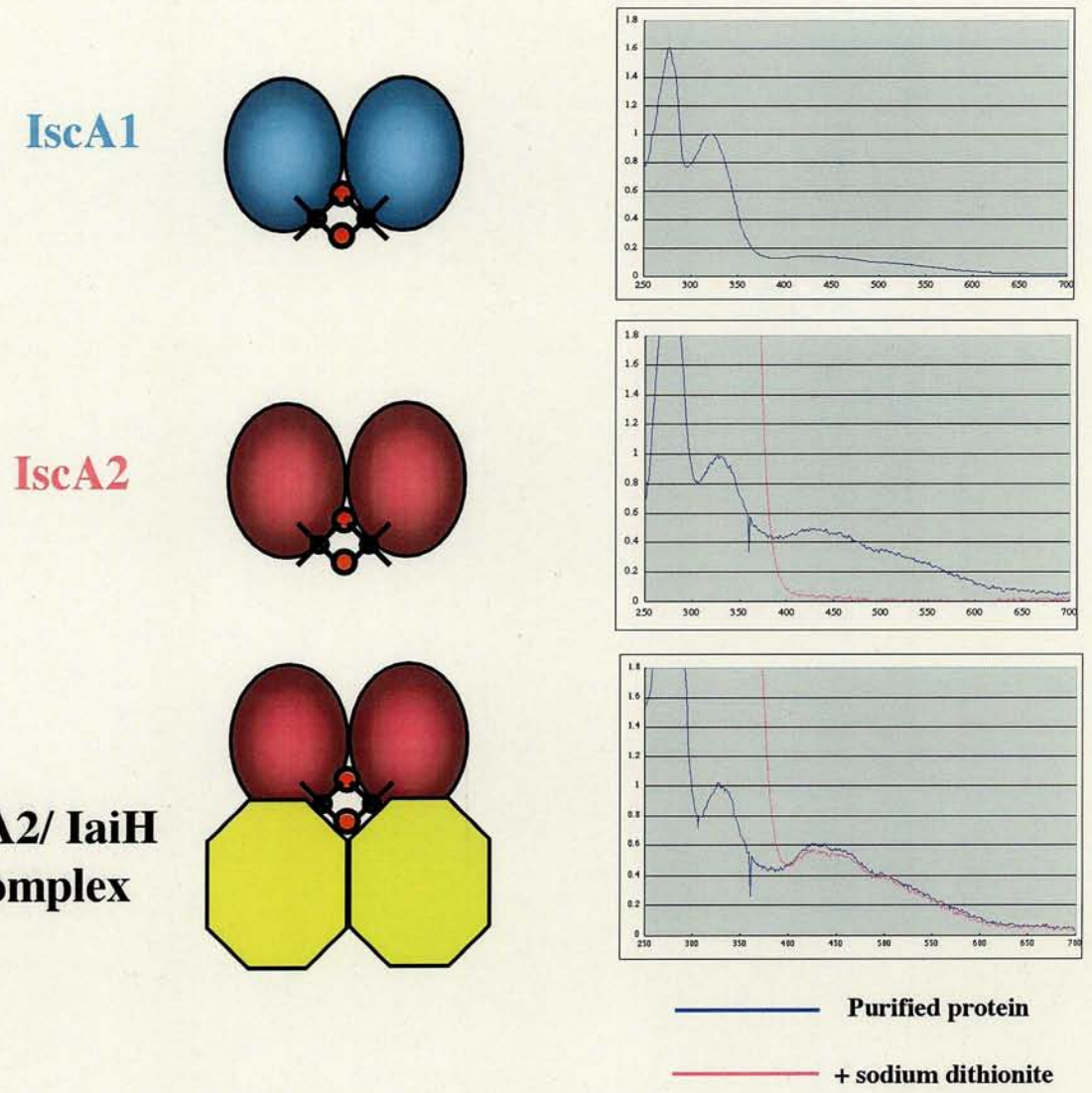

Fig. 0-5 UV/visible absorption spectra of recombinant proteins.
UV/visible absorption spectra of purified proteins were measured before (blue line) and after (pink line) adding sodium dithionite in the presence of dithiothreitol.

Upper panel; IscA1
Middle panel; IscA2
Lower panel; The IscA2/IaiH complex

IscA2 and the IscA2/IaiH complex exhibit a characteristic UV-visible spectra typical for [2Fe-2S] cluster-containing iron-sulfur proteins. In the presence of dithiothreitol, the [2Fe-2S] cluster of IscA2, but not of the IscA2/IaiH complex, became reductively labile upon the addition of sodium dithionite.

a

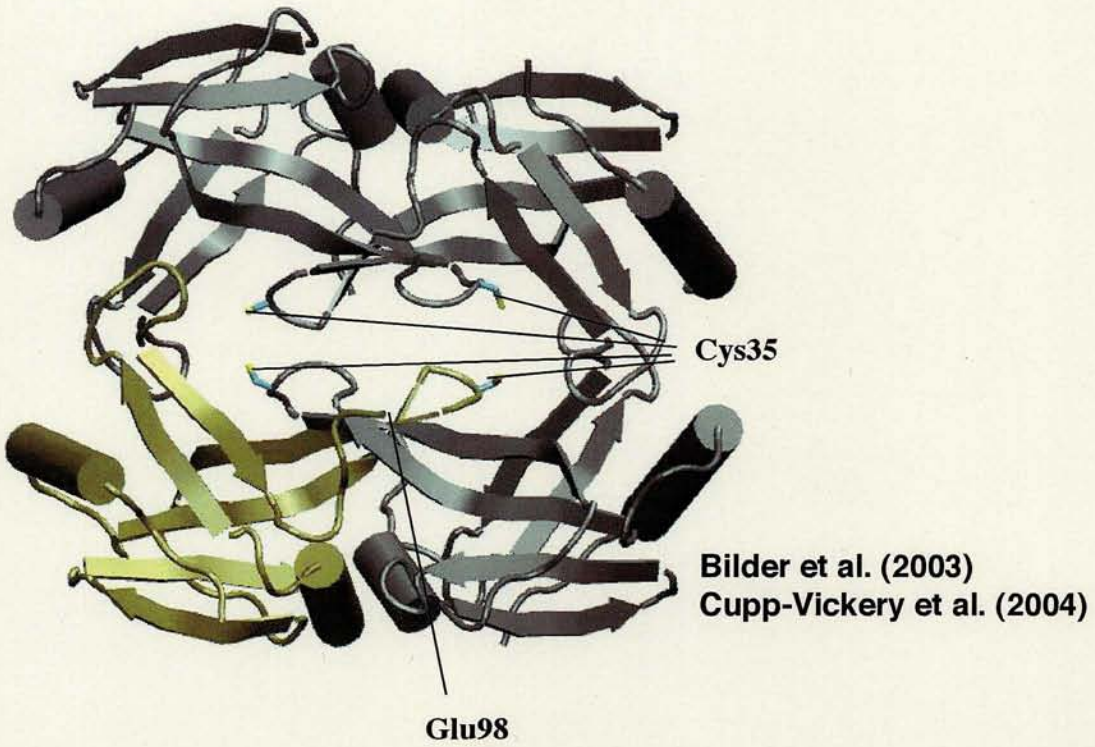

b

```
                                    35
 1  MSITLSDSAAARVNTFLANRGKGFGLRLGVRTSGCSGMAYVLEFVDEPTPEDIVFEDKGV
51  KVVVDGKSLQFLDGTQLDFVKEGLNEGFKFTNPNVKDECGCGESFHV 107
                                    99 101
```

Fig. 0-6
(a) Crystal structure of *E. coli* apo IscA.
One monomer is highlighted by tan color, and the C-terminal visible residue, Glu98, of ton-colored monomer is indicated. Side chains of Cys35 are shown in a bond model and indicated.

(b) Amino acid sequence of *E. coli* IscA.
Red letter indicates three evolutionally conserved cysteine residues, Cys35, Cys99, and Cys101.
Green shading indicates the C-terminal region that was missing in the crystal structure.
Note that this C-terminal region contains two conserved cysteines, Cys99 and Cys101.

CHAPTER1; A HEAT-repeats containing protein, IaiH, stabilizes the iron-sulfur cluster bound to the cyanobacterial IscA homologue, IscA2

ABSTRACT

IscA homologues are involved in iron-sulfur cluster biosynthesis. In the non-nitrogen-fixing cyanobacterium Synechocystis PCC 6803, there are two IscA homologues, SLR1417 and SLR 1565 (designated IscA1 and IscA2), of which only IscA2 exists as a protein complex with the HEAT-repeat-containing protein, SLR1098 (IaiH). We observed that the absorption spectrum of the recombinant IscA2/IaiH complex resembles that of IscA2 alone, although it is sharper. In the presence of dithiothreitol, the [2Fe-2S] cluster of IscA2 alone, but not of the IscA2/IaiH complex, became reductively labile upon the addition of sodium dithionite. This implies that the IscA2 moiety of the [2Fe-2S] cluster is stabilized by the presence of IaiH. The [2Fe-2S] cluster of the IscA2/IaiH complex was destabilized by sodium dithionite in the absence of dithiothreitol, suggesting that the *in vivo* stability of the iron-sulfur cluster in the IscA2/IaiH complex is influenced by the redox state of cellular thiols. When any one of three conserved cysteine residues in IscA2, poteintial ligands for the [2Fe-2S] cluster, was replaced with serine, the amount of assembled [2Fe-2S] cluster and protein complex was significantly recuced in *E. coli* cells. The cystein mutated IscA2/IaiH complexes that were present all contained a [2Fe-2S]-like cluster suggesting that the assembly of a stable iron-sulfur cluster bound to IscA2 is required for efficient and stable complex formation. Truncated IaiH proteins were analyzed using the yeast two-hybrid assay to identify the essential domain of IaiH that interacts physically with IscA2. At least 2 of the 5 N-terminal HEAT-repeats of IaiH were found to be required for interaction with IscA2.

INTRODUCTION

IscA, together with other Isc proteins, has been identified in a wide range of organisms, and participates in the process of iron-sulfur cluster biosynthesis (Lill et al., 2000). Although gene disruption studies in *Eschericiae coli* (*E. coli*) (Tokumoto et al., 2001) and *Saccharomyces cerevisiae* (Jensen et al., 2000; Pelzer et al., 2000; Kaut et al., 2000) have demonstrated an important, albeit nonessential, role for IscA proteins in iron-sulfur cluster biosynthesis, the precise role of these proteins is unclear.

IscA is about 110 amino acid residues in length and contains three revolutionary conserved cystein residues thought to bind iron or iron-sulfur clusters. Ollagnier-de-choudens, et al. purified IscA from recombinant *E. coli* in a colorless metal free form (Ollagnier-de- choudens et al., 2001). This apo-IscA protein was shown to assemble an air-labile [2Fe-2S] cluster under anaerobic conditions, and the resultant holo-IscA, but not the apo-IscA, was able to form a complex with the holo-Fdx protein, a [2Fe-2S] - containing ferredoxin encoded in the *isc* operon. Krebs et al described the purification and characterization of an IscA homologue encoded in the *nif* operon of the nitrogen-fixing bacterium *Azotobactor vnelandii* (Krebs et al., 2001). When this homologue, termed ^{Nif}IscA, was purified from recombinant *E. coli*, it was also colorless and metal-free. Further investigation revealed that ^{Nif}IscA could bind the ferrous ion in a tetrahedral, predominantly cysteinyl-ligated, coordination environment. In addition, like the previously identified IscA, ^{Nif}IscA was able to assemble an air-labile [2Fe-2S] cluster under anaerobic conditions. They also found that the [2Fe-2S] cluster could be converted to a [4Fe-4S] cluster *in vitro*, although the resultant [4Fe-4S] cluster was extremely labile even under anaerobic conditions. The IscA homologues of *E. coli* and *A. vnelandii* are thought to act as alternative scaffold proteins to NifU or IscU for iron-sulfur cluster biosynthesis (Ollagnier-de- choudens et al., 2001; Krebs et al., 2001).

Genome analyses of different organisms have revealed the presence of IscA isologues, even in a same organism. For example, *E. coli* contains at least three IscA isologues and yeast mitochondria contain two IscA isologues, Isa1p and Isa2p. Disruption of either Isa1p or Isa2p results in respiratory deficiency (Jensen et al., 2000). The disruption of both genes did not produce an additive effect suggesting that these IscA homologues are not redundant in yeast. Functional differences, similarities or cooperation between the two yeast IscA homologue, or among other IscA isologues,

have not been determined.

We reported recently that the non-nitrogen-fixing cyanobacterium, *Synechocysits* PCC6803, contains two IscA homologues, SLR1417 and SLR1565 (designated IscA1 and IscA2) (Nakamura et al., 1998; Morimoto et al., 2002). The absorption spectrum of purified recombinant IscA2 is typical of [2fe-2S]-cluster-containing proteins, whereas the absorption spectrum of IscA1 shows predominantly the presence of the iron ion (Morimoto et al., 2002). Although both IscA1 and IscA2 localize in the soluble fraction of the cyanobacterial cell and represent about 0.01% of soluble cellular proteins, their molecular states are remarkably different with IscA1 residing in the cell as a homo-dimer and IscA2 existing as a complex with another 30-kDa protein. This 30-kDa protein was identified as SLR1098 (termed IaiH for IscA-interacting Heat-repeats-containing protein), the function of which has not been elucidated. When IscA2 and IaiH were co-expressed in *E. coli*, they formed a stable complex with 1:1 stoichiometry and exhibited the UV-visible spectral characteristic of [2Fe-2S] cluster-containing iron-sulfur proteins. The stable nature of the [2Fe-2S] cluster bound to IscA2 and IscA2/IsaiH complex is in stark contrast to the extremely labile nature of the reconstituted iron-sulfur cluster bound to IscA from *E. coli* or *A. vinelandii* (Ollagnier-de- choudens et al., 2001; Krebs et al., 2001). In the present study, we characterized the purified IscA2/IaiH complex and identified a HEAT-repeats domain in IaiH required for complex formation with IscA2. We also used amino acid substitutions to investigate the role of the three conserved cysteine residues of IscA2 in [2Fe-2S]-cluster binding and IaiH complex formation.

MATERIALS AND METHODS

Bacterial strains and culture conditions

The *E. coli* strain TG1 was used as the host for plasmid propagations. *E. coli* strain BL-21(DE3)RIL (Stratagene) was used for the over-expression of recombinant proteins. Both *E. coli* strains were grown using standard procedures in LB-liquid or agar-solidified medium with appropriate antibiotics. The expression and purification of recombinant proteins have been described (Morimoto et al., 2002; Nishio et al., 2000).

Spectroscopic methods

UV-visible absorption spectra of proteins were recorded using a UV-2500PC UV-visible recording spectrophotometer (Shimazu). The concentration of the [2Fe-2S] clusters bound to IscA2, IscA2/IaiH complex, or ferredoxin (PetF) were estimated using the molecular extinction coefficient 9.68 $mM^{-1}cm^{-1}$ at 422 nm as described previously (Morimoto et al., 2002).

Spectroscopic changes in the presence of a metal chelator, ethylenediaminetetraacetic acid (EDTA), were analyzed as follows: Purified IscA2 or IscA2/IaiH complexes were prepared in 500 μl of buffer containing 50 mM Tris-HCl (pH 7.5), 150 mM NaCl, 5 mM dithiothreitol (DTT) and 10 mM EDTA, to give a final protein concentration of about 10 μM. The mixture was then divided into aliquots and the UV-visible absorption spectra of each aliquot was recorded at 0, 30, and 60 min. Spectroscopic changes in the presence of the reducing agent, sodium dithionite ($Na_2S_2O_4$), were analyzed as follows: Purified ferredoxin, IscA2 or IscA2/IaiH complex was prepared in 100 μl of buffer containing 50 mM Tris-HCl (pH 7.5), 150 mM NaCl, with or without 5 mM DTT, to give a protein concentration of about 10 μM. UV-visible absorption spectra of the basic states of these proteins were recorded first. The reduced state was analyzed following the addition of 1 μl of 100 mM sodium dithionite to the protein solution. Oxidized state were then analyzed after exposure to air for 20 min.

Yeast two-hybrid analysis between of IscA2 and various truncated fragments of IaiH

The *iscA2* gene was PCR-amplified from *Synechocystis* PCC6803 genomic DNA, and cloned as an *EcoRI*/*PstI* fragment into pAS2-1, a bait vector for yeast two-hybrid

analysis (Clontech). The resultant plasmid was called pAS2-1/*iscA2*. The prey vector for two-hybrid assay derivatives, pACT2 (Clontech), was used to construct truncated IaiH derivatives. Intact IaiH and several turncated IaiH fragments were amplified independently by PCR from cyanobacterial genomic DNA. Each PCR product was cloned into pACT2. Individual pACT2 derivatives, along with pAS2-1, were co-transformed into the yeast strain PJ69-4A. Co-transformed yeast cells were transferred onto histidine-lacking synthetic media supplemented with 5 mM 3-aminotriazole (3-AT), and grown at 30 °C for 4 days for analysis of hybrid formation. Yeast two-hybrid analyses were carried out essentially as described in the Yeast Protocols Handbook (Clontech). The two-hybrid assay was also used to evaluate mutated *iscA2* genes cloned into pAS2-1.

Site-directed mutagenesis of IscA2

Site-directed mutagenesis of IscA2 was performed using the PCR-based QuikChange™ site-directed mutagenesis kit (Stratagene). Plasmids carrying the desired amino acid substitutions were confirmed by DNA sequencing with the BigDyeTM terminator cycling sequencing ready reaction (ABI Prism) and used to transform *E. coli* strain BL-21(DE3)RIL with or without pET/*IaiH*. The resultant transformed cells were spotted onto a nitrocellulose membrane filter (Millipore) placed on a LB-agar solid medium supplemented with appropriate antibiotics, 0.3 mg/ml ammonium iron citrate, and 1 mM L-cysteine. Cells were t grown at 37 °C for 16 h, and then the expression of recombinant proteins was induced by transferring the membrane onto LB-agar solid medium supplemented with 0.4 mM IPTG. Cells were then grown for an additional 16 h at 20 °C.

Other Methods

Protein concentration was determined using the Bio-Rad Protein Assay (Bio-Rad). Western blot analysis was carried out using HRP-Protein A (Zymed) as a secondary antibody and the ECL™ detection system (Amersham Pharmacia) (Nishio et al., 1999; Nakai et al., 2001).

RESULTS

Effect of EDTA on the spectroscopic properties of IscA2 and the IscA2/IaiH complex

As reported previously, IscA2 and the IscA2/IaiH complex can bind [2Fe-2S] clusters and have a characteristic UV-visible absorption peak at approximately 330nm and lower broad peaks at around 420nm and 460nm. Stably assembled [2Fe-2S] clusters, such as those bound to photosynthetic ferredoxin, are difficult to disrupt with the metal chelator EDTA (data not shown). In contrast, the cyanobacterial NifU-like protein, now termed CnfU for a protein homologues to the carboxy-terminal domain of NifU and proposed as a major scaffold protein for iron-sulfur cluster biosynthesis in cyanobacteria, carries a labile [2Fe-2S] cluster that is sensitive to chelating agents such as EDTA (Nishio et al., 2000). To determine whether the [2Fe-2S] cluster bound by IscA2 or the IscA2/IaiH complex is stable or labile in the presence of a metal chelator, we analyzed purified proteins in the presence of EDTA. When purified IscA2 was incubated with 10 mM EDTA for 60 min at 25 °C, the intensity of the visible absorption spectrum characteristic of the [2Fe-2S] cluster decreased slightly (Fig. 1-1 A). By comparison, the absorption spectrum of the IscA2/IaiH complex was unaffected by the addition of EDTA (Fig. 1-1 B). Therefore unlike the [2Fe-2S] cluster bound to CnfU, the [2Fe-2S] cluster bound by IscA2 is stable in the presence of a metal chelator, and this stability is greater in the presence of IaiH.

Effect of sodium dithionite on the spectroscopic properties of IscA2 and the IscA2/IaiH complex

To analyze whether [2Fe-2S] clusters bound to IscA2 or IscA2/IaiH complex are redox-active or reductively labile, spectroscopic changes were monitored after the addition of a powerful reducing agent, sodium dithionite. As shown in Fig. 1-2 A, the absorption spectrum of ferredoxin (PetF), a cyanobacterial photosynthetic protein typical of [2Fe-2S] cluster-containing electron carrier proteins, disappears at 420-460 nm in the presence of excess dithionite. This is due to the reduction of all bound [2Fe-2S] clusters. The original absorption spectrum, characteristic of the presence of oxidized [2Fe-2S] clusters, can be regained by air-oxidation. The absorption spectrum of IscA2 at 420-460 nm also dropped off drastically in a few seconds following the addition of

dithionite (Fig. 1-2 B). In this case, air-oxidation could not recover the original absorption spectrum. In the absence of dithionite, the [2Fe-2S] cluster bound to IscA2 was resistant to air-oxidation (data not shown). These data show that the [2Fe-2S] cluster bound to IscA2 is removed or disassociated from the protein upon reduction by dithionite.

The effect of IaiH in the presence of dithionite on the stability of the [2Fe-2S] cluster bound to IscA2 was then analyzed. As shown in Fig. 1-2 C, the absorption spectrum of the [2Fe-2S] cluster-containing IscA2/IaiH complex at 420-460 nm was essentially unaffected by dithionite or by subsequent air-oxidation. Although sodium dithionite is a small inorganic compound (Mw = 174.11), it is possible that the [2Fe-2S] cluster bound to the IscA2 moiety of the IscA2/IaiH complex is largely covered by IaiH rendering the [2Fe-2S] cluster-binding pocket inaccessible. Alternatively, IaiH may mechanically stabilize the binding of the [2Fe-2S] cluster bound to IscA2 thereby lowering the redox potential of the iron-sulfur cluster and the effectiveness of dithionite in reducing the [2Fe-2S] cluster.

All experiments described above were carried out in the presence of 5 mM DTT. Omitting DTT resulted in the [2Fe-2S] cluster bound to the IscA2/IaiH complex becoming reductively labile (Fig. 1-2 D). Possible explanations for this phenomenon will be discussed later.

Site-directed mutagenesis of IscA2

IscA has three evolutionally conserved cysteine residues, which are the best candidates for binding the [2Fe-2S] clusters (Jensen et al., 2000; Kaut et al., 200; Krebs et al., 2001). Cyanobacterial IscA2 also has three conserved cysteine residues, Cys35, Cys99, and Cys101, and there are no other cysteine residues in the sequence (Fig. 1-3 A). To investigate the role of these cysteine residues, we used site-directed mutagenesis to convert each cysteine residue to a serine residue as described in Materials and Methods. Resultant IscA2 mutant were called C35S, C99S, and C101S, with the S referring to the replacement of the serine residue at position 35, 99, and 101, respectively. These mutants were expressed independently in *E. coli*.

Analysis of the color of transformed *E. coli* colonies was used as an initial assessment of the [2Fe-2S] cluster-binding ability of each IscA2 mutant. As shown in Fig. 1-3 B, the expression of wildtype IscA2 in *E. coli* resulted in brown red colonies,

even in the absence of IaiH, and colonies expressing the IscA2 mutant proteins were colorless apart from C35S IscA2, which turned a very pale pink. Although the expression levels of the mutant IscA2 proteins were similar to that of wildtype IscA2 (Fig. 1-4 A), most of the mutant proteins were not recovered in as soluble form (Fig. 1-4 B).

Co-expression of IaiH resulted in colonies that expressed the wildtype IscA2 protein being a deeper red brown color (Fig. 1-3 B). The presence of co-expressed IaiH had no effect on the color of mutant IscA2 colonies (Fig. 1-3 B), but greatly enhanced the solubility of all mutant IscA2 proteins (Fig. 1-4, A and B)

Physical interaction was between IaiH and the IscA2 mutants were confirmed by immunoprecipitation (Fig. 4-4, C and D). Although all IscA2 mutants could form complexes with IaiH, the efficiency of complex formation was low. This was confirmed by yeast two-hybrid analyses as described below (Fig. 1-6 B).

Protein complexes of IaiH and IscA2 mutants were purified. Although significant levels of individual proteins were present in the extracts, the recovery of mutant complexes was low, implying that these complexes are either unstable or inefficiently assembled in *E. coli.* Fig. 1-5 A shows that all purified mutant complexes displayed absorption spectra similar to [2Fe-2S] clusters. The absorption spectra at 420-460 nm of the C35S and C101S IscA2/IaiH complexes were obviously affected by the cysteine substitutions, whereas the absorption spectrum of the C99S IscA2/IaiH complex rather resembled that of the wildtype complex. However, by contrast with the [2Fe-2S] cluster of wildtype complex, all [2Fe-2S]-like clusters bound to the mutant complexes, including C99S IscA2/IaiH, were reductively labile even in the presence of DTT (Fig. 1-5 B).

These results suggest that substituting serine for cysteine either decreases the efficiency of [2Fe-2S] cluster assembly or renders the assembled cluster unstable. For this reason we conclude that all three conserved cysteine residues are important for [2Fe-2S] cluster assembly, and most likely act as ligands for iron-sulfur cluster binding. However we could not totally exclude the possibility that these substitutions might have an indirect effect (e.g. improper folding of the IscA2 molecule) that causes inefficient [2Fe-2S] cluster binding. In any case, without the assembled iron-sulfur cluster, IscA2 and IaiH are unable to form a stable complex. This result was also confirmed by yeast two-hybrid analyses (Fig. 1-6, A and B).

Yeast two-hybrid analysis between IscA2 and truncated IaiH

IaiH is 246 amino acid residues long (Mw = *ca.* 27 k) and shows no strong sequence similarities to proteins with known functions. As described previously, *in silico* analysis of IaiH amino acid sequence revealed the presence of HEAT-repeats throughout the molecule (Morimoto et al., 2002). Figure. 1-6 C shows 5 and a half HEAT motifs in tandem repeat following the extra 50 residues on the N-terminus; these are designated H0-H5. The HEAT-repeats was initially found in a diverse family of eukaryotic proteins that includes huntington, elongation factor 3, the PR65/A subunit of protein phosphatase 2A, the lipid kinase TOR, and importin β (Neuwald et al., 2000; Andrade et al., 2001). Although HEAT-repeats containing proteins are involved in a great variety of cellular processes, the mediation of protein-protein interactions is thought to be a common function. For example, importin β binds to various protein substrates destined for nuclear import, and the PR65/A subunit of protein phosphatase 2A interact with various regulatory subunits of PP2A. The crystal structures of several proteins containing HEAT repeats have already been determined (Neuwald et al., 2000; Andrade et al., 2001). Structural information has revealed that the canonical HEAT-repeat consists of two helices forming a helical hairpin. Between the two antiparallel helices, one electrostatic interaction and several hydrophobic interactions play important roles in stabilizing this structural unit. Neighboring repeats stack together into a single domain with a continuous hydrophobic core, forming an elongated curlicue-like or solenoid-like super-helix. The resultant concave surface of the super-helix in the HEAT-repeats containing protein is known to serve as a ligand-binding domain.

The interaction of IscA2 with IaiH may occur via some or all of these HEAT-repeats. Yeast two-hybrid analysis was performed to investigate this possibility. Figure. 1-6 C shows the various truncated IaiH proteins constructed with different N-terminal or C-terminal fragments, including N1-59, N1-90, N1-122, N1-156, N1-195, 60-246C, 91-246C, 123-246C, 157-246C, and 196-246C, where numberings correspond to the amino acid residues of IaiH. DNA fragments were constructed as described in Fig. 1-6 A and yeast two-hybrid analysis was performed as described above.

Among the fusion constructs containing truncated IaiH domains, only N1-122, N1-156, N1-195 and 60-246C fragments were found to interact with IscA2. These fragments contain amino acid residues 60 to 122, a region containing two HEAT-repeats

designated H1 and H2. We conclude that the two HEAT-repeats H1 and H2 of IaiH are the minimum requirement for the interaction of this protein with IscA2.

DISCUSSION

In this study we demonstrated that IscA2 forms a stable protein complex with the HEAT-repeats containing protein, IaiH, which functions to stabilize the [2Fe-2S] cluster bound to IscA2. Three evolutionarily conserved cysteine residues in IscA2 are important for efficient [2Fe-2S] cluster binding, and the stable retention of the iron-sulfur cluster bound is required for the tight interaction with IaiH. Normally, four conserved cysteine residues are found in [2Fe-2S] cluster-containing proteins, although histidine or aspartic acid residues can also serve as ligands for [2Fe-2S] cluster binding. IscA2 possesses four histidine and several aspartate residues, one of which might serve as the fourth ligand for [2Fe-2S] cluster binding. It is also possible that an amino acid residue, such as cysteine, in IaiH acts as a ligand for [2Fe-2S] cluster binding in IscA2/IaiH complex. However, this possibility is unlikely because purified IscA2 alone shows the characteristic [2Fe-2S]-type absorption spectrum that is essentially similar to that of the IscA2/IaiH complex. Further investigation is necessary to define other residues in IscA2 that act as ligands for [2Fe-2S] cluster binding.

The physiological role of the IscA2/IaiH complex is unknown. IscA2 proteins from other organisms (Ollagnier-de- choudens et al., 2001; Krebs et al., 2001), such as IscU and NifU-like proteins (Nishio et al., 2000; Yuvaniyama et al., 2000; Agar et al., 2000; Smith et al., 2001), function as scaffold proteins in iron-sulfur cluster assembly. The iron-sulfur cluster bound to these proteins is extremely labile, suggesting that the cluster may be preformed transiently on IscA and transferred either directly or indirectly to an apoprotein. IscA1, another cyanobacterial IscA homologue, may function in such a way. By contrast, the iron-sulfur cluster bound to cyanobacterial IscA2 is stable and is further stabilized when complexed with IaiH. Data from our previous experiments showed that nearly all cellular IscA2 and IaiH exist in IscA2/IaiH complexes. In the present sturdy there was virtually no stable complex formed between apo-IscA2 and IaiH *in vitro*, suggesting that all cellular IscA2/IaiH complexes bind an iron-sulfur cluster. The stable nature of the holo-IscA2/IaiH complex implies that cyanobacterial IscA2 may be involved in physiological functions other than iron-sulfur cluster delivery. It is also possible that the [2Fe-2S] cluster bound to the IscA2/IaiH complex becomes transferable following other interactions. This interaction may be via the remaining HEAT-repeats domain of IaiH, which leads to the formation of a transient tertiary

complex and transfer of the iron-sulfur cluster. The possibility that the holo-IscA2/IaiH complex functions as a redox electron carrier is unlikely because we found that the iron-sulfur cluster bound to the IscA2/IaiH complex is not reduced by dithionite *in vitro*. Instead, the iron-sulfur cluster became labile when the complex was incubated with dithionite in the absence of DTT, a thiol reductant. It is possible that the iron-sulfur cluster can be destabilized and transferred when the redox state of cellular thiols is largely oxidized. Alternatively, the iron-sulfur cluster bound to IscA2 could be a molecular sensor by which the redox state of cellular thiols is monitored. These questions may be answered in further investigations that aim to identify and characterize proteins that interact with the IscA2/IaiH complex. We are also currently investigating the physiological role of the IscA2/IaiH complex by analyzing cyanobacterial mutants in which one or both genes have been disrupted.

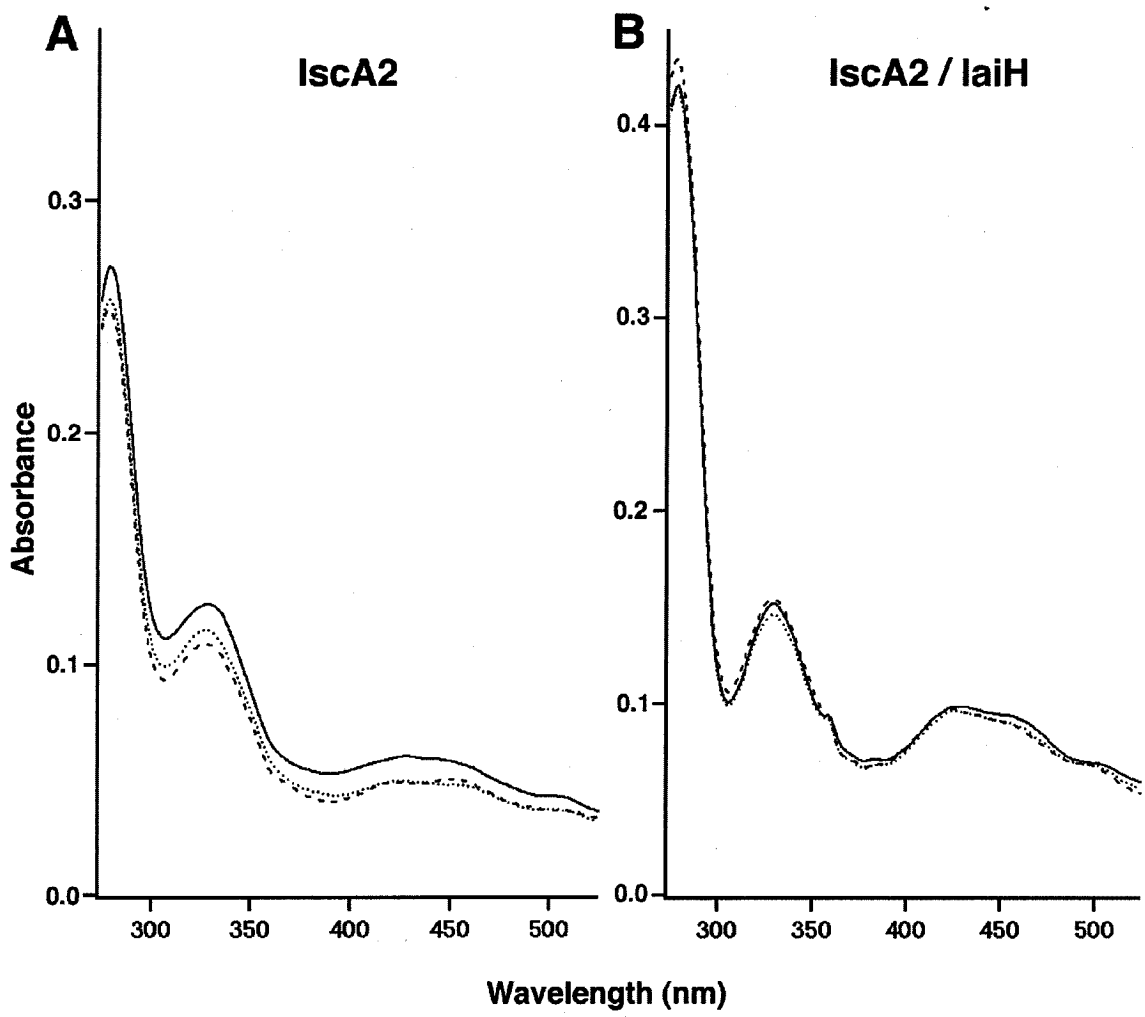

Fig. 1-1. Effect of EDTA on the spectroscopic properties of IscA2 and the IscA2/IaiH complex. Samples containing either purified IscA2 (A) or IscA2/IaiH complex (B) were prepared in buffer containing 50 mM Tris-HCl (pH 7.5), 150 mM NaCl, 5 mM DTT, and 10 mM EDTA, to give a final protein or protein complex concentration of about 10 μM. UV-visible absorption spectra were recorded at 0 min (plain lines), and after 30 min (dotted lines) and 60 min (dashed lines).

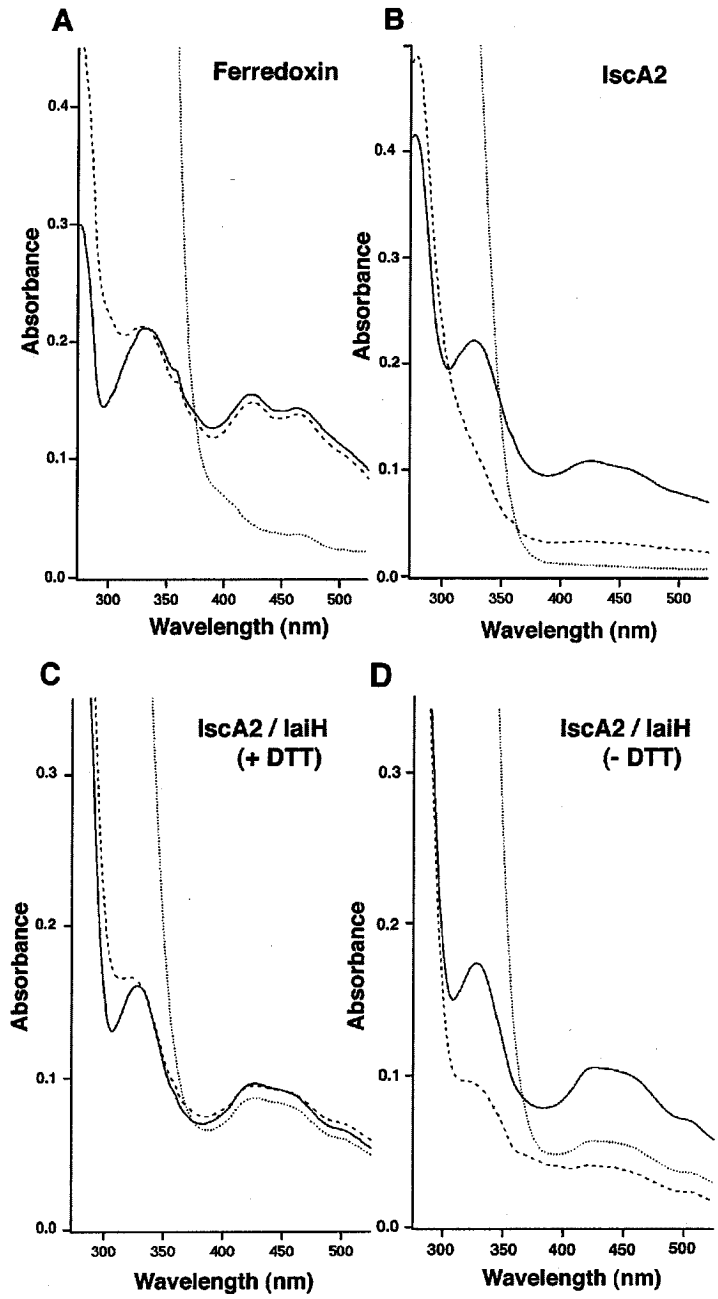

Fig. 1-2 Effect of sodium dithionite on the spectroscopic properties of IscA2 and the IscA2/IaiH complex. Samples containing either purified ferredoxin (PetF; SSL0020) (A), IscA2 (B) or IscA2/IaiH complex (C) were prepared in 100 μl of buffer containing 50 mM Tris-HCl (pH 7.5), 150 mM NaCl, and 5 mM DTT, to give a final protein or protein complex concentration of about 10 μM. UV-visible absorption spectra were recorded initially to generate a base line (solid lines). Then, 1 μl of 100 mM sodium dithionite ($Na_2S_2O_4$) was added to the mixture. Immediately following gentle, but thorough mixing, the absorption spectra of the reduced state were recorded (dashed lines). Absorption spectra of the oxidized state (dotted lines) were recorded following oxidation of the mixture, achieved by exposing the mixture to air for 20 min. Spectra of the IscA2/IaiH complex shown in (D) were recorded as in (C) with DTT omitted from the buffer.

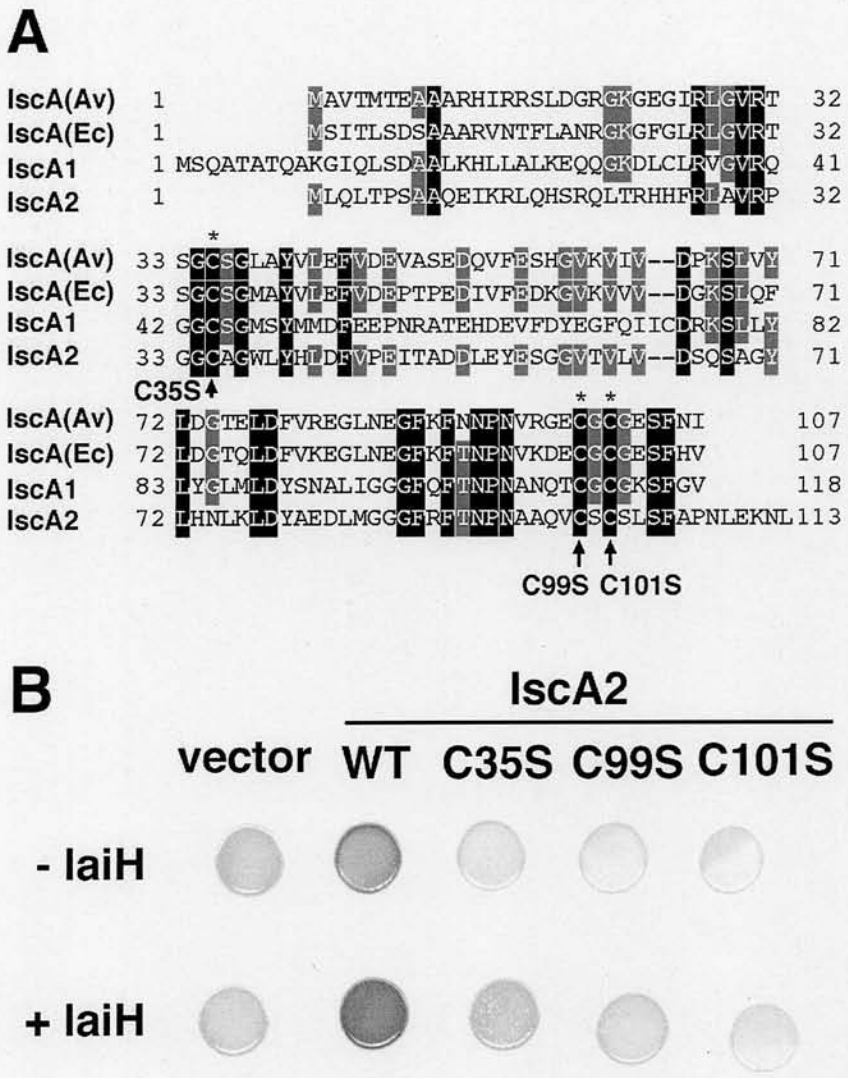

Fig. 1-3 Iron-sulfur cluster assembly in wildtype and cysteine-substituted mutant IscA2 proteins in *E. coli*. A: Alignment of IscA proteins from *Azotobactor vinelandii* (Av), *E. coli* (Ec), and *Synechocystis* PCC6803 (IscA1 and IscA2). Arrows indicate positions of amino acid substitutions in IscA2. B: Formation of holo-IscA2 in *E. coli* was analyzed as described in Materials and Methods. Vector alone (vector) or plasmid encoding either the wildtype (WT) or cysteine-substituted IscA2 (C35S, C99S, C101S) was transformed into E. coli with (+IaiH) or without (-IaiH) a co-expression plasmid for IaiH. Transformed cells were spotted onto a nitrocellulose membrane layered on solid LB-medium supplemented with iron and cysteine. The expression of IscA2 and IaiH was induced by transferring the membrane onto LB-media containing 0.4 mM IPTG.

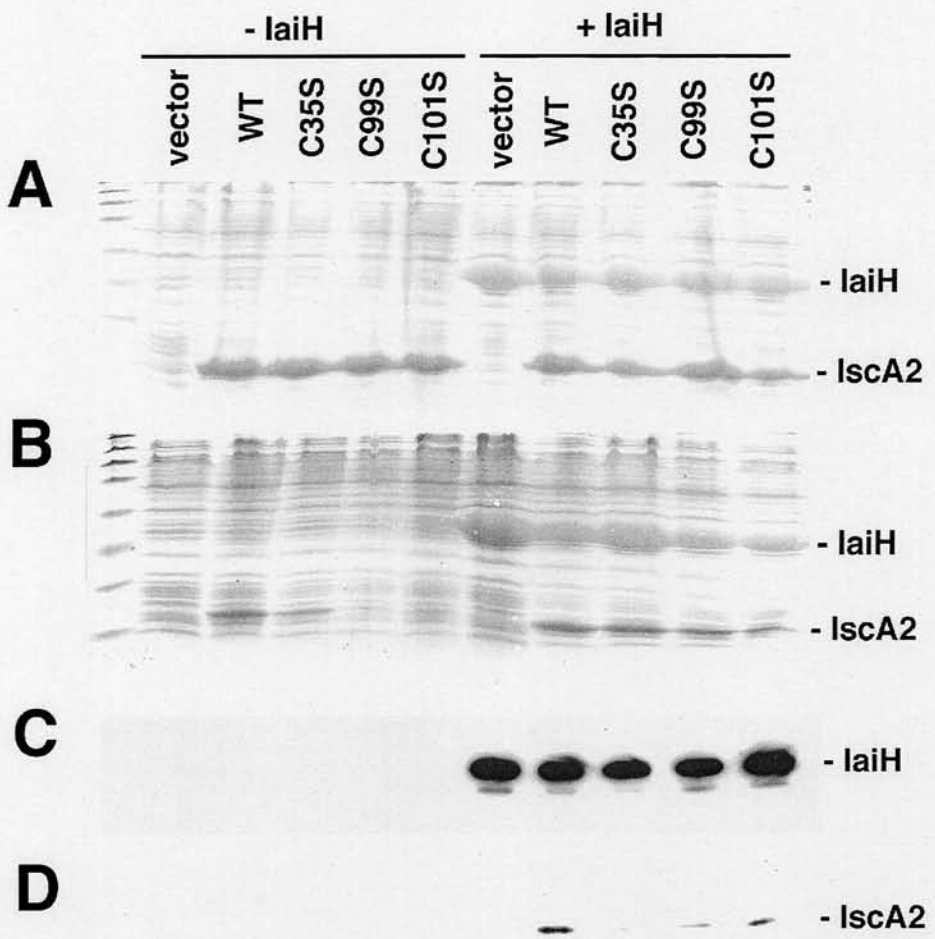

Fig. 1-4 Complex formation between IaiH and various IscA2 mutants as analyzed by immunoprecipitation. Various transformed *E. coli* cells used in the experiments shown in Fig. 1-3 were cultivated in liquid LB-medium supplemented with iron and cysteine, and the expression of IaiH and IscA2 proteins was induced by the addition of 0.4 mM IPTG. After further cultivation for 16 h at 20 °C, the cells were harvested, ruptured by sonication, and fractionated into soluble and membrane fractions. Total cell lysates (A) and soluble fractions (B) were analyzed by staining with Coomassie Brilliant Blue following SDS-PAGE. Soluble fractions were used for immunoprecipitation with purified anti-IaiH antibodies, and precipitated proteins were analyzed by Western blotting either with anti-IaiH antibodies (C) or anti-IscA2 antibodies (D).

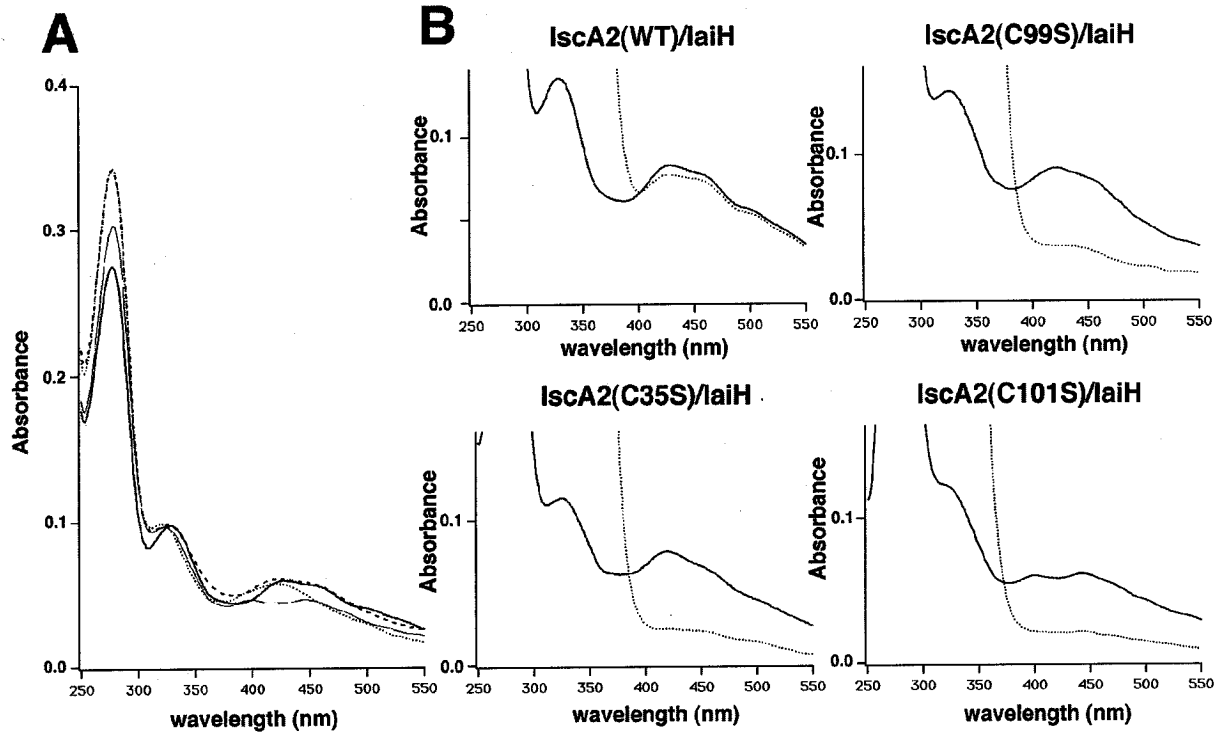

Fig. 1-5 UV/visible absorption spectra of purified mutant IscA2/IaiH complexes. A: Various IscA2/IaiH proteins were purified as described previously (Morimoto et al, 2002). UV/visible absorption spectra of purified wildtype IscA2/IaiH (solid line), IscA2(C35S)/IaiH (dotted line), IscA2(C99S)/IaiH (dashed line), and IscA2(C101S)/IaiH (thin line) complexes were adjusted using the absorption values at 330 nm and compared. B: Changes in the absorption spectra of various IscA2/IaiH complexes as indicated were monitored before (solid lines) and after (dotted lines) reduction by the addition of 1 mM sodium dithionite as described in the legend of Fig. 1-2.

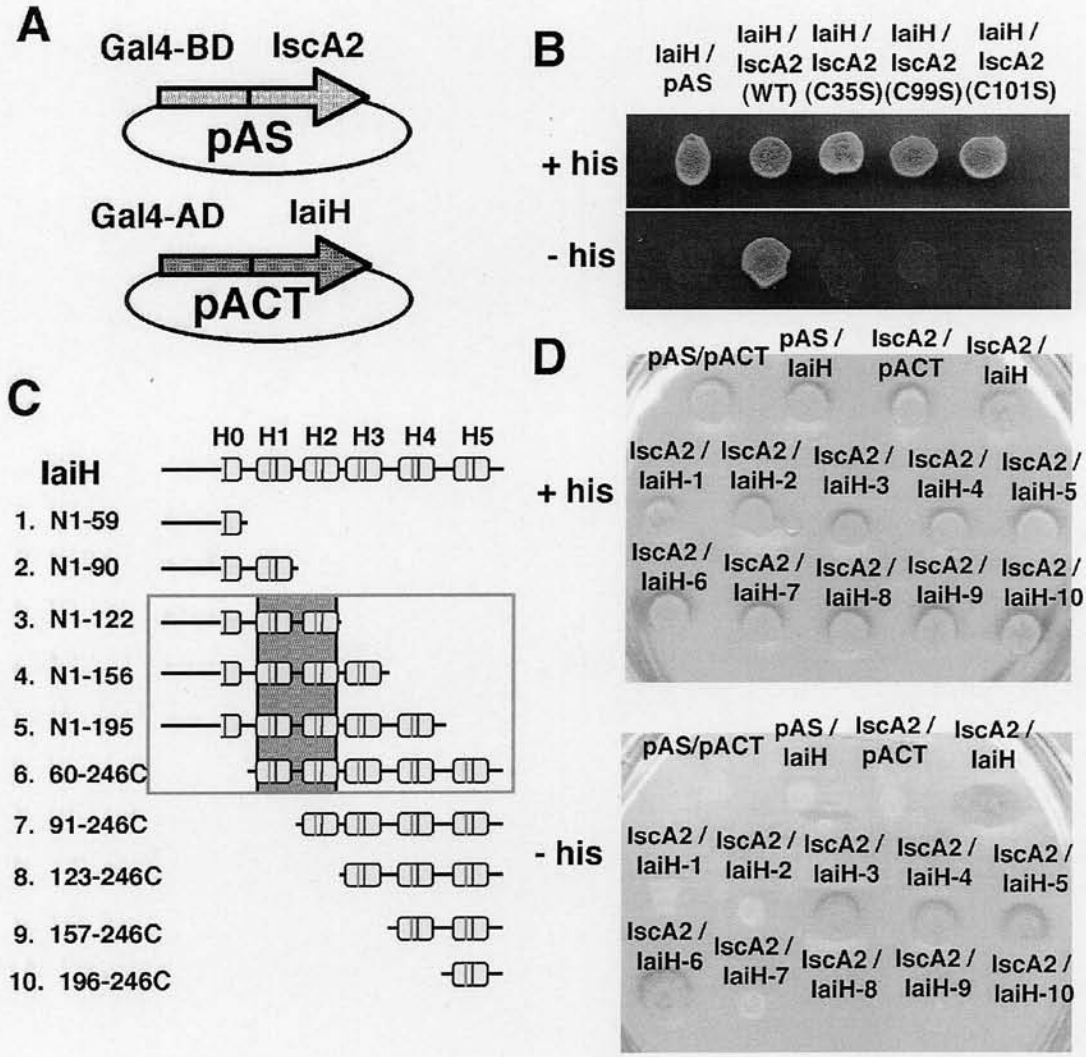

Fig. 1-6 Yeast two-hybrid analysis of the interaction between IscA2 and IaiH proteins. A: Schematic representations of pAS and pACT plasmids used for the yeast two-hybrid analysis of the interaction between IscA2 and IaiH variants. B: Various pAS derivatives, each encoding wildtype IscA2 or one of the cysteine-substituted IscA2 mutants, as indicated, were co-transformed withe the wildtype IaiH-encoding pACT derivative. All co-transformed yeast cells grew on medium with added histidine (+his). Only wildtype IscA2 was able to allow growth of the co-transformed yeast cells on medium lacking histidine (-his). C: Various truncated IaiH proteins were designed so each contained an N-terminal or C-terminal fragment; IaiH-1 (N1-59), IaiH-2 (N1-90), IaiH-3 (N1-122), IaiH-4 (N1-156), IaiH-5 (N1-195), IaiH-6 (60-246C), IaiH-7 (91-246C), IaiH-8 (123-246C), IaiH-9 (157-246C), IaiH-10 (196-246C). D: All co-transformed yeast cells grew on medium with added histidine (+his). Only the N1-122, N1-156, N1-195, 60-246C, and wildtype (IaiH) constructs were able to interact with IscA2 sufficiently to allow growth of the co-transformed yeast cells on medium lacking histidine (-his).

CHAPTER2; Partially exposed [2Fe-2S] cluster bound by asymmetric IscA homodimer suggests the structural basis for its scaffold function in iron-sulfur cluster biosynthesis.

ABSTRACT

IscA has been identified in a wide range of organisms, and participates in the process of iron-sulfur cluster biosynthesis. IscA is defined as a scaffold protein from which pre-assembled clusters are transferred to substrate proteins. Although the crystal structure of the apo-protein form of IscA from *Escherichia coli* was reported recently, the C-terminal region that contains two invariant cysteine residues critical for the iron-sulfur cluster binding was disordered. Therefore, the question of how the iron-sulfur cluster is coordinated in IscA remained unsolved. In this chapter, we report the crystal structure of holo protein form of IscA2 from *Thermosynechococcus elongatus*. This is the first of IscA to be structurally characterized with iron-sulfur clusters. Interestingly, the [2Fe-2S] cluster was asymmetrically coordinated by four cysteine residues from two IscA2 monomers; three cysteines from one monomer, and one cysteine from another. Partially exposed [2Fe-2S] cluster bound by asymmetric IscA homodimer suggests the structural basis for its scaffold function in iron-sulfur cluster biosynthesis. We propose a molecular mechanism of the iron-sulfur cluster transfer from holo IscA to apo substrate proteins.

INTRODUCTION

Iron-sulfur proteins are known to play important physiological roles not only in electron transfer or metabolic reactions but also in gene regulation (Beinert, 1997, 2000). These activities rely upon protein-bound iron-sulfur clusters which exhibit a wide range in geometry, oxidation state, and chemical reactivity (Fig. 0-1). While iron-sulfur proteins themselves have been the focus of extensive genetic, biochemical, or biophysical characterization, the biosynthetic process by which iron and sulfur atoms are mobilized from their storage sources and combined in a controlled way to generate iron-sulfur cluster is in an early phase of exploration. It requires complex protein machinery that is only now becoming identified and characterized (Fig. 0-2).

The *iscA* gene encodes a small soluble protein that contains three evolutionally conserved cysteine residues thought to bind iron-sulfur clusters (Fig. 2-1). The genetic studies of the *iscA* gene in *Escherichia coli* (Takahashi et al.,1999; Tokumoto et al., 2001) and the homologous *ISA1* and *ISA2* genes of *Saccharomyces cervisiae* (Kaut et al., 2000; Jensen et al., 2000; Pelzer et al., 2000) established the importance of IscA in iron-sulfur protein formation. Even though the precise role of IscA is still unsettled, IscA has been proposed as a scaffold for the iron-sulfur cluster assembly, because purified IscA from *Escherichia coli* (Ollagnier-de-Choudens et al., 2001, 2004) and its homologues from *Azotobacter vinelandii* (Krebs et al., 2001), cyanobacterium *Synechocystis* PCC 6803 (Wollenberg et al., 2003), and *Schizosaccharomyces pombe* (Wu et al., 2002; Wu et al., 2003) could host iron-sulfur clusters and transfer the assembled clusters to target proteins.

Recent X-ray crystal structure of the *E. coli* IscA (Bilder et al., 2004; Cupp-Vickery et al., 2004) showed that *E. coli* IscA existed as a homotetramer (Fig. 0-6). Cys35, one of three evolutionally conserved cysteine residues, was located in a central cavity formed at the tetramer interface. However, the crystal structure of the *E. coli* IscA lacked the electron density map of the C-terminal region that contains two conserved cysteines, Cys99 and Cys101. We still do not know how the iron-sulfur cluster is coordinated in IscA because a crystal structure of the holo protein form of IscA has not been reported. Difficulty to crystallize holo IscA is probably due to the iron-sulfur cluster loss during the crystallization.

In the non-nitrogen fixing cyanobacterium *Synechocystis* sp. PCC6803, there are

two IscA protein homologues (Nakamura et al., 1998), IscA1 and IscA2. In our previous work (Morimoto et al., 2002, 2003), we analyzed molecular status of IscA1 and IscA2 in the cyanobacterial cell extracts and performed a molecular characterization of their recombinant proteins that were expressed in and purified from *E. coli*. Recombinant IscA2 was purified from *E. coli* in the status containing the [2Fe-2S] cluster. The rather stable retention of [2Fe-2S] cluster in cyanobacterial IacA2 is quite contrastive to extreme labile property of iron-sulfur cluster reconstituted into IscA from *E. coli* or *A. vinelandii*. We revealed that the [2Fe-2S] cluster of IscA2 became reductively labile upon the addition of sodium dithionite in the presence of dithiothreitol (Morimoto et al., 2003; Fig 0-5, middle panel, compare blue and pink line). The iron-sulfur clusters of IscA protein from other organisms are also known to be reductively labile. Therefore, IscA2 seems to have structural similarity to holo IscA from other organisms.

Taking advantage of this stable property of iron-sulfur cluster assembled in the cyanobacterial IscA, we tried to determine the crystal structure of cyanobacterial IscA2 as holo form. In this paper, we report a crystal structure of *Thermosynechococcus elongatus* IscA2 with the [2Fe-2S] cluster. This is the first of IscA to be structurally characterized with iron-sulfur clusters. On the basis of structural information and additional biochemical evidence, we further suggest a molecular mechanism of the iron-sulfur cluster transfer from holo IscA to apo substrate proteins.

MATERIALS AND METHODS

Bacterial strains and culture conditions

The *E. coli* strain TG1 was used as the host for plasmid propagations. *E. coli* strain BL-21(DE3)RIL (Stratagene) was used for the expression of recombinant native proteins. *E. coli* strain BL-21-CodonPlus™(DE3)RIL-X (Stratagene) was used for the expression of recombinant selenomethionine derivative. *E. coli* strains were grown using standard procedures in liquid or agar-solidified medium with appropriate antibiotics.

IscA2 protein expression

For expression of the *Thermosynechococcus elongatus* IscA2 protein in *E. coli*, a plasmid, pET21/*iscA2*, was constructed as a derivative of the expression vector pET-21 (Novagen). A DNA fragment of about 350 bp encompassing the *T. elongatus iscA2 gene* (*tll0464*) was obtained by PCR amplification from the genomic DNA of *T. elongatus* using forward and reverse primers containing digestive site for restriction enzymes. The PCR product was digested with appropriate restriction enzymes and cloned into the cloning site of pET-21. The pET21/*iscA2*-transformed *E. coli* strain BL-21(DE3)RIL was grown at 310 K in LB medium containing ampicillin (50 $\mu g\ ml^{-1}$) to an OD_{600} of 0.6 – 0.8, induced by addition of 0.4 mM isopropyl-β-D-thiogalactoside (IPTG), and grown for another 16 h at 293 K. The cells were harvested by centrifugation and stored at 193 K.

IscA2 protein purification

All steps in the purification were carried out at 277 K and all solutions used for purification were purged with argon prior to use. 30 ml of the *E. coli* pellet was suspended in 270 ml of lysis buffer (50 mM Tris-HCl pH7.5, 10 mM NaCl, 1 mM DTT) and broken by sonication. After centrifugation, the supernatant was loaded onto a 200 ml of DE52 column equilibrated with lysis buffer. After washing with 300 ml of lysis buffer, the protein was eluted with 300 ml of 100 mM NaCl buffer (50 mM Tris-HCl pH7.5, 100 mM NaCl, 1 mM DTT). Solid ammonium sulfate was added to the eluate and a fraction between 30 and 40% saturation was collected by centrifugation. The precipitate was suspended in 50 ml of ammonium sulfate buffer (50 mM Tris-HCl

pH7.5, 1 mM DTT, 25% (w/v) ammonium sulfate) and subjected to centrifugation followed by filtration through a Millex™-LG syringe driven filter unit (Millipore) to strictly remove any insoluble materials. The protein solution was loaded onto a 150 ml of Butyl TOYO-PEARL column (Tosoh) equilibrated with ammonium sulfate buffer. Decreasing the ammonium sulfate concentration to 0% (w/v) in ammonium sulfate buffer induced IscA2 elution. The IscA2-containing fractions were concentrated using a Centriprep YM-10 (Amicon) to 5 ml and diluted with 50 ml of Tris buffer (50 mM Tris-HCl pH7.5, 1 mM DTT). This step was repeated two times. The protein solution was loaded onto a 150 ml of DEAE TOYO-PEARL anion-exchange column (Tosoh) equilibrated with Tris buffer. The protein was eluted with a linear gradient of 0-500 mM NaCl in Tris buffer. The IscA2-containing fractions were concentrated using a Centriprep YM-10 to 4 ml and injected onto a Hiprep™ 26/60 Sephacryl S-100 HR gel-filtration column (Pharmacia) equilibrated with a buffer containing 50 mM Tris-HCl pH7.5, 1 M NaCl, 1 mM DTT. The eluted IscA2 was concentrated using a Centriprep YM-10 to 800 μl and desalted by NAP™10 column to the buffer containing 10 mM Tris-HCl pH 7.5 and 5 mM DTT (or without DTT for the use of some biochemical experiments). Purity of each fraction was confirmed by SDS-17.5% PAGE.

Spectroscopic method

UV-visible absorption spectrum of protein was recorded using a UV-2500PC UV-visible recording spectrophotometer (Shimazu).

Concentration measurement of the protein and the iron-sulfur cluster

Protein concentration was determined with Bio-Rad Protein Assay (Bio-Rad) according to the suggested protocol. This assay is based on the method of Bradford. BSA was used as a standard protein.

Protein concentration was also estimated from the absorption peak value at 280 nm in the UV-visible absorption spectrum of the protein solution. Using the equations cited below and the idiosyncratic values for the protein (in the case of IscA2; W = 2, Y = 2, Mw = 12350), we can estimate the protein concentration.

$E_{280} = (5500 \times W + 1400 \times Y) \times 1.05$ W = tryptophan, Y = Tyrosine

$A_{280} = E_{280} / Mw$ Mw = Molecular weight

The [2Fe-2S] cluster concentration was estimated using the molar extinction coefficients of 9.68 mM-1 cm-1 at 422 nm (Tagawa et al., 1968). We calculated holo IscA2 concentration using the cluster concentration, hypothesizing that holo IscA2 is composed of two IscA2 molecules and one [2Fe-2S] cluster.

Gel filtration analysis

IscA2 was loaded onto a Superdex^{TM}75 3.2/30 column (Pharmacia) equilibrated with a buffer containing 50 mM Tris-HCl pH7.5, 150 mM NaCl, 1 mM DTT. The flow rate was 100 μl min^{-1}. The elution time of each protein was measured by monitoring the absorption at 280, 330 and 420 nm. The following molecules with known molecular mass were used for the calibration of the column; BSA (67 kDa), Ovalbumin (43 kDa), Myoglobin (17.6 kDa), Ribonuclease A (13.7 kDa).

Iron-sulfur cluster transfer from IscA2 to apo ferredoxin

Apo ferredoxin was obtained from holo ferredoxin as described by Nishio et al. For the iron-sulfur cluster transfer reaction, 20 μg apo ferredoxin and 50 μg holo IscA2 were incubated in 40 μl of a buffer containing 50 mM Tris-HCl pH7.5, 50 mM KCl, 5 mM DTT, 1 mM EDTA for 1 h at 310 K. Analysis of the transfer reaction was made by nondenaturing PAGE using 17.5 % polyacrylamide gel as described by Nishio et al.

Crystallization

Under a glove box enclosing an argon atmosphere, crystals were grown at 277 K by the hanging-drop vapour-diffusion method with a reservoir containing 100 mM K phosphate pH 6.2, 2.5 M NaCl, 5 mM DTT. Drops were made by mixing 2 μl protein solution (30 mg ml^{-1} in 10 mM Tris-HCl pH 7.5, 5 mM DTT) and 2 μl reservoir solution. Crystal plate was stored in a vinyl bag containing an oxygen absorption agent (Azuwan). Small crystals appeared after 4 d and continued to grow for about two weeks.

Preparation of selenomethionine derivative

In parallel with the native form, a selenomethionine derivative of the IscA2 protein was prepared and crystallized for MAD (multiwavelength anomalous diffraction). The pET21/*iscA2* plasmid was transformed to the *E. coli* methionine auxotroph strain BL21-

CodonPlus™(DE3)-RIL-X. Transformed *E. coli* was grown at 310 K in M9 medium supplemented with amino acids (40 mg l^{-1} each; 19 amino acids except methionine), selenomethionine (25 mg l^{-1}), nucleic acids (0.5 g l^{-1} each; 4 nucleic acids), vitamin mixture (10 ml l^{-1} of Kao and Michayluk Vitamin Solution, Sigma) and ampicillin (50 μg ml^{-1}) to an OD_{600} of 0.4 – 0.6, induced by addition of 0.4 mM isopropyl-β-D-thiogalactoside (IPTG), and grown for another 16 h at 293 K. Selenomethionine derivative of the IscA2 protein was purified and crystallized by the same methods described for native IscA2.

Data collection and structure determination

Crystals were transferred from the hanging drop to reservoir solution containing 5% (w/v) PEG400. Stepwise increase of PEG400 concentration up to 20% (w/v) was achieved by changing the reservoir solution. Crystals were picked up with a nylon loop and flash-cooled at 100 K in liquid nitrogen. Diffraction data were collected at 100 K using beamline BL44XU at the SPring-8 synchrotron-radiation facility, Japan. Imaging plates (DIP6040) were used as detectors. The MAD data set was collected using a different crystal at the iron-absorption edge (1.7423 Å). Another MAD data set was collected using a selenomethionene derivative crystal at the selenium-absorption edge (0.9791 Å). All diffraction-image data were indexed and integrated with MOSFLM and scaled using SCALA from the CCP4 suite. The IscA2 crystal belonged to the orthorhombic space group I222, with unit-cell parameters a = 77.5, b = 102.8, c = 137.0 Å. The atomic model was completed using O (Jones et al., 2000) and refined with REFMAC (Murshudov et al., 2000).

Analytical ultracentrifugation

Prior to analysis by analytical ultracentrifugation, IscA2 was dialyzed against a buffer containing a physiological concentration of salt (50mM Tris-HCl pH7.5, 150 mM NaCl, 1 mM DTT) or the crystal buffer containing a high concentration of salt (100 mM K phosphate pH 6.2, 2.5 M NaCl, 1 mM DTT) at 277 K over night to give a final concentration of 1 mg ml^{-1}. The dialysate was used as a reference solution. Sedimentation velocity experiment was performed in an Optima XL-I analytical ultracentrifuge (Beckman) in a 4-hole An60Ti rotor at a rotor speed of 40,000 rpm at 293 K with standard double-sector centerpieces and quartz windows. Scans by

absorbance at 280 nm were recorded in a continuous mode without intervals between successive scans. The resulting data were analyzed by a program, sedfit, which has been developed by Peter Schuck at NIH (Schuck, 2002).

Computer-based models of non-domain-swapped IscA2 dimer

As a general rule of 3D domain swapping, original protein structures can be guessed by cutting and reconnecting the domain-swapped origomeric structure. Two model structures of IscA2 dimer in a physiological solution were constructed by cutting and reconnecting the crystal structure of *T. elongatus* IscA2 tetramer.

Model (a) was made as follows; Molecule *B'* was made by connecting residue 1-36 of molecule *D* and residue 37-108 of molecule *B*; Molecule *D'* was made by connecting residue 1-36 of molecule *B* and residue 37-108 of molecule *D*.

Model (b) was made as follows; Molecule *B'* was made by connecting residue 1-36 of molecule *B*, residue 37-97 of molecule *D*, and 98-108 of molecule *B*; Molecule *D'* was made by connecting residue 1-36 of molecule *D*, residue 37-97 of molecule *B*, and 98-108 of molecule *D*.

The structure of each model was refined with REFMAC (Murshudov et al., 2000).

AMS (4-acetamido-4'-maleimidylstilbene-2,2'-disulfonic acid) modification of IscA2

800 μl of IscA2 solution (50 μM IscA2, 50mM Tris-HCl pH7.5, 150 mM NaCl, 1 mM TCEP) was mixed with 20 μl of AMS solution (20 mM AMS, 50mM Tris-HCl pH7.5, 150 mM NaCl, 1 mM TCEP) on ice. UV-visible absorption spectra of AMS-reacted IscA2 were recorded on time course using a UV-2500PC UV-visible recording spectrophotometer (Shimazu). After remnant AMS was quenched by adding β-mercaptoethanol, AMS modification of IscA2 was confirmed by SDS-15% PAGE.

Carboxymethylation and Mass spectroscopy

120 μl of AMS-reacted IscA2 protein solution was mixed with 7.5 ml of urea buffer (8 M urea, 0.5 M Tris-HCl pH9, 5 mM EDTA). After being added with 100 μl of β-mercaptoethanol under an argon atmosphere, protein solution was incubated at 310 K for 3 h. Iodoacetic acid solution (1 g dissolved in 1 ml MilliQ) and 50 μl of β-mercaptoethanol were added under an argon atmosphere, and protein solution was

incubated in the dark for 2 h at room temperature. Sample was dialyzed against 4 l of 50 mM NH_4HCO_3 at 277 K. The buffer was changed 3 times with the last step being overnight. Protein solution was freeze-dried overnight to become a white precipitate. The precipitate was suspended in 100 μl of SDS-PAGE sample buffer. 40 μl of sample was separated by SDS-17.5% PAGE. Right after the electrophoresis, the protein bands were visualized by Coomassie brilliant blue R (Sigma). The band was cut out, broken and desiccated. Dried-gel was suspended in 50 μl of 50 mM NH_4HCO_3 containing 10 μg ml^{-1} *Pichia pastoris* trypsin (Roche) and digested for 12 h at 310 K. Digested IscA2 fragments were extracted from the gel by adding, vortex and reserving of a series of extraction buffer; 50 μl of 0.1% TFA (trifluoroacetic acid), 100 μl of 0.1% TFA in acetonitril, 50 μl of 0.1% TFA in 50% acetonitril, 80 μl of 0.1% TFA in acetonitril. After being filtrated through an ULTRAFREE® -MC 0.22 μm Filter Unit (Millipore), the volume of the extract was reduced to 50 μl using the vacuum dryer centrifuge. The sample was desalted using a C18™ zip tip (Millipore) according to the manufacturer's instructions and eluted in 10 μl of 0.1 % TFA in 50% acetonitrile. After mixing with the matrix, α-cyano-4-hyroxycinnamic acid, samples were air-dried and analyzed by matrix-assisted laser-desorption ionization-time of flight mass spectrometry using a Voyager Elite XL (Applied Biosystems).

Trypsin digestion of AMS-reacted IscA2

50 μl of AMS-reacted IscA2 protein solution was mixed with 5 μl of 0.2 mg ml^{-1} *Pichia pastoris* trypsin (Roche) (or graded concentration of trypsin from 4.5 x 10^{-4} to 1 mg ml^{-1} as a final concentration) and incubated on ice for 30 min. 5 μl of 10 mg ml^{-1} trypsin inhibitor (Sigma) was added and kept for another 15 min. Trypsin digestion of AMS-reacted IscA2 was confirmed by SDS-PAGE using 16 % polyacrylamide gel as described by Hermann et al.

Amino-terminal sequence determination

Right after the electrophoresis, the protein bands were transferred to a polyvinylidene difluoride membrane (Millipore). Protein bands were visualized by Coomassie brilliant blue R (Sigma). The band was cut out and applied on a protein sequencer (Shimadzu PPSQ-21). The first 5 amino-terminal residues were determined.

RESULTS AND DISCUSSION

Cloning, expression and purification of the *Thermosynechococcus elongatus* IscA2.

The *iscA2* (*tll0464*) gene was cloned from the genomic DNA of *T. elongatus* into a plasmid, and IscA2 protein was expressed from this plasmid in *E. coli* as a recombinant protein. IscA2 protein was purified by the methods described in Materials and Methods, and purity was confirmed by SDS-PAGE (Fig. 2-2). Single protein band of IscA2 indicates that only IscA2 exists in a purified protein solution (Fig. 2-2 Lane 9).

Purified IscA2 protein solution showed brown red color (Fig. 2-3 (a)). By measuring the UV/absorption spectrum, we investigated which type of the iron-sulfur cluster is contained in the IscA2 protein. The UV/absorption spectrum of purified IscA2 (Fig. 2-3 (b)) showed a sharp peak at 280 nm, which derives from the absorption of both tryptophan and tyrosine residues in the protein, and peaks at 330 nm and around 420 nm. These characteristic peaks at 330 nm and around 420 nm have been reported for the proteins with the [2Fe-2S] clusters. This result suggests that purified IscA2 protein has the [2Fe-2S] cluster. From the absorption spectrurm (refer to Materials and Methods), we estimated that holo IscA2 accounts for about 70% of all IscA2 molecule.

To investigate the molecular status of purified IscA2, the gel filtration analysis was applied (Fig. 2-4). Purified IscA2 eluted through a Superdex 75 column as a sharp single peak (Fig. 2-4 (a)). The molecular weight of IscA2 was calculated to be 20 kDa by comparing its elution time with that of other proteins with known molecular weight (Fig. 2-4 (b)). Because this value of 20 kDa is near the molecular weight of IscA2 dimer (24.8 kDa), this result suggests that purified IscA2 exists as predominant dimer.

Crystallization and structure determination

Crystals of IscA2 were obtained by the hanging-drop vapour-diffusion method with a reservoir containing 100 mM K phosphate pH 6.2, 2.5 M NaCl, 5 mM DTT (Fig. 2-5). Note that the protein crystallized in a solution containing a high concentration of salt, 2.5 M NaCl. The IscA2 protein in the crystal seemed to still have iron-sulfur clusters because the crystal showed brown red color that is characteristic for a protein with iron-sulfur clusters. IscA2 crystallized in the space group of *I222* with unit-cell parameters of a = 77.5, b = 102.8, and c = 137.0 Å ($\alpha = \beta = \gamma = 90°$) (Table. 2-6). The structure was determined by the MAD (multiwavelength anomalous dispersion) technique performed

at both the Fe edge (1.7423 Å) using native crystals and the Se edge (0.9791 Å) using cristals of selenomethionyl derivatives. The electron density was well defined so that we could construct the atomic model of *T. elongates* IscA2. The current 2.3 Å resolution structure has excellent refinement statistics (Table. 2-7).

IscA2 crystallized as a tetramer with the [2Fe-2S] cluster asymmetrically bound by IscA2 dimer

To our surprise, *T. elongatus* holo IscA2 crystallized as a tetramer. The crystallographic asymmetric unit contained four molecules of IscA2 and two [2Fe-2S] clusters (Fig. 2-8 (a)). Each IscA2 molecule was designated as monomer *A*, *B*, *C*, and *D*. Although residues around 15-25 and a few residues of N- and C- terminal in each monomer were missing, other protein part was clearly visible.

Monomer *A* and monomer *C* exhibit compact globular structures (Fig. 2-8 (a), blue and red molecules). The central core is composed of two closely packed beta-sheets forming a sandwitch-like structure with a hydrophobic interior. Two amphipathic alpha helices frame opposite sides of the sandwitch. These structural features are almost similar to the crystal structure of *E. coli* IscA subunit. However, in contrast to *E. coli* IscA whose C-terminal regions were disordered and missing, *T. elongatus* IscA2 shows clear structure of the C-terminal region. In monomer *A* (and monomer *C*), the C-terminal region (residues 97-111, see Fig. 2-1) is fixed by the [2Fe-2S] cluster via two cysteine ligands, Cys101 and Cys103, and bends double near this site. This makes S-shaped conformation of the C-terminal region.

In contrast to globular structures of monomer *A* and monomer *C*, entire molecules of monomer *B* and monomer *D* intertwined with each other. We suggest that this intertwined structure is a result of "domain-swapping", about which we will discuss in detail later. Intertwined structure of monomer *B* and monomer *D* contains a long beta-sheet on the front side of the crystal structure (Fig 2-8 (a), front side). C-terminal region is also visible and positioned near the [2Fe-2S] cluster (see Fig 2-8 (a)). However, the conformation of it is straight, and only one cysteine residue, Cys103, ligates to the cluster.

Interestingly, the [2Fe-2S] cluster is asymmetrically coordinated in a tetrahedral fashion by four cysteine residues from two IscA2 monomers. In the case of one [2Fe-2S] cluster ligated by both monomer *A* and monomer *B* (Fig. 2-8 (b)), three cysteine

residues (*A*-Cys37, *A*-Cys101, and *A*-Cys103) are from monomer *A*, and one cysteine residue (*B*-Cys103) is from monomer *B*. *B*-Cys103 and *A*-Cys37 ligate to the same iron atom of the [2Fe-2S] cluster whereas *A*-Cys101 and *A*-Cys103 ligate another iron atom. Another [2Fe-2S] cluster is asymmetrically coordinated in the same way by both monomer *C* and monomer *D*.

The [2Fe-2S] cluster itself of IscA2 seems to be same as that of other proteins, although the current resolution of 2.3 Å is insufficient to correctly measure the bond lengths and angles.

Holo IscA2 exists as a dimer in a physiological solution

Although purified IscA2 was estimated as predominant dimer by gel filtration analysis (Fig. 2-4 (b)), IscA2 crystallized as a tetramer. What is the reason of this discrepancy? We hypothesized that originally dimeric form of IscA2 might change its oligomeric state to a tetramer depending on the experimental conditions. There are several differences between two experimental conditions of gel filtration analysis and crystallization. One of them is the protein solution composition. The gel filtration analysis used a protein solution containing a physiological concentration of salt (150 mM NaCl) whereas the crystallization used a protein solution containing a high concentration of salt (2.5 M NaCl).

To investigate the effects of each solution over oligomeric state of IscA2 protein, the analytical ultracentrifugation study was applied (Fig. 2-9). In a solution containing a physiological concentration of salt (Fig. 2-9 (a)), two peaks were observed. The major peak was assigned to be from IscA2 dimer, and the minor peak was assigned to be from IscA2 monomer. On the other hand, three peaks were observed in the solution containing a high concentration of salt (Fig. 2-9 (b)). In addition to two peaks that seemed to be from IscA2 monomer and dimer, the peak with a calculated molecular weight of 56.7 kDa was observed. This peak was assigned to be from IscA2 tetramer. The difference between the measured value and the calculated molecular weight of IscA2 tetramer, 49.4 kDa, is probably due to a measurement error. This result indicates that a part of IscA2 can form a tetramer in a solution containing a high concentration of salt.

Tetrameric form of IscA2 observed in the crystal structure is a result of 3D domain

swapping

It is reasonable to think that IscA2 tetramer observed in the analytical ultracentrifugation studies and in the crystal structure was made from a pair of IscA2 dimers. In the IscA2 crystal structure, monomer *A* and monomer *B* are covalently linked by an iron-sulfur cluster (Fig. 2-8). Therefore, monomer *A* and monomer *B* must be subunits of a dimer. Besides, as we will show later, holo IscA2 exists as an asymmetric homodimer even in a physiological solution. Putting all things together, it seems that only monomer *B* unfolds and exchanges homologous parts with another unfolded IscA2 dimer to form an intertwined IscA2 tetramer.

We suggest that these processes are a kind of 3D (three dimensional) domain swapping (Fig. 2-10). As Eisenberg and colleagues defined (Bennett et al., 1995), 3D domain swapping is a mechanism by which one protein subunit exchanges homologous part with other protein subunits. The result is an intertwined dimer or higher oligomer.

We will discuss about the mechanism of 3D domain swapping and its physiological meaning after we construct a model structure of holo IscA2.

Construction of two model structures of holo IscA2: from the crystal structure

Analytical ultracentrifugation studies indicated that holo IscA2 is a homodimer in a physiological solution. Then what is the structure of IscA2 dimer? As a general rule of 3D domain swapping, the original protein structure can be guessed from the domain-swapped origomeric structure (Bennett et al., 1995). One domain in the origomeric structure, which is made from several proteins, represents the original protein structure.

Following the rule, we constructed model structures of IscA2 dimer by cutting and reconnecting the crystal structure of IscA2 tetramer (Fig. 2-11). Although monomer *B* and monomer *D* are intertwined in the crystal structure of IscA2 (Fig. 2-11 crystal structure), two globular domains are easily recognized (Fig. 2-11 panel1 and panel2, gray domains). Their core structures are almost similar to those of monomer *A* and monomer *C* (data not shown). Monomer *A* is linked to the C-terminal region of monomer *B* via the [2Fe-2S] cluster (Fig. 2-11 panel3, blue molecule & green fragment). Then, which domain is the core structure of monomer *B* that forms a homodimer with monomer *A*?

Two distinct model structures, Model (a) and Model (b), are possible (Fig. 2-11 lower panels). In Model (a), monomer *B'* (' means a model-constructed structure) is

arranged side by side with monomer *A* and C-terminal region of monomer *B'* is extended towards an iron-sulfur cluster on monomer *A*. In Model (b), monomer *B'* is arranged in another position, and the iron-sulfur cluster is just between monomer *B'* and monomer *A*. In the model construction, the crystal structure was cut and reconnected at two sites near the twofold axis (= center) of the protein (Fig. 2-11 panel2). One site is on the front side of the crystal structure, and another site is on the back side (Fig. 2-12 crystal structure). Fig. 2-12 shows the structural comparison before and after the model construction at these two sites, front site and back site. Only a few residues change its structure at both sites after the model construction (see Fig. 2-12 Merge panel). Model (a) changed its structure only at front site whereas Model (b) changed its structure at both front and back sites.

Deciding one model structure of holo IscA2: by the biochemical experiments

Which model is the correct structure of holo IscA2 in a physiological solution?

We tried to distinguish these two model structures by biochemical experiments. There was a difference between two model structures, which was expected to be distinguishable by biochemical experiments. In holo IscA2 dimer, there should be two free cysteine residues, *B'*-Cys37 and *B'*-Cys101, which both belong to monomer *B'*. In Model (a), two sulfur atoms of these free cysteine residues are completely exposed to the solvent (Fig. 2-13 (a)). On the other hand, only one sulfur atom of *B'*-Cys37 is exposed in Model (b) (Fig. 2-13 (b)). Another sulfur atom of *B'*-Cys101 is buried deep in the protein structure.

We thought that we could distinguish the protein structure using a free thiol modification reagent. If the reagent is added to IscA2 protein solution, only fully exposed sulfur atoms would be modified. An experimental result comes depending on the protein structure.

1. If Model (a) is the correct structure, half of IscA2 monomers would be modified by two reagent molecules at both Cys37 and Cys101.
2. If Model (b) is the correct structure, half of IscA2 monomers would be modified by one reagent molecule only at Cys37.
3. Alternative possibility that should be considered is; if the [2Fe-2S] cluster is symmetrically ligated by two IscA2 monomers in the solution, all IscA2 molecules

would be modified by one reagent molecule.

Biochemical experiments using a free thiol modification reagent, AMS, indicated that only Model (b) was plausible. Being reacted with 10 equivalent of AMS, half of IscA2 was modified by one AMS (Fig. 2-14 (a)). We emphasize that one-AMS-modified IscA2 and unmodified IscA2 were always major products even when much higher concentration of AMS was used (data not shown). AMS-modified position was confirmed by peptide mass spectroscopy. Cys37-containing peptide was observed comparably to other peptides only in remaining unmodified IscA2, not in AMS-modified IscA2 (Fig. 2-15 (a)). This implies that Cys37 is the modification position. Trypsin digestion experiment also implied that Cys37 is the modification position, because only Cys37-containing fragments changed its migration profile after being modified by AMS (Fig. 2-16, compare Lane 3 and Lane 4). These results are in good agreement with Model (b) in which one monomer, monomer *B'*, has one solvent accessible free cysteine residue, *B'*-Cys37.

As shown in Fig. 2-17, AMS-modified IscA2 monomer showed almost same sensitivity against trypsin digestion compared to unmodified-IscA2 (compare patterns of two bands indicated as AMS-IscA2 and IscA2). This implies that two monomers in IscA2 homodimer have essentially similar overall structure. Model (b), in which monomer *A* and monomer *B'* have similar overall structure except around conserved cysteine residues as will be discussed later, also meets this result.

Please note that all experiments mentioned above were carried out in a physiological solution. This also means that the asymmetry of IscA2 homodimer exists even in a physiological solution. We propose that Model (b) is a genuine structure of holo IscA2 in a physiological solution, and we will use it for the following discussions.

Molecular mechanism of 3D domain swapping of IscA2 and its physiological meaning

In the early discussion, we suggested that IscA2 tetramer observed in the crystal structure and analytical centrifugation study was made from a pair of IscA2 dimers and that these processes are a kind of 3D domain swapping.

Fig. 2-18 shows a model mechanism of 3D domain swapping of *T. elongatus* IscA2. Holo IscA2 exists as an asymmetric homodimer in a physiological solution (Fig. 2-18,

panel1). However when the solution is changed to a particular condition such as a high concentration of salt, a certain proportion of monomer *B'* undergoes unfolding of its structure (from panel1 to panel3 via panel2). If an unfolded molecule does not meet another unfolded molecule, IscA2 returns to its original structure of completely folded homodimer (from molecule3 to molecule1 via molecule2). This is because molecules are in an equilibrium state and that the original globular structure is thermodynamically stable. However, if an unfolded molecule meets with another unfolded molecule, the situation changes. They exchange homologous parts to form tetrameric form (from panel3 to panel4). This tetrameric structure seems to be very stable because intertwined two monomers form a long beta-sheet on the front surface of the tetrameric structure. IscA2 tetramer probably can not easily separate into a pair of dimers again. Because of its structural stability, the IscA tetramer presumably crystallized preferentially.

We believe that occurrence of domain swapping between *B* and *D* monomers in the crystal must be relevant to functional significance why holo IscA2 exists as an asymmetric homodimer in which one monomer is unstable. In other words, we intend to propose that instability of one monomer is suitable for the iron-sulfur transfer especially when the iron-sulfur cluster is located between monomers. The iron-sulfur transfer occurs by the protein-protein interaction between apo substrate protein and holo IscA protein. If unstable monomer moves or changes its structure during the interaction with the substrate protein, the iron-sulfur cluster will be more exposed and will have more chances to be transferred to the substrate protein. We will discuss the asymmetric-IscA-dimer-directed iron-sulfur cluster transfer in detail later.

Flexible regions around evolutionally conserved cysteine residues of IscA2

The most outstanding feature of the deduced structure of holo IscA2 dimer is that two monomers in IscA2 homodimer are asymmetric even though their overall structures are similar. The asymmetry is conspicuous especially around three evolutionally conserved cysteine residues, Cys37, Cys101, and Cys103. (Fig. 2-19 (a), purple regions).

Fig. 2-19 shows structural comparison of two IscA monomers with other IscA homologues from different organisms, *E. coli* (Fig. 2-19 (b); Cupp-Vickery et al., 2004) and *Aquifex aeolicus* (Fig. 2-19 (c); Xu et al., 2004). In all IscA, the central core is composed of two closely packed beta-sheets forming a sandwitch-like structure with a

hydrophobic interior. Two amphipathic alpha helices frame opposite sides of the sandwitch. However, both the crystal structure of *E. coli* IscA and the NMR structure of the *A. aeolicus* IscA homologous protein lacked ordered structure of entire C-terminal region which contains two conserved cysteine residues. This is probably due to the lack of iron-sulfur cluster ligation. In the case of holo form of *T. elongatus* IscA2, clear structure of the C-terminal region is visible. In monomer *A*, the C-terminal region is fixed by the [2Fe-2S] cluster via two cysteine ligands, Cys101 and Cys103, and bends double near this site. This makes S-shaped conformation of the C-terminal region. In monomer *B'*, the C-terminal region extends straight, and only *B'*-Cys103 is a ligand for the [2Fe-2S] cluster. These various conformations indicate that the C-terminal region is highly flexible when IscA is apo form and that it will be fixed only when IscA assembles an iron-sulfur cluster.

The asymmetry around another conserved cysteine residue, Cys37 of *T. elongatus* IscA2, is conspicuous, too. This cysteine residue is located at a loop which connects two beta-strands. In monomer *A*, Cys37-containing loop is bent towards the [2Fe-2S] cluster, and *A*-Cys37 is used as a ligand for the cluster. On the other hand, Cys37-containing loop of monomer *B'* turns a different direction, and *B'*-Cys37 is not used for iron-sulfur cluster ligation. Furthermore, in *E. coli* IscA, homologous loop region turns in a direction completely opposite of the cluster binding pocket of its own, and the loop interacts with another subunit of IscA tetramer (Fig. 0-6). NMR structures of *A. aeolicus* IscA homologue take various conformations at homologous Cys-containing loop. These various conformations indicate that the Cys-containing loop is potentially flexible and that this flexible Cys-containing loop is fixed in distinct conformations depending on situations. When IscA assemble the cluster, the Cys-containing loop bends towards the [2Fe-2S] cluster to ligate it. When IscA forms an oligomeric complex, the Cys-containing loop turns away from the cluster binding site to interact with another IscA monomer. This interaction may stabilize the oligomeric form.

Amino acid residues with small side chains around the [2Fe-2S] cluster

Amino acid residues with small side chains, such as glycine, alanine, and serine, are well conserved around evolutionally conserved three cysteine residues (Fig. 2-1). We suggest that these amino acid residues with small side chains are important at least in two means.

First, they are important for the conformational changes around cysteine residues. Having residues with small side chains at nearby sites, cysteine-containing regions can gather around the iron-sulfur cluster without large steric hindrance when IscA assembles the cluster (Fig. 2-20).

Second, they are important for the iron-sulfur cluster transfer. Small side chains are not prone to obstacle the interactions with other proteins. Furthermore, they do not cover over the iron-sulfur cluster. Taking these advantages, holo IscA can make a close contact with apo substrate protein, where the iron-sulfur cluster can be directly transferred from holo IscA to apo substrate protein smoothly.

Phe107 plays a "key" role to stabilize the C-terminal region of monomer *A*

The C-terminal region takes two distinct conformations in holo IscA2 asymmetric homodimer. While the C-terminal region of monomer *A* is bent, the C-terminal region of monomer *B'* is straight (Fig. 2-21). The C-terminal region seems to be essentially flexible. What factor(s) stabilize the structure of the C-terminal region? In early discussion, we indicated that the [2Fe-2S] cluster stabilizes the structure of the C-terminal region. Other than the [2Fe-2S] cluster, we found another factor which is important to stabilize the structure of the C-terminal region.

We suggest that Phe107 plays a "key" role to stabilize the structure of C-terminal region especially in monomer *A*. Phe107 is an evolutionally conserved phenylalanine residue located at the C-terminal region following Cys101 and Cys103 (Fig. 2-1). In monomer *A*, Phe107 is inserted into the protein core structure made by the alignment of hydrophobic residues (Fig 2-21 and Fig. 2-1). As a result, the C-terminal region is forced to turn sharply, and both *A*-Cys101 and *A*-Cys103 are positioned suitable for the [2Fe-2S] cluster ligation. *A*-Phe107 seems to fix the structure of the C-terminal region as like as a key lock. On the other hand, in monomer *B'*, Phe107 is out of the core structure. The C-terminal region is extended straight, and free *B'*-Phe107 does not contribute to the stability of monomer *B'* at all.

Partially exposed [2Fe-2S] cluster suggests a molecular mechanism of the iron-sulfur transfer

The structure around the [2Fe-2S] cluster has not been changed by the model construction at all. The [2Fe-2S] cluster of holo IscA2 is asymmetrically coordinated by

four cysteine residues of two IscA monomers. Three cysteine residues (*A*-Cys37, *A*-Cys101, and *A*-Cys103) are from monomer *A*, and one cysteine residue (*B'*-Cys103) is from monomer *B'*.

One of the outstanding features of the [2Fe-2S] cluster in holo IscA2 is that the cluster is partially exposed (Fig. 2-22 (a)). In addition to the iron-sulfur cluster itself, cluster ligands are also exposed to the solution. Two sulfur atoms of *B'*-Cys103 and *A*-Cys37 are exposed to the solution. Please note that these two exposed sulfur atoms ligate to the same Fe atom of the [2Fe-2S] cluster. On the other hand, sulfur atoms of *A*-Cys101 and *A*-Cys103 are completely buried in the protein. Partially exposed structure of the [2Fe-2S] cluster in IscA2 is very unique and different from the usual iron-sulfur clusters of other proteins. For example, *Spirulina* ferredoxin contains a [2Fe-2S] cluster coordinated by four cysteine residues (Fig. 2-22 (b)). However, the iron-sulfur cluster and its ligands are all buried in the protein structure.

Partial exposure of the iron-sulfur cluster of holo IscA2 is reasonably suitable for the iron-sulfur cluster transfer. It is important for holo IscA protein to keep the iron-sulfur cluster stable until IscA meets a substrate protein. If the iron-sulfur cluster is completely exposed to the solvent, the cluster might be too labile to be held. On the other hand, if the iron-sulfur cluster is completely buried in the protein, the iron-sulfur cluster might be hardly transferred to the substrate protein. Partially exposed cluster might be the best structure to achieve the efficient cluster transfer.

Furthermore, partially exposed [2Fe-2S] cluster bound by asymmetric IscA homodimer suggests the structural basis for its scaffold function in iron-sulfur cluster biosynthesis. Importantly, two exposed cysteines, *B'*-Cys103 and *A*-Cys37, are ligating a single Fe atom and are therefore expected to be substituted first when apo substrate protein interacts with holo IscA. Based on the structural information, we suggest a molecular mechanism of the iron-sulfur transfer from holo IscA to apo substrate protein as follows (Fig. 2-23).

1. When apo substrate protein interacts with holo IscA, the cluster transfer begins. Apo substrate proteins have two reactive cysteine residues in a correct position (for example; Cys41 and Cys46 of *Spirulina* ferredoxin). These two reactive cysteine residues attack and substitute with two exposed sulfur ligands of IscA to coordinate one Fe atom.

2. Then, monomer *B'* can move or change its structure dramatically, because monomer *B'* is not ligated to the cluster anymore. As a result, the "mixo-ligated" iron-sulfur is further exposed to apo substrate protein so that originally buried two cysteine ligands can be attacked and substituted by substrate protein.

3. Substrate protein with the iron-sulfur cluster folds into the correct holo structure as it detaches from the protein complex. Apo IscA will be used for another cycle of the iron-sulfur cluster transfer after it reassembles the cluster.

In this work, we suggested a molecular mechanism of the iron-sulfur cluster transfer from holo IscA to apo substrate proteins based on both the crystal structure of *T. elongatus* holo IscA2 and biochemical experiments. Can we consider the asymmetric IscA dimer with the partially exposed [2Fe-2S] cluster proposed in this study as a representative structure of holo form of IscA-type scaffold?

In vivo, cyanobacterial IscA2 protein exists as a protein complex with the HEAT-repeat-containing protein, IaiH, whose function has not yet been elucidated (Morimoto et al, 2002). Therefore, *in vivo* role of the cyanobacterial IscA2 is not likely to be a mere scaffold protein. Nevertheless, purified recombinant holo *T. elongatus* IscA2 alone can transfer its iron-sulfur cluster to apo ferredoxin *in vitro* (Fig. 2-24). This indicates that asymmetric structure of holo IscA2 homodimer actually has a potential to transfer its iron-sulfur cluster to substrate proteins and thus can function as a molecular scaffold in iron-sulfur cluster biosynthesis. Further investigations are needed to examine whether or not holo IscA from other organisms also have an asymmetric structure as shown in this study.

There are also reports which indicate that IscA can assemble the [4Fe-4S] cluster in addition to the [2Fe-2S] cluster (Krebs et al., 2001; Ollagnier-de-Choudens et al., 2004). How IscA assembles the [4Fe-4S] cluster is still an open question.

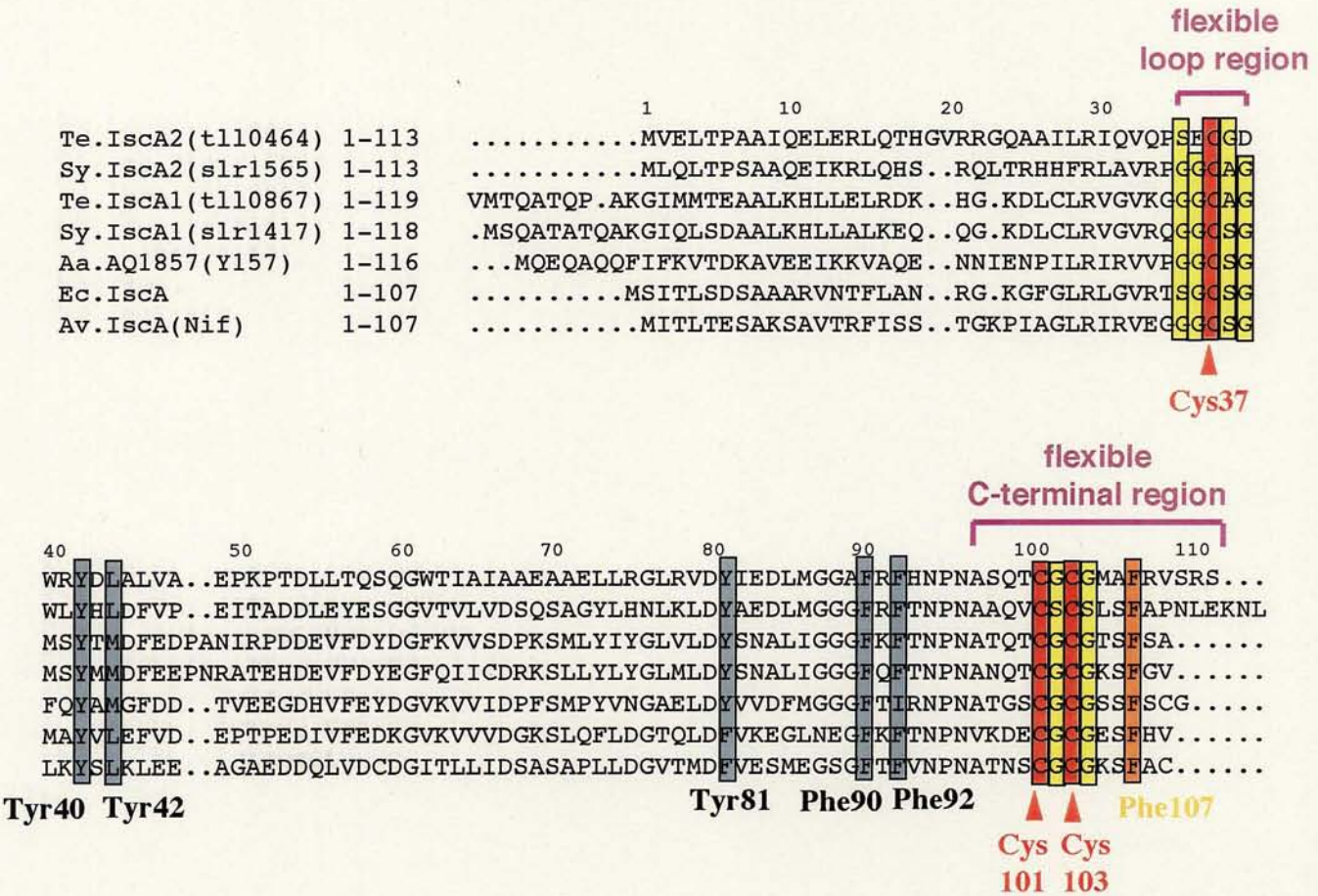

Fig. 2-1 Sequence alignment of *T. elongatus* IscA2 with bacterial homologues.
Red shading indicates three evolutionally conserved cysteine residues.
Orange shading indicates evolutionally conserved phenylalanine residues on the C-terminal region.
Gray shading indicates hydrophobic residues which make up the IscA protein core structure.
Yellow shading indicates well-conserved residues with small side chains around evolutionally conserved cysteine residues.
Below each shading (except yellow shading), residues of *T. elongatus* IscA2 are indicated.
Above sequence alignment, "flexible loop region" and "flexible C-terminal region" are indicated.
Note that each region contains evolutionally conserved cysteine residues.

Te, *Thermosynechococcus elongatus*; Sy, *Synechocystis* sp. PCC6803; Aa, *Aquifex aeolicus;* Ec, *Escherichia coli*; Av, *Azotobacter vinelandii.*
The alignment was generated using the Multalin program (Corpet, 2001).

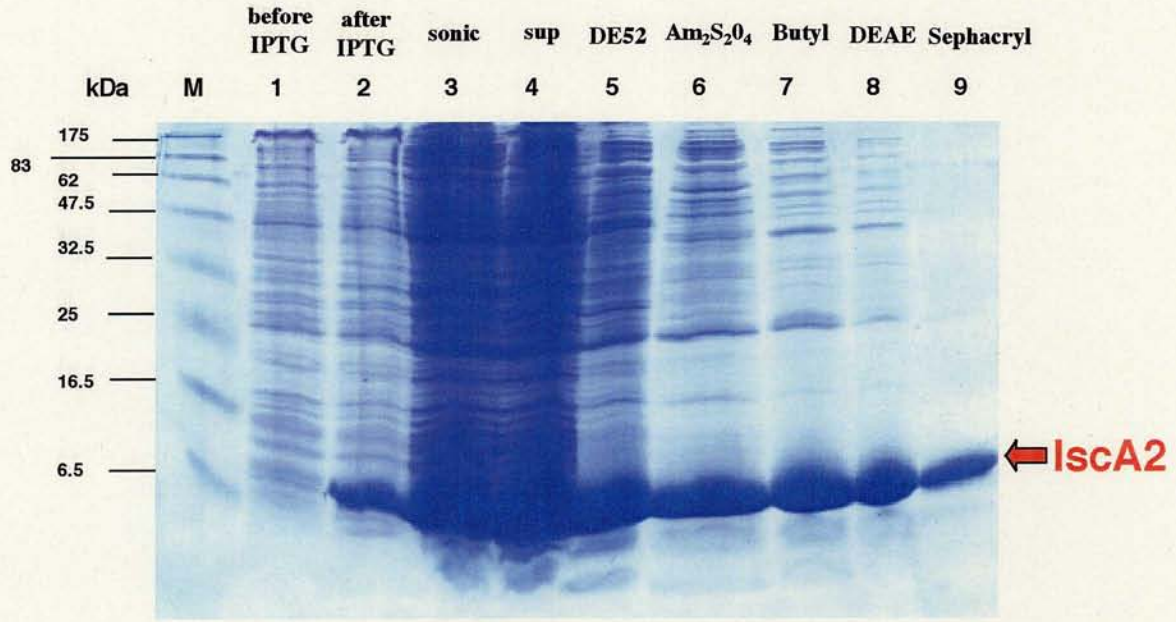

Fig. 2-2. SDS-PAGE analysis of the purification steps of recombinant *T. elongatus* IscA2.

Lane 1: crude cell extract from pET21/*IscA2*-transformed *E. coli* BL21(DE3)RIL before IPTG induction.
Lane 2: crude cell extract from pET21/*IscA2*-transformed *E. coli* BL21(DE3)RIL after IPTG induction.
Lane 3: crude cell extract from IscA2-expressing *E. coli* after sonication.
Lane 4: supernatant after centrifugation.
Lane 5: eluted fraction after the DE52 column.
Lane 6: protein pellet after ammonium sulfate precipitation.
Lane 7: eluted fraction after the Butyl TOYO-PEARL column.
Lane 8: eluted fraction after the DEAE TOYO-PEARL column.
Lane 9: eluted fraction after the Sephacryl S-100 HR column.

Lane M: molecular mass standard. From top to bottom: MBP-β–galactosidase (175.0 kDa), MBP-paramyosin (83.0 kDa), glutamic dehydrogenase (62.0 kDa), aldolase (47.5 kDa), triosephosphate isomerase (32.5 kDa), β–Lactoglobulin A (25.0 kDa), lysozyme (16.5 kDa), aprotinin (6.5 kDa)

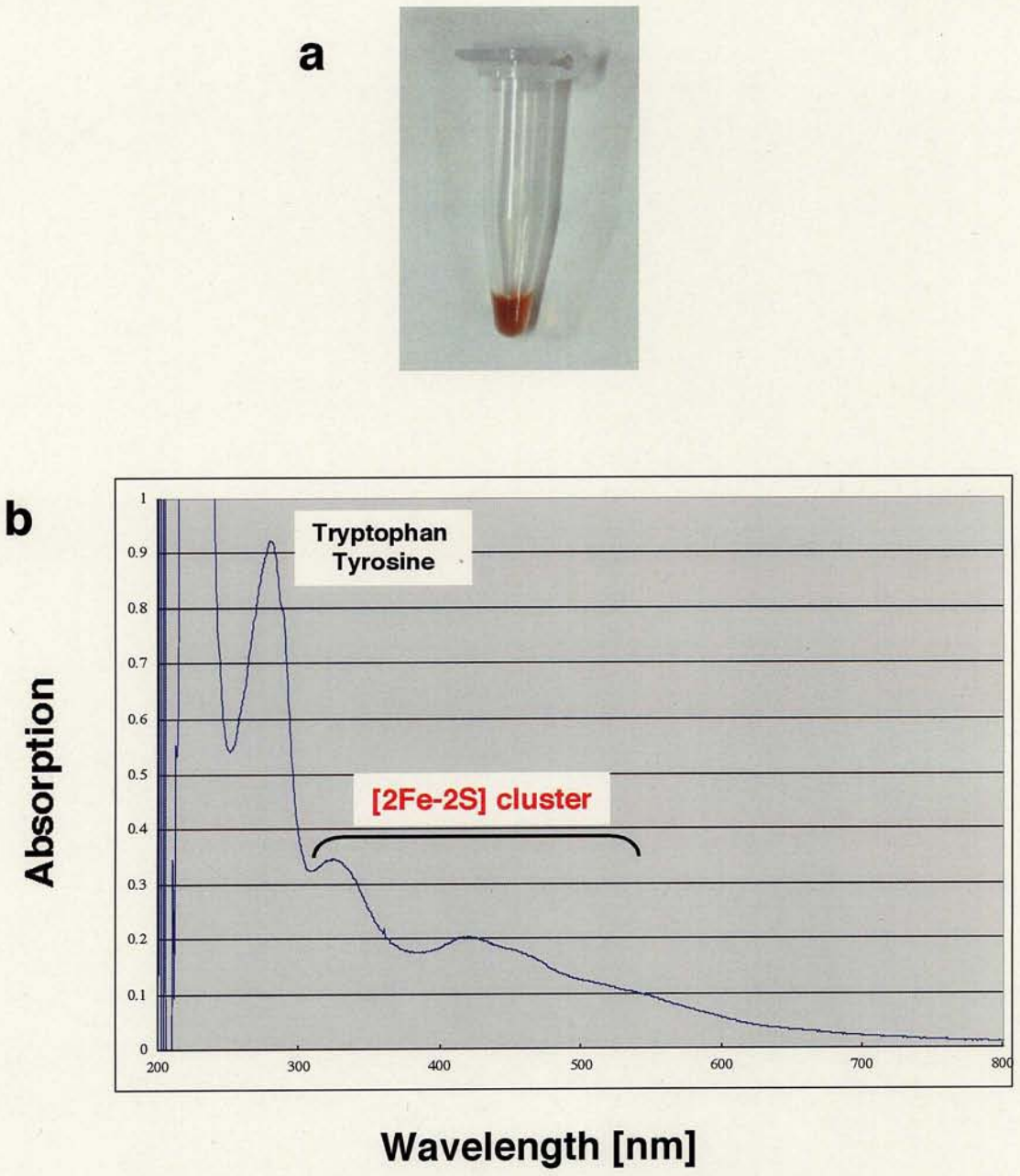

Fig. 2-3.
(a) Purified IscA2 protein solution.
(b) UV/absorption spectrum of purified IscA2.
The protein concentration of IscA2 was 1 mg ml^{-1} in 10 mM Tris-HCl pH7.5, 5 mM DTT.
A sharp peak at 280 nm, which derives from the absorption of both tryptophan and tyrosine residues in the protein, is indicated by black letter.
Peaks at 330 nm and around 420 nm, which derives from the absorption of the [2Fe-2S] cluster, is indicated by red letter.

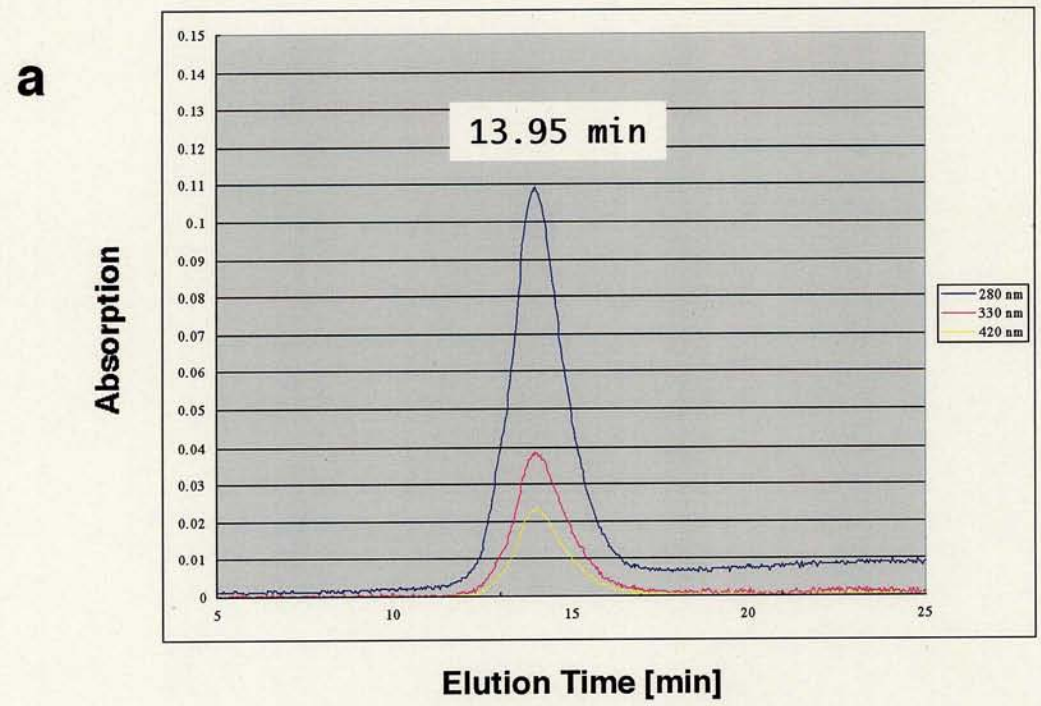

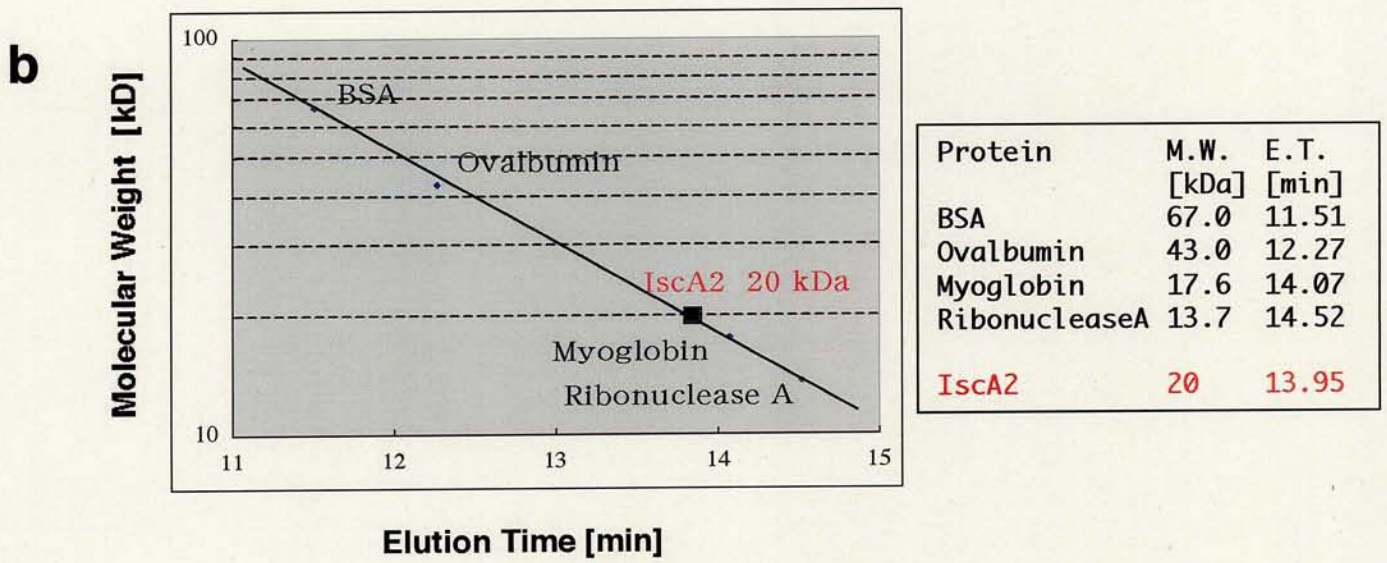

Protein	M.W. [kDa]	E.T. [min]
BSA	67.0	11.51
Ovalbumin	43.0	12.27
Myoglobin	17.6	14.07
RibonucleaseA	13.7	14.52
IscA2	20	13.95

Fig. 2-4. Gel filtration analysis of purified IscA2
Protein was loaded onto a Superdex 75 gel-filtration column equilibrated with a buffer containing 50 mM Tris-HCl pH7.5, 150 mM NaCl, 1 mM DTT.
(a) The elution profile of IscA2 was monitored by absorption at 280 (blue line), 330 (pink line), and 420 nm (yellow line). IscA2 elutedas a sharp peak at an elution time of 13.95 min.
(b) The molecular weight of IscA2 was calculated using the following proteins with known molecular weight; BSA (67 kDa), Ovalbumin (43 kDa), Myoglobin (17.6 kDa), Ribonuclease A (13.7 kDa). *Filled square* shows the position of IscA2. From the elution time, IscA2 was estimated to be a 20 kDa protein.

Fig. 2-5 A crystal of *T. elongatus* IscA2.
Crystals of IscA2 were obtained by the hanging-drop vapour-diffusion method with a reservoir containing 100 mM K phosphate pH 6.2, 2.5 M NaCl, 5 mM DTT.
Note that the protein crystallized in a solution contained a high concentration of salt, 2.5 M NaCl.

The crystal showed brown red color which is characteristic for a protein with iron-sulfur clusters.

Table 2-6 Details of data collection and heavy-atom refinement statistics.

	Native	Fe	Se
Wavelength (Å)	0.9000	1.7423	0.9791
Resolution Range (Å)	83.1-2.3	84.5-3.0	62.0-3.2
Space group	*I222*	*I222*	*I222*
Unit-cell parameters			
a (Å)	77.47	77.36	77.51
b (Å)	102.79	103.70	103.43
c (Å)	137.03	138.31	138.69
Measured reflections	213810	55608	75328
Unique reflections	23851	10717	9371
I/σ(I)	33.1	18.5	26.6
R_{merge} (%) [a]	6.6	7.1	7.0
Completeness (%)	96.6	93.0	99.4
R_{iso} (%) [b]	-	11.0	12.3
Phasing Power (acentric) [c]	-	0.62	0.14
R_{cullis} [d]			
Anomalous (acentric)	-	0.83	0.88
Isomorphous (centric)	-	0.79	0.99
(acentric)	-	0.91	0.99
F.O.M [e]	0.327		

(a) $R_{merge} = \Sigma_{hkl}\Sigma_i|I_i(hkl) - \langle I(hkl)\rangle| / \Sigma_{hkl}\Sigma_i \langle I(hkl)\rangle$ where I_i is the intensity of the measured reflection. (b) $R_{iso} = \Sigma_{hkl}|F_{PH} - F_P| / \Sigma_{hkl}|F_P|$ where F_P is the native structure factor and F_{PH} is the heavy atom derivative structure factor. (c) Phasing power = $\Sigma_h f_c/\Sigma_h \varepsilon$ where f_c is calculated heavy atom factor and ε is the lack-of-closure error. (d) $R_{cullis} = \Sigma||F_{PH}| - |F_P + f_c||/\Sigma||F_{PH}| - |F_P||$ (e) FOM (figure of merit) calculated by the program MLPHARE, in parentheses the FOM after phase improvement with noncrystallographic symmetry averaging and solvent flattening considering 55% of solvent by the program DM

Table 2-7 Refinement statistics of the native structure

Resolution (Å)	2.3
R_{cryst} (%)	24.6
R_{free} (%)	28.6
Number of molecules in the asymmetric unit	4
Number of protein atoms	3059
Number of water molecules	8
Number of [2Fe-2S] clusters	2
Overall B-factor	67.6
r.m.s.d. bond (Å)	0.020
r.m.s.d. angles (°)	2.013
Ramachandran Plot (%)	
Most favored	90.9
Additional allowed	8.5
Generously allowed	0.6

$R_{cryst} = \Sigma||F_{obs}| - |F_{calc}||/\Sigma|F_{obs}|$, where F_{calc} and F_{obs} are the calculated and observed structure factor amplitudes, respectively. R_{free} = as for R_{cryst}, but for 5.0% of the total reflections chosen at random and omitted from refinement.

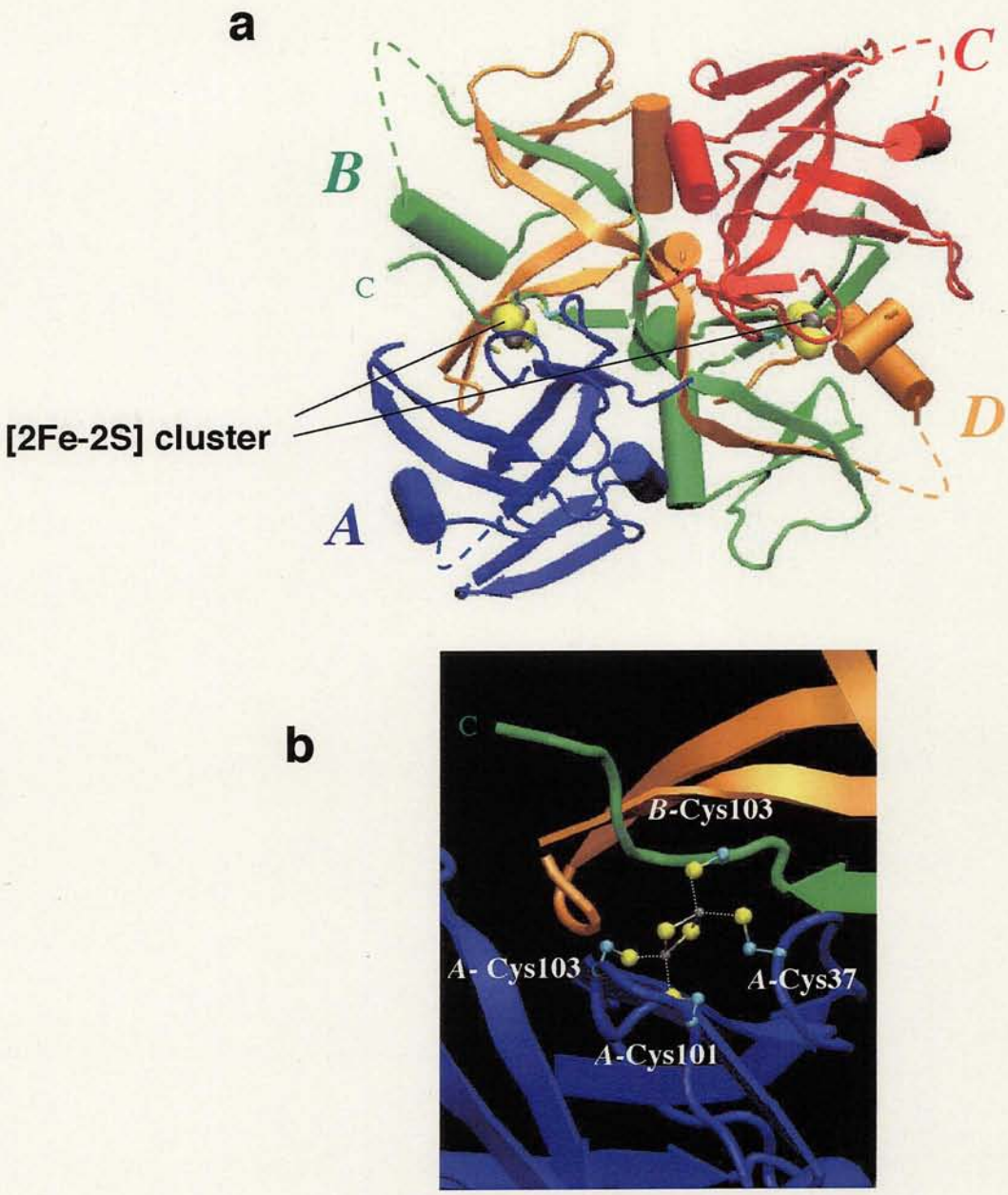

Fig. 2-8 Crystal structure of *T. elongatus* IscA2.
(a) Overall structure of IscA2 illustrating the main secondary structural elements.
IscA2 molecules are shown as a ribbon model and colored blue (*A*), green (*B*), red (*C*), or orange (*D*).
Dotted line connects missing region of each monomer (around residues 15-25).
The C-terminal of monomer *B* is indicated by green letter of "C".
The [2Fe-2S] clusters are shown as a space-filling model and indicated. Note that both clusters are on the front side. Side chains of cysteine residues used for the cluster ligations are shown as a bond model.
Atoms are colored cyan (carbon), gray (iron), or yellow (sulfur).
The figures was created using VMD (Humphrey et al., 1996).
(b) Structure around the [2Fe-2S] cluster.
Molecules are colored in the same way as (a) except that the [2Fe-2S] cluster and side chains of cysteine residues are shown as a ball-and-stick model. Cysteine ligands are indicated.

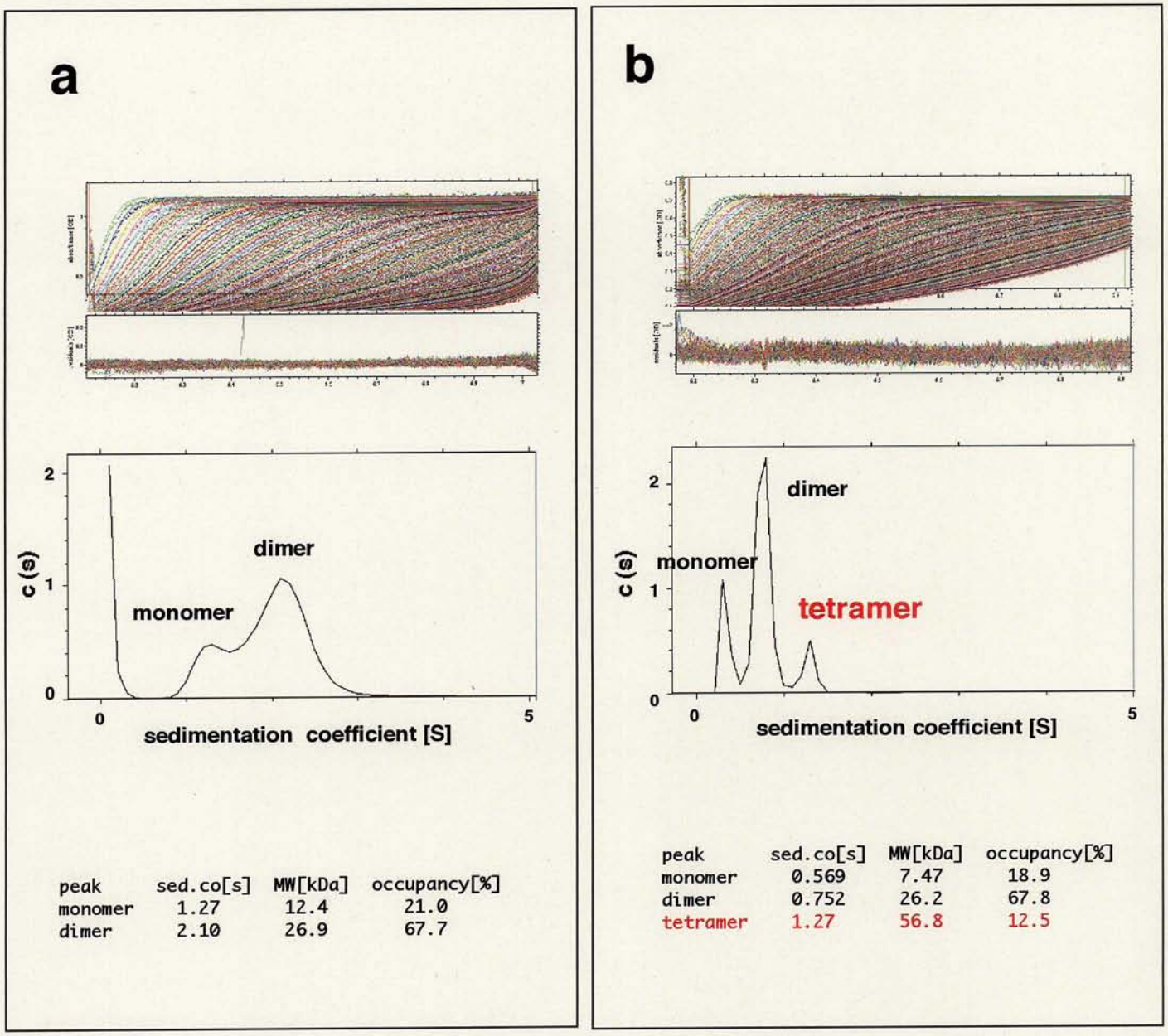

peak	sed.co[s]	MW[kDa]	occupancy[%]
monomer	1.27	12.4	21.0
dimer	2.10	26.9	67.7

peak	sed.co[s]	MW[kDa]	occupancy[%]
monomer	0.569	7.47	18.9
dimer	0.752	26.2	67.8
tetramer	1.27	56.8	12.5

Fig. 2-9 Analytical ultracentrifugation
Analytical ultracentrifugation was applied for 1 mg ml $^{-1}$ IscA2 in each following solution.
(a) solution containing a physiological salt;
50mM Tris-HCl pH7.5, 150 mM NaCl, 1 mM DTT
(b) solution containing a high concentration of salt (used for the crystallization);
100 mM K phosphate pH 6.2, 2.5 M NaCl, 1 mM DTT
Scans by absorbance at 280 nm were recorded in a continuous mode without intervals between successive scans.The resulting data were analyzed by a program, sedfit. (Schuck, 2002, lower tables).

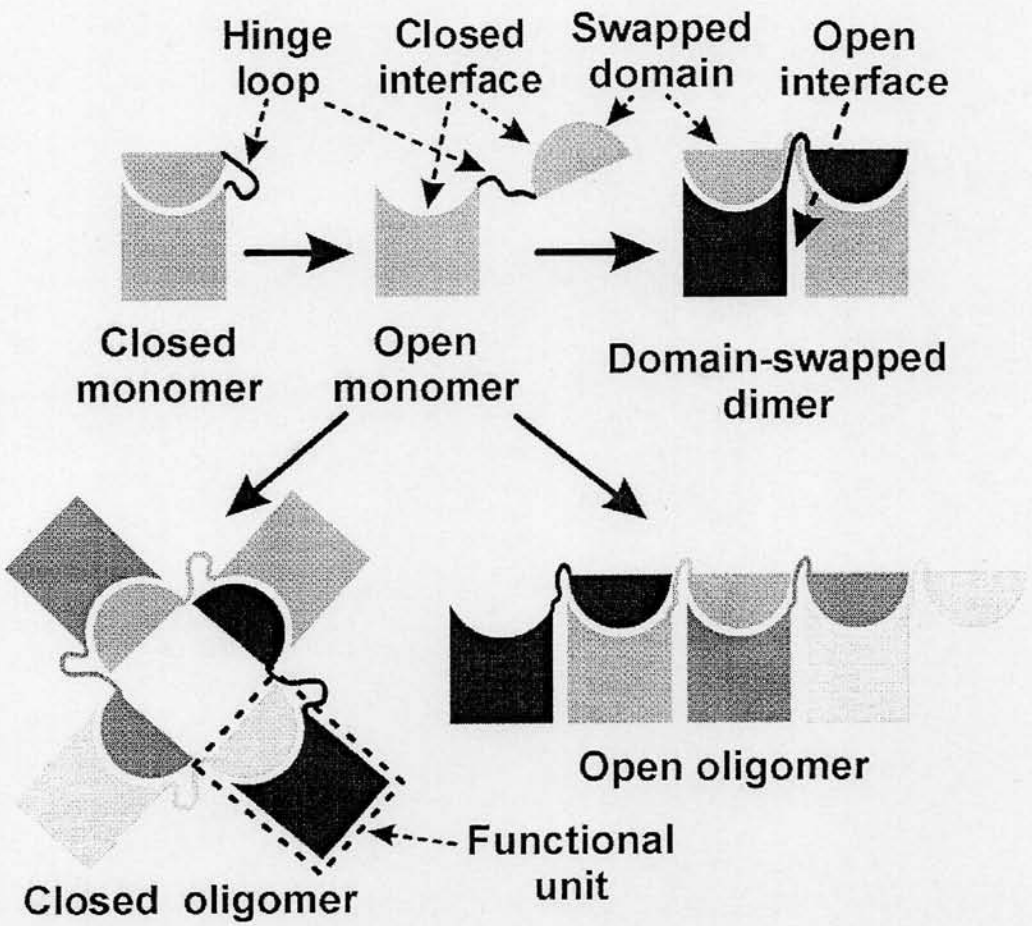

Fig. 2-10. Schematic diagram illustrating terms related to 3D domain swapping.

Yanshun Liu et al. Protein Sci 2002; 11: 1285-1299

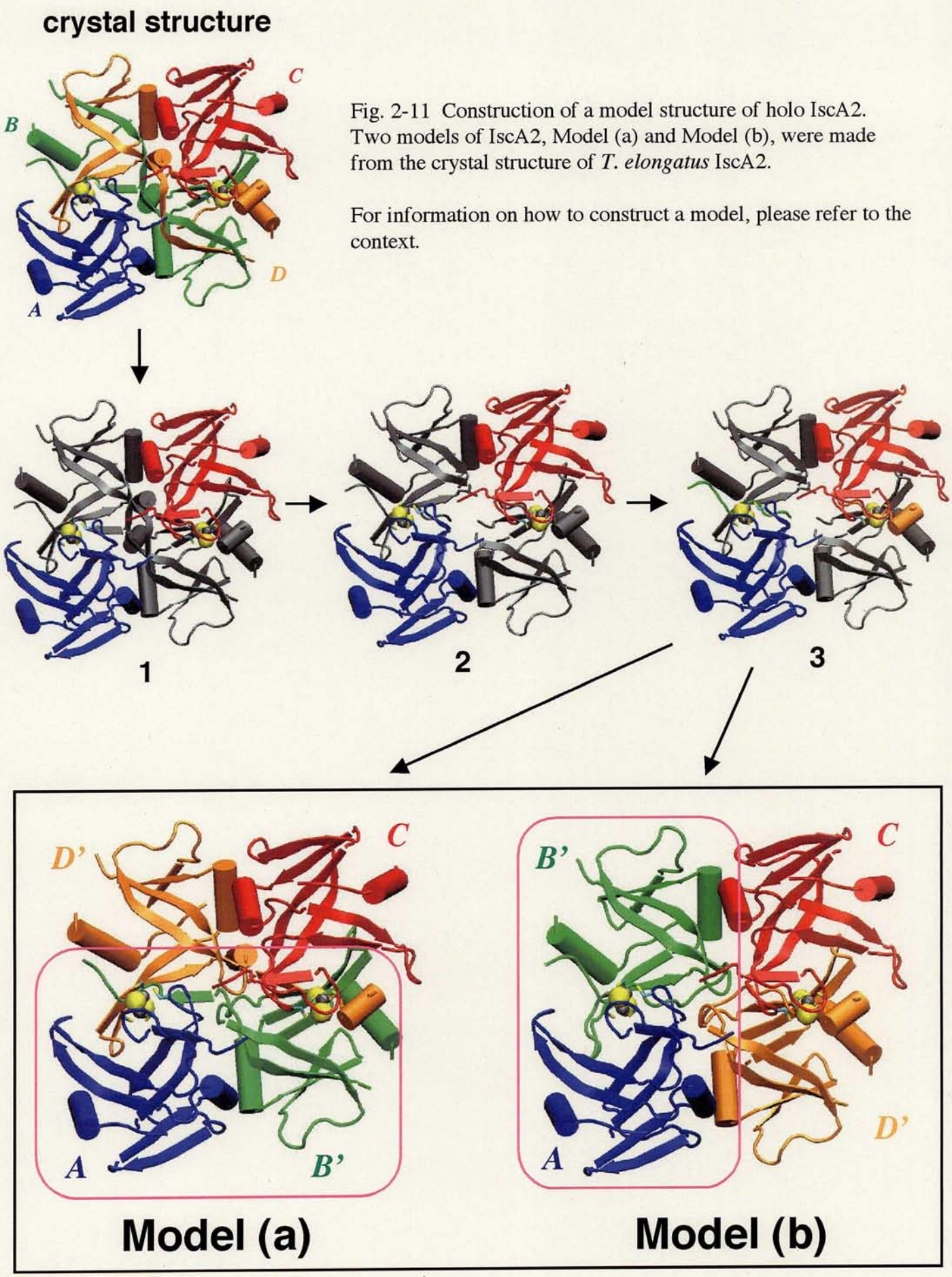

Fig. 2-11 Construction of a model structure of holo IscA2. Two models of IscA2, Model (a) and Model (b), were made from the crystal structure of *T. elongatus* IscA2.

For information on how to construct a model, please refer to the context.

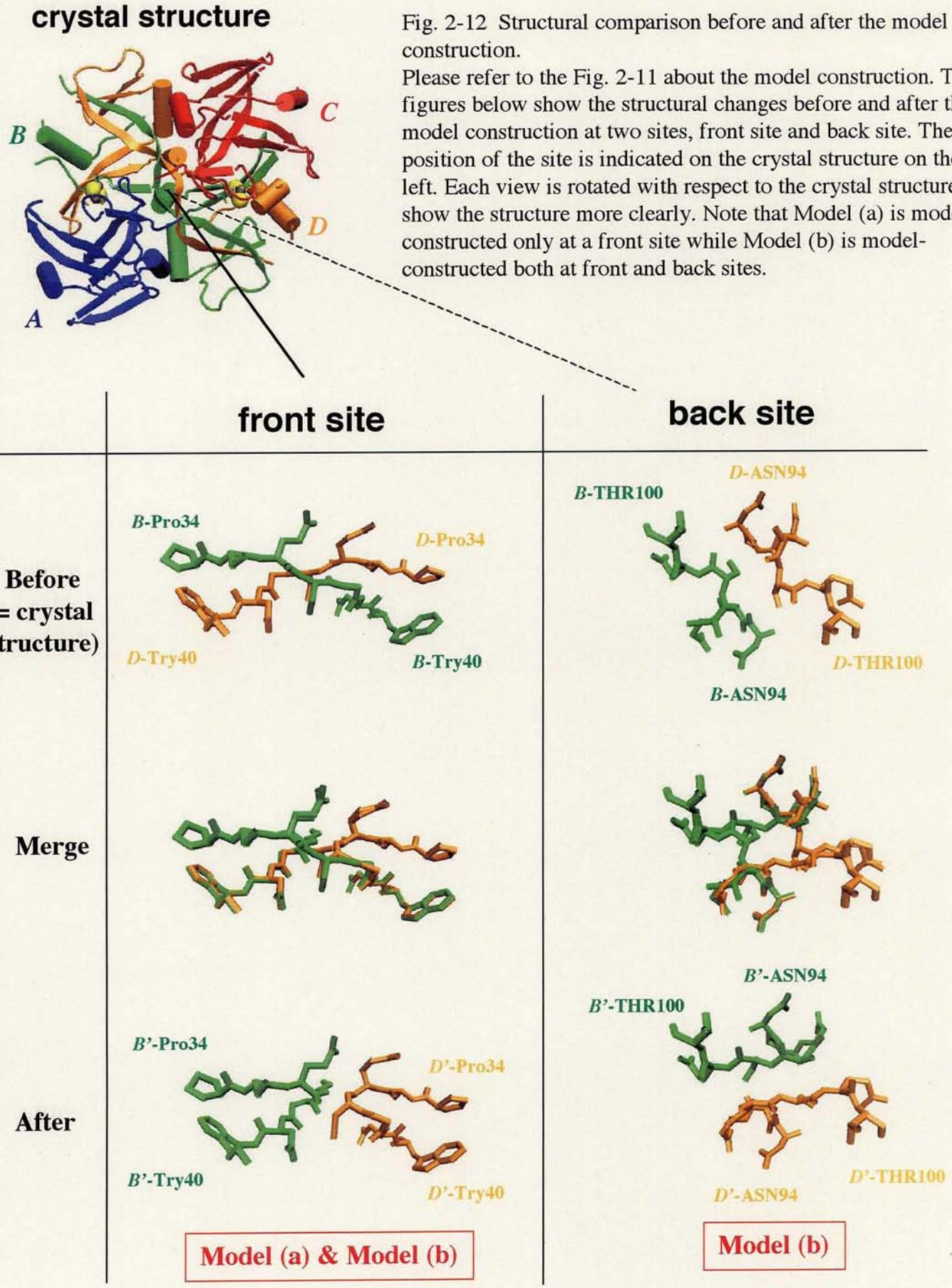

Fig. 2-12 Structural comparison before and after the model construction.
Please refer to the Fig. 2-11 about the model construction. The figures below show the structural changes before and after the model construction at two sites, front site and back site. The position of the site is indicated on the crystal structure on the left. Each view is rotated with respect to the crystal structure to show the structure more clearly. Note that Model (a) is model-constructed only at a front site while Model (b) is model-constructed both at front and back sites.

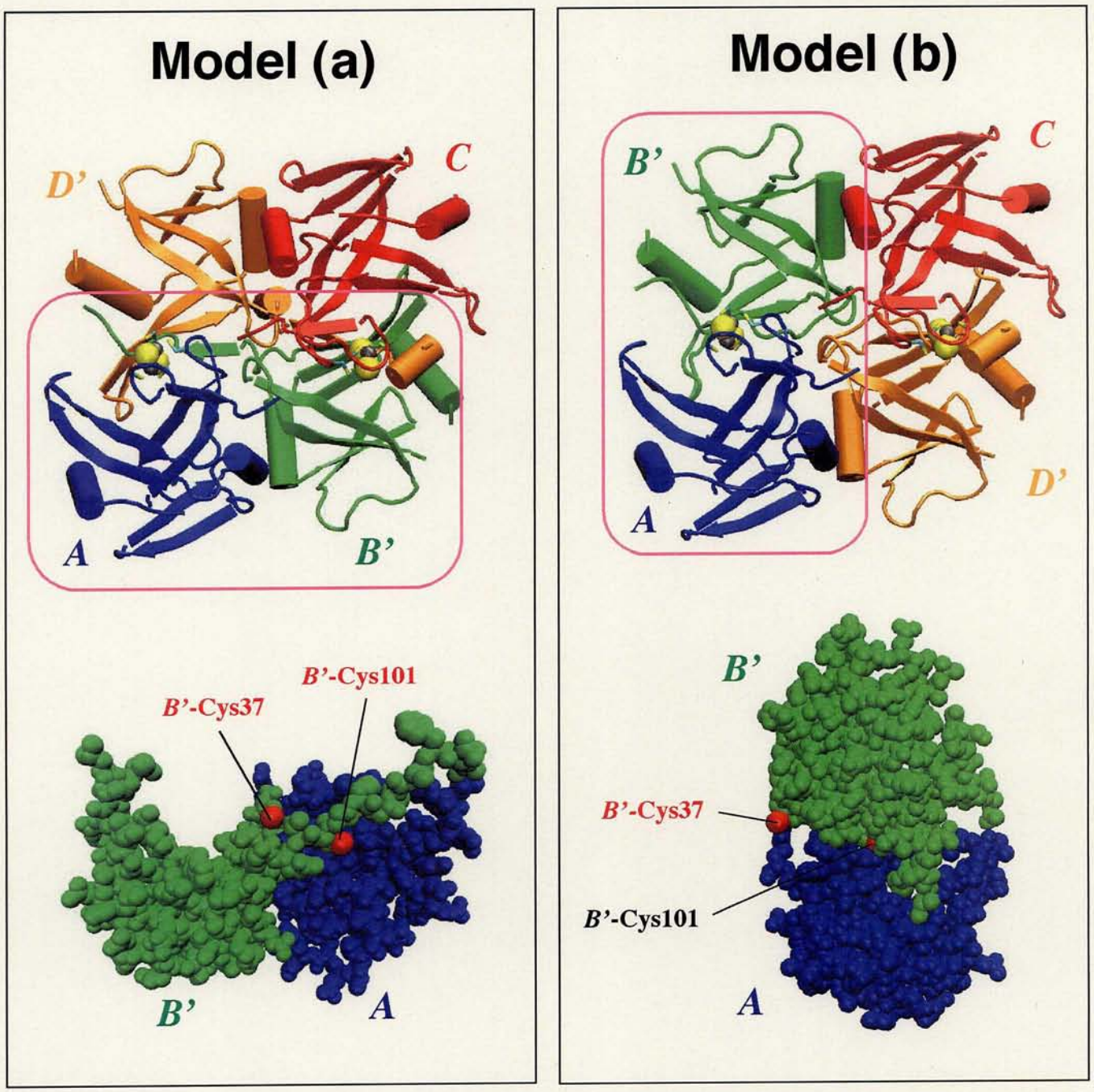

Fig. 2-13 Position of free cysteine residues.
Upper molecule shows model structures of holo IscA2, Model (a) or Model (b), constructed in Fig. 2-11.

Lower molecule depicts monomer *A* and monomer *B'* of each upper molecule.
Sulfur atoms of free cysteine residues are highlighted by red colored red and indicated.
Molecules are shown as a space-filling model.

The view of lower molecule is rotated 180° with respect to each upper molecule.

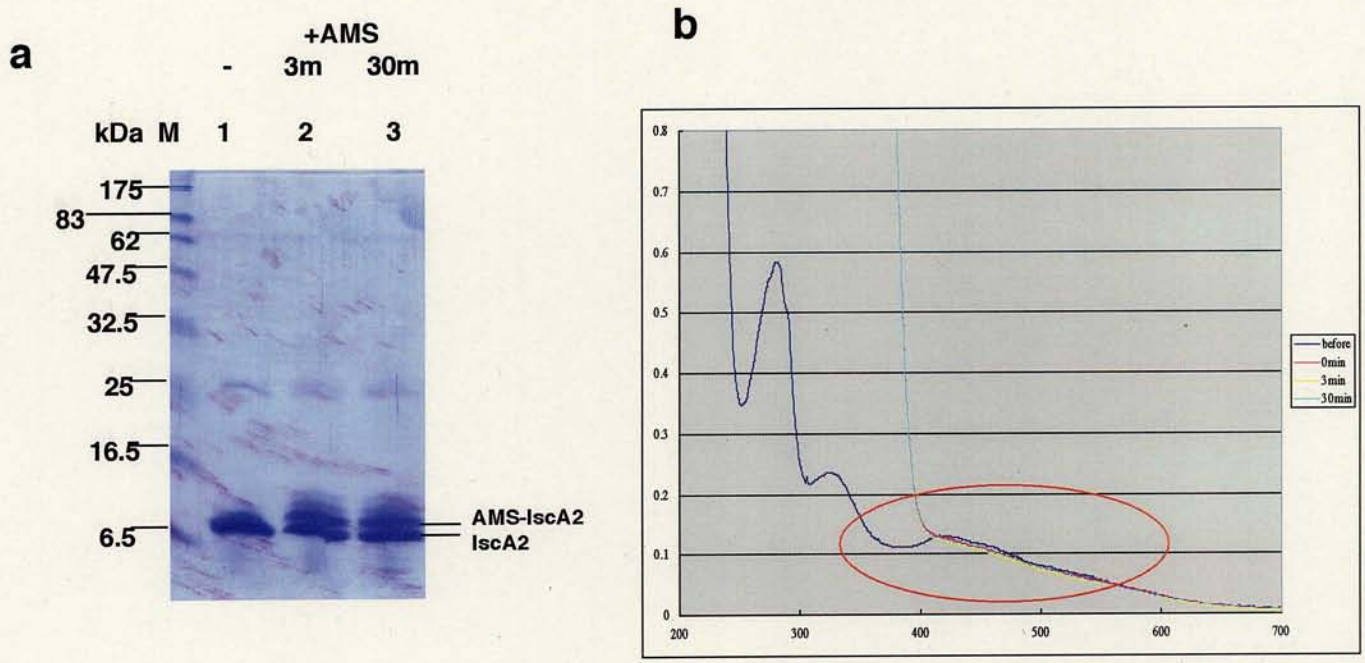

Fig. 2-14 AMS modification of IscA2.
IscA2 (50 μM) was modified by free thiol modification reagent, AMS (500 μM).
(a) SDS-PAGE after AMS modification.
Lane 1: before adding AMS.
Lane 2: 3 min after adding AMS.
Lane 3: 30 min after adding AMS.
Lane M: molecular mass standard same as Fig. 2-2.
Protein bands of IscA2 and AMS-modified IscA2 are indicated.

(b) UV-visible absorption spectra during the AMS modification.
Blue line: before adding AMS.
Purple line: 0 min after adding AMS.
Yellow line: 3 min after adding AMS.
Cyan line: 30 min after adding AMS.
Note that the absorption peaks around 420 nm, which derives from the absorption of the [2Fe-2S] cluster, did not change during the reaction (red circle).

a

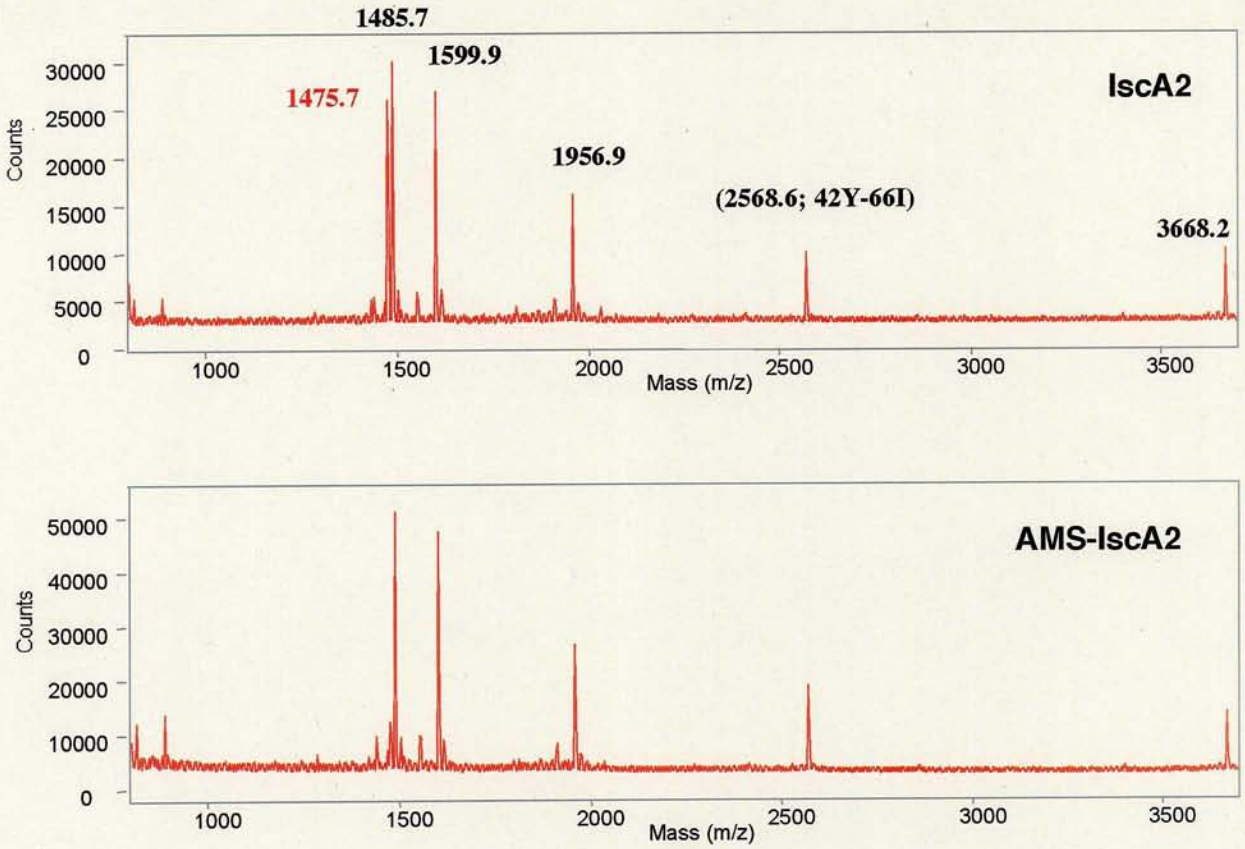

b

mass	position	modification(s)	peptide sequence
3667.9581	42-75		YDLALVAEPKPTDLLTQSQGWTIAIAAEAAELLR
1956.7785	92-108	Cys_CM: 101, 103	FHNPNASQTCGCGMAFR
1599.8410	1-14		MVELTPAAIQELER
1485.7042	79-91		VDYIEDLMGGAFR
1475.6583	30-41	Cys_CM: 37	IQVQPSECGDWR
810.4580	15-21		LQTHGVR
728.4413	23-29		GQAAILR

```
1          11         21         31         41         51
MVELTPAAIQ ELERLQTHGV RrGQAAILRI QVQPSECGDW RYDLALVAEP KPTDLLTQSQ
GWTIAIAAEA AELLRglrVD YIEDLMGGAF RFHNPNASQT CGCGMAFRvs rs
61         71         81         91         101
```

Fig. 2-15 Mass spectroscopy of IscA2 and AMS-modified IscA2.
(a) After carboxymethylation and trypsin digestion, digested products of IscA2 (upper panel) and AMS-modified IscA2 (lower panel) were examined by mass spectroscopy. Note that a peak with m/z value of 1475.7 (highlighted by red color) specifically dropped off in AMS-modified IscA2.
(b) The table shows molecular weight mass, residue position, modifications, and peptide sequence of trypsin digestion products of carboxymethylated IscA2.
The figure was made using PeptideMass (http://au.expasy.org/tools/peptide-mass.html).

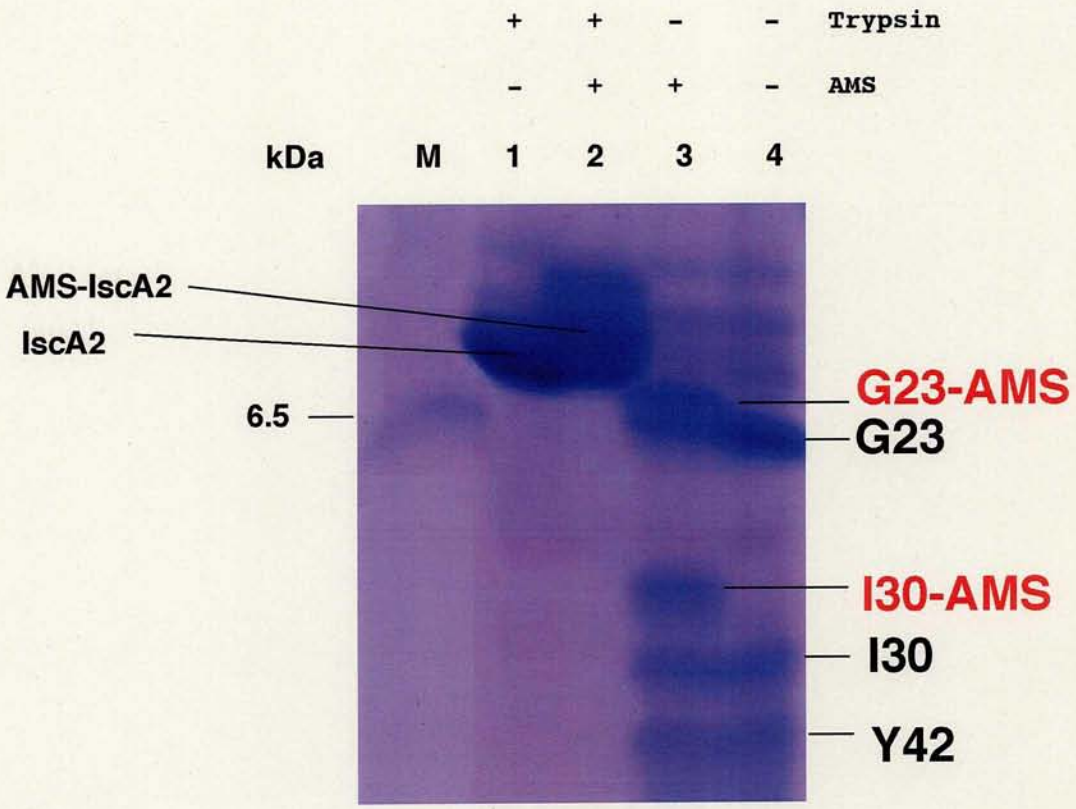

Fig. 2-16. Trypsin digestion of AMS-reacted IscA2 and identification of the AMS-reacted peptide. AMS-reacted IscA2 was digested by trypsin, and digested products were separated by SDS-PAGE using 16 % polyacrylamide gel as described by Hermann et al.
Lane 1: IscA2.
Lane 2: AMS-reacted IscA2.
Lane 3: AMS-reacted IscA2 after trypsin digestion.
Lane 4: IscA2 after trypsin digestion.
Lane M: molecular mass standard same as Fig. 2-2.

The digested products were confirmed by N-terminal amino acids sequencing.
The first amino acid with its sequence number is shown on the right side of each digested product.
The digested product modified by AMS is marked by -AMS and colored red.

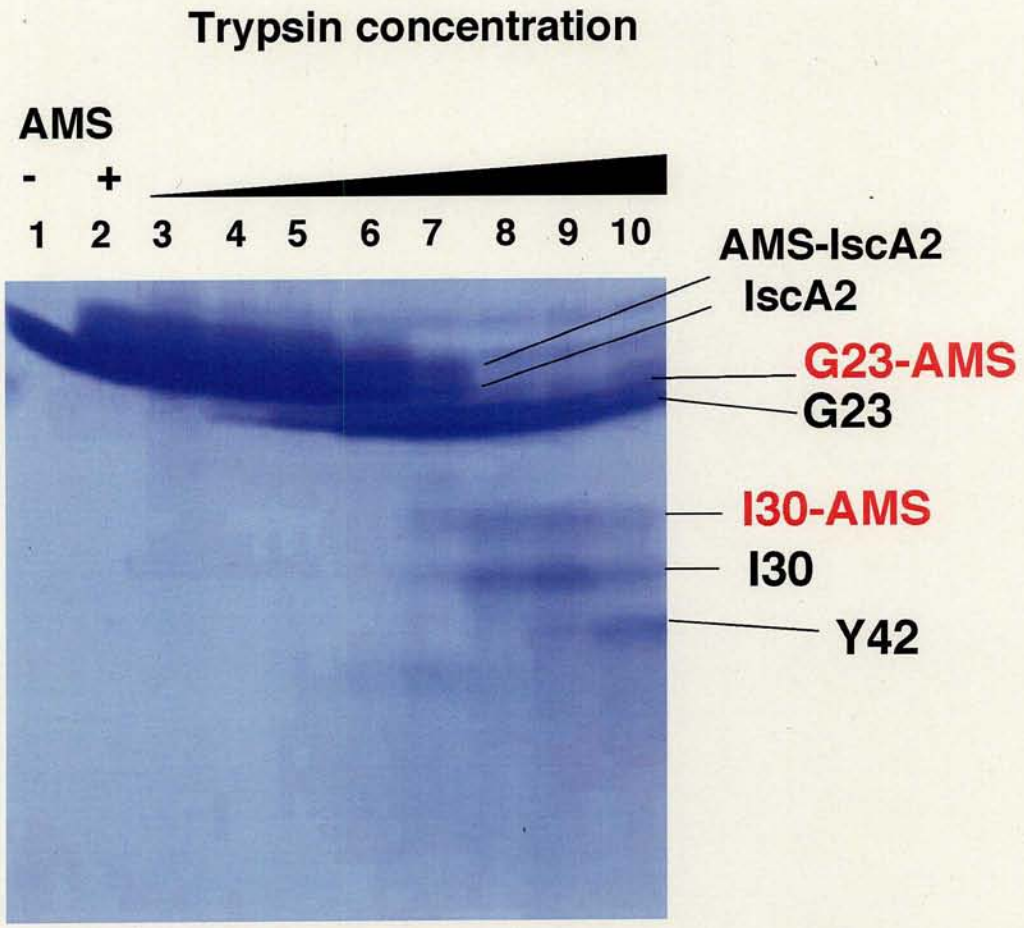

Fig. 2-17. Sensitivity of AMS-reacted IscA2 against trypsin digestion.
AMS-reacted IscA2 was digested by graded concentration of trypsin , and digested products were separated by SDS-PAGE using 16 % polyacrylamide gel as described by Hermann et al.
Lane 1: IscA2.
Lane 2: AMS-reacted IscA2.
from Lane 3 to Lane 10: AMS-reacted IscA2 after digestion by graded concentration of trypsin (from 4.5×10^{-4} to 1 mg ml^{-1}).

The first amino acid with its sequence number is shown on the right side of each digested product. The digested product modified by AMS is marked by -AMS and colored red.

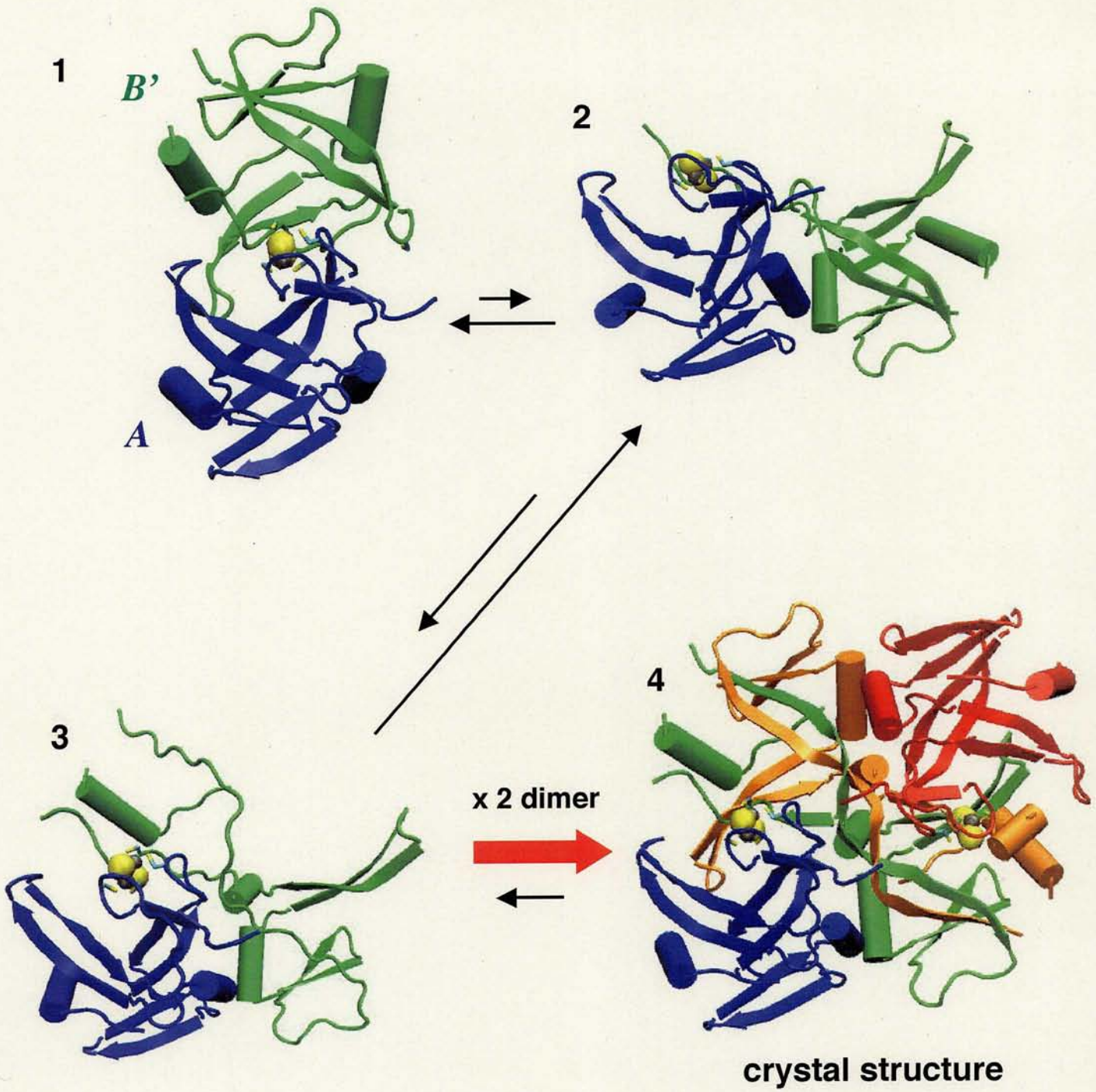

Fig. 2-18 A model mechanism of 3D domain swapping of *T. elongatus* IscA2. Please refer to the context for details.

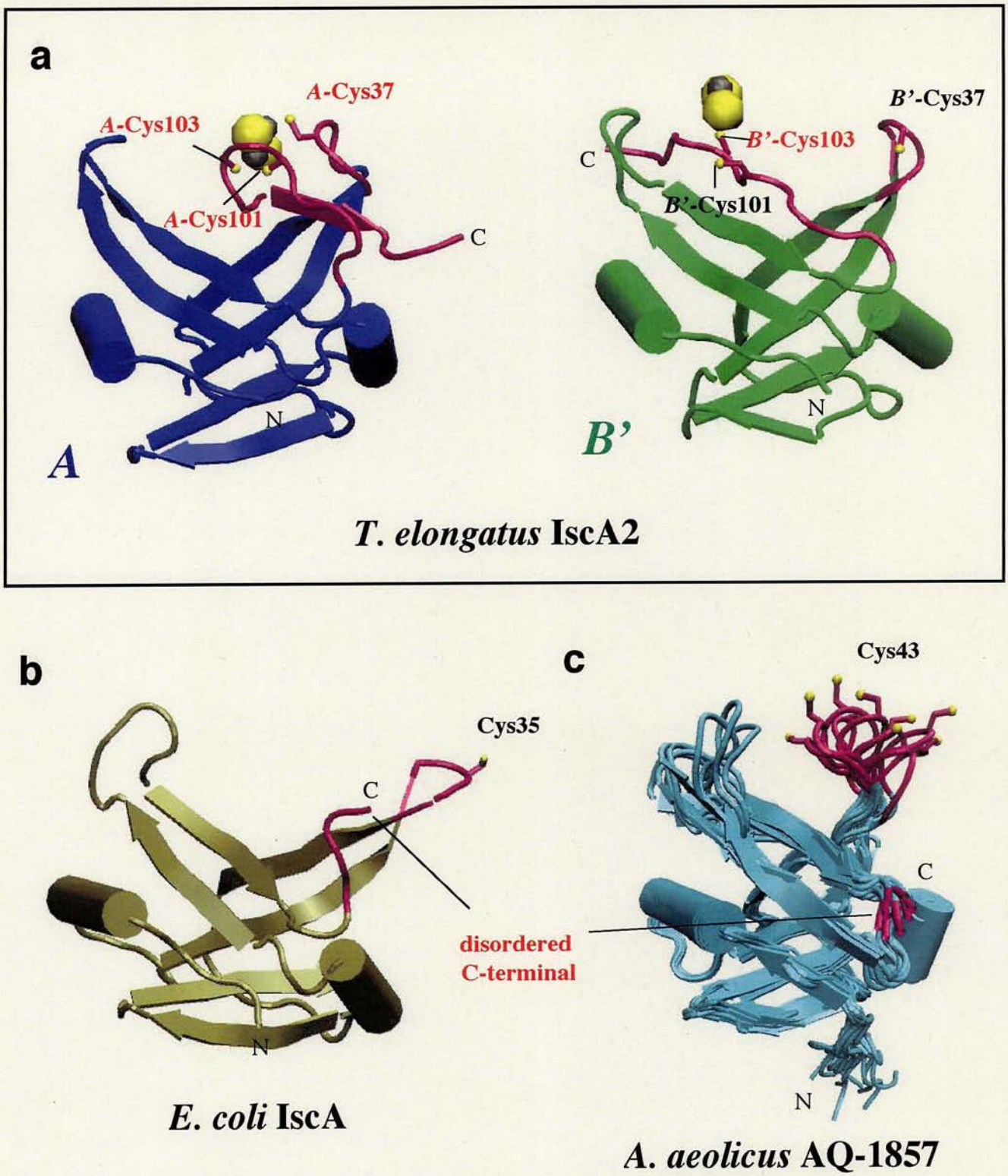

Fig. 2-19 Structural comparison of IscA monomer.
T. elongatus IscA2 monomer *A* (a, left), *T. elongatus* IscA2 monomer *B'* (a, right), *E. coli* IscA subunit (b), and *A. aeolicus* AQ-1857 protein (c) are compared.
Flexible loop region and flexible C-terminal region (see Fig. 2-1) are colored purple.
Evolutionally conserved cysteine residues are indicated by red letters (cluster ligands) or black letters (not cluster ligands).

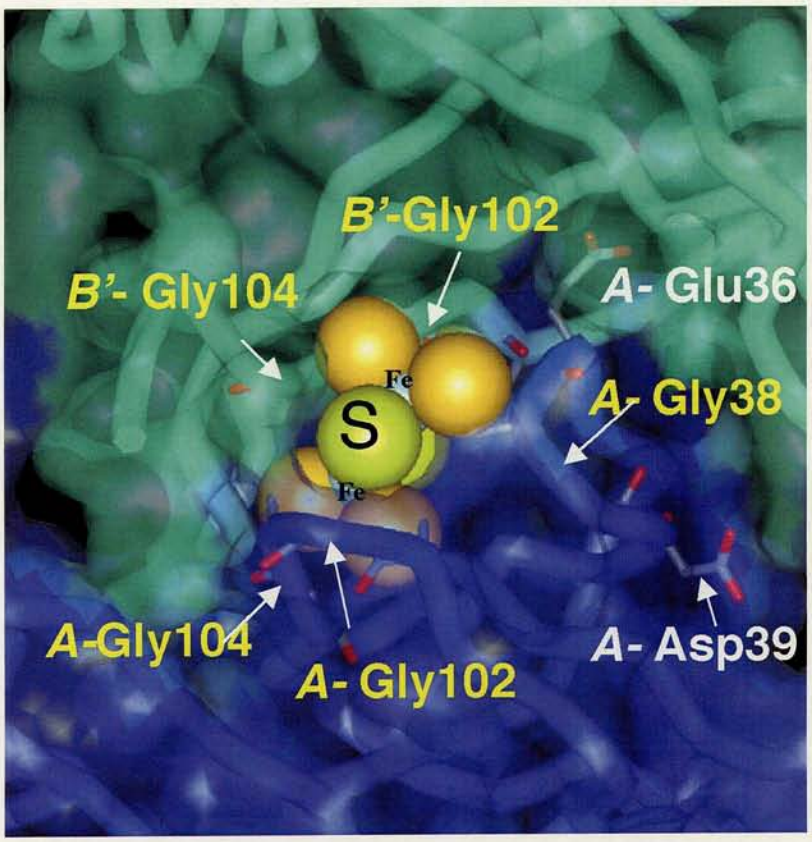

Fig. 2-20. Residues with small side chains around the [2Fe-2S] cluster.
Yellow letter indicates the well-conserved residues with small side chains around evolutionally conserved cysteine residues.
White letter indicates the residues where those with small side chain are normally positioned in other IscA homologues (see Fig. 2-1).

The figure was created using WebLab.

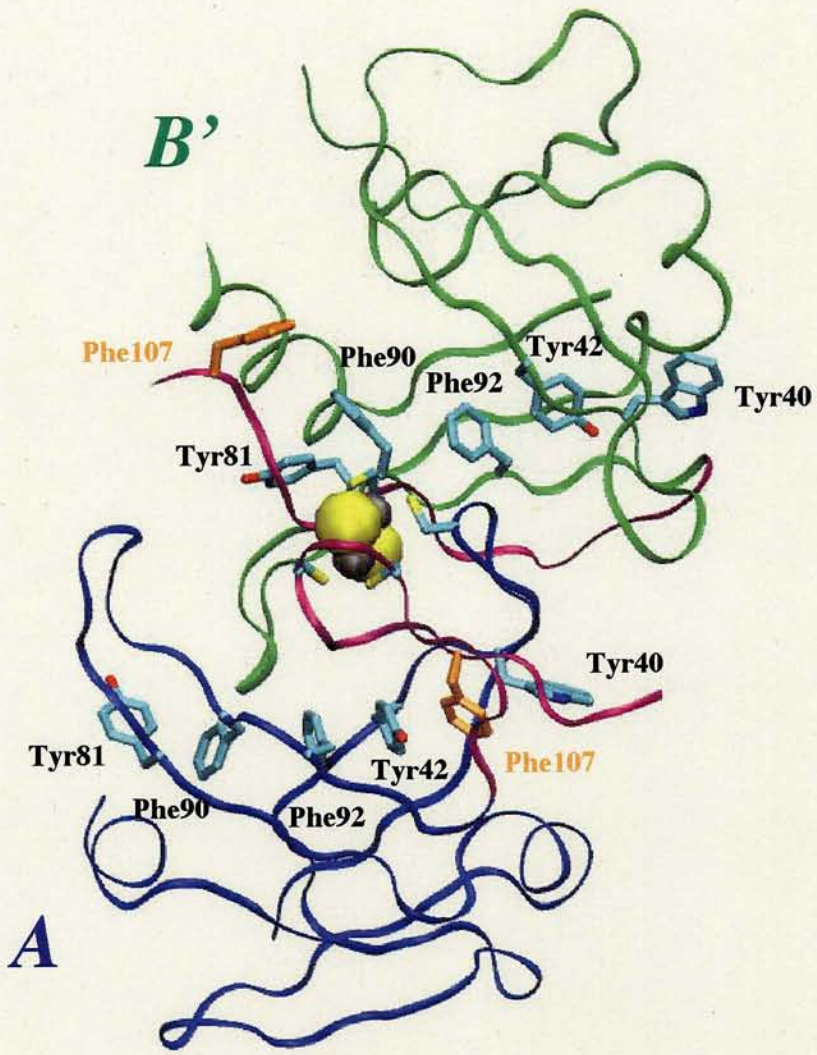

Fig. 2-21 Position of Phe107 and the conformation of C-terminal region.
Phe107, an evolutionally conserved phenylalanine residue on the C-terminal region, is colored orange. Lined up aromatic residues (Tyr81, Phe90, Phe92, Tyr42, Phe107, and Tyr40) forming a part of the protein core structure are also shown.

IscA2 molecules are shown as a tube model and colored blue (monomer *A*) or green (monomer *B'*) except C-terminal regions (colored purple).
[2Fe-2S] cluster atoms are shown as a space-filling model and colored gray (iron) or yellow (sulfur).Side chain atoms are shown as a stick model and colored cyan (carbon), red (oxygen), blue (nitrogen), or yellow (sulfur). The view is rotated slightly with respect to Fig.2-12 (a) to show side-chain positions more clearly.

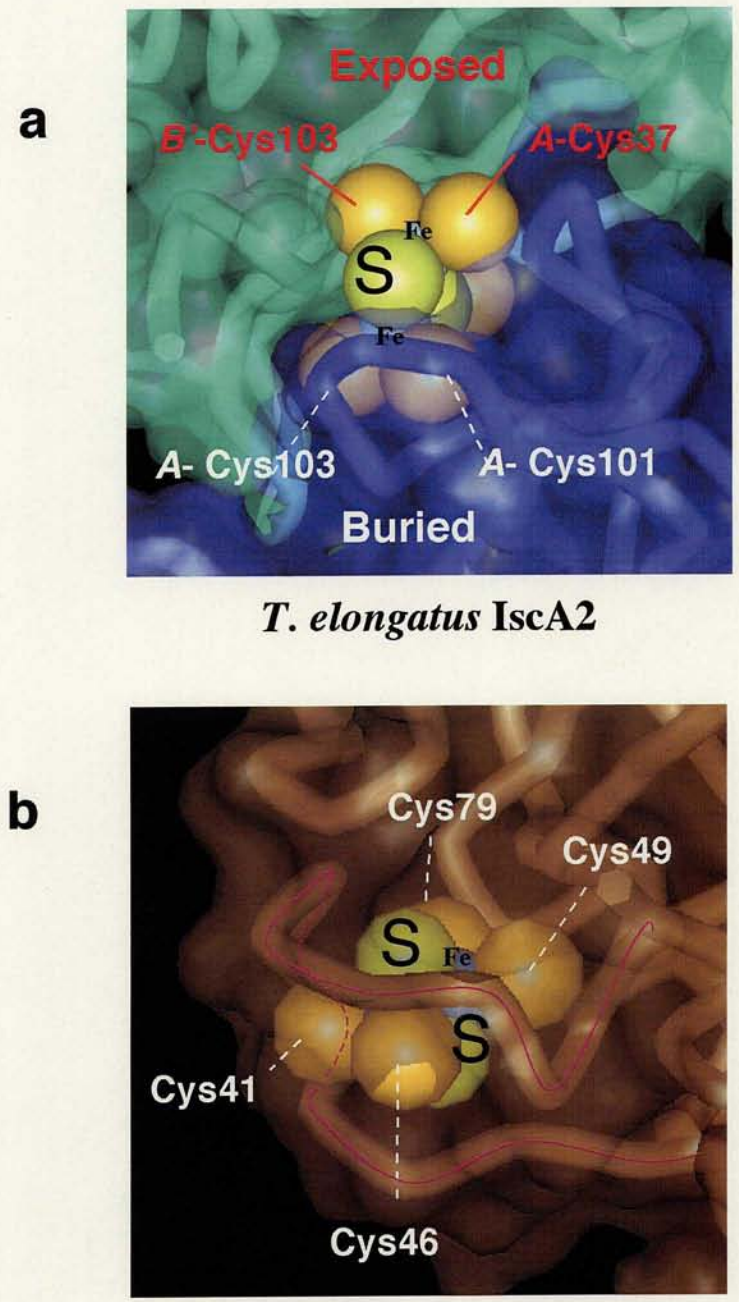

Fig. 2-22. Partially exposed [2Fe-2S] cluster of *T. elongatus* IscA2.
(a) The [2Fe-2S] cluster of *T. elongatus* IscA2.
(b) The [2Fe-2S] cluster of *Spirulina* ferredoxin.
In addition to the [2Fe-2S] clusters and ligating cysteinyl Sγ atoms shown by space-filing model, solvent accessible areas were drawn by transparent surfaces.
Note that three cysteine residues of ferredoxin, Cys41, Cys46, and Cys49, are located on a same loop (indicated by a pink line).

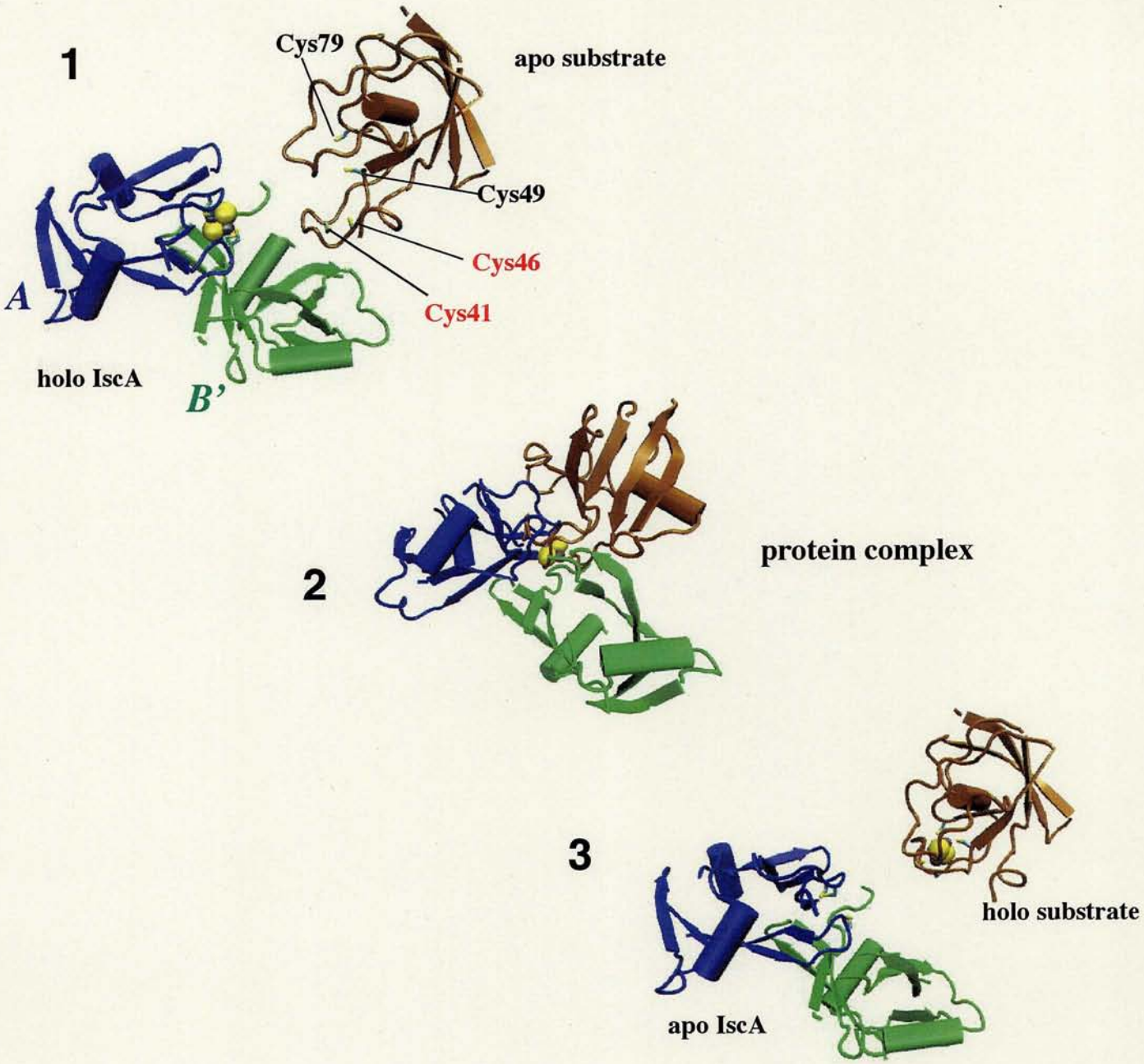

Fig. 2-23 Model mechanism of the iron-sulfur cluster transfer from holo IscA to apo ferredoxin. Please refer to the context for details.

Protein molecules are shown as a ribbon model and colored blue (monomer *A*), green (monomer *B'*), or brown (*Spirulina* ferredoxin). The [2Fe-2S] clusters are shown as a space-filling model, and side chains of cysteine residues used for the cluster ligations are shown as a stick model and indicated. Atoms are colored cyan (carbon), gray (iron), or yellow (sulfur).

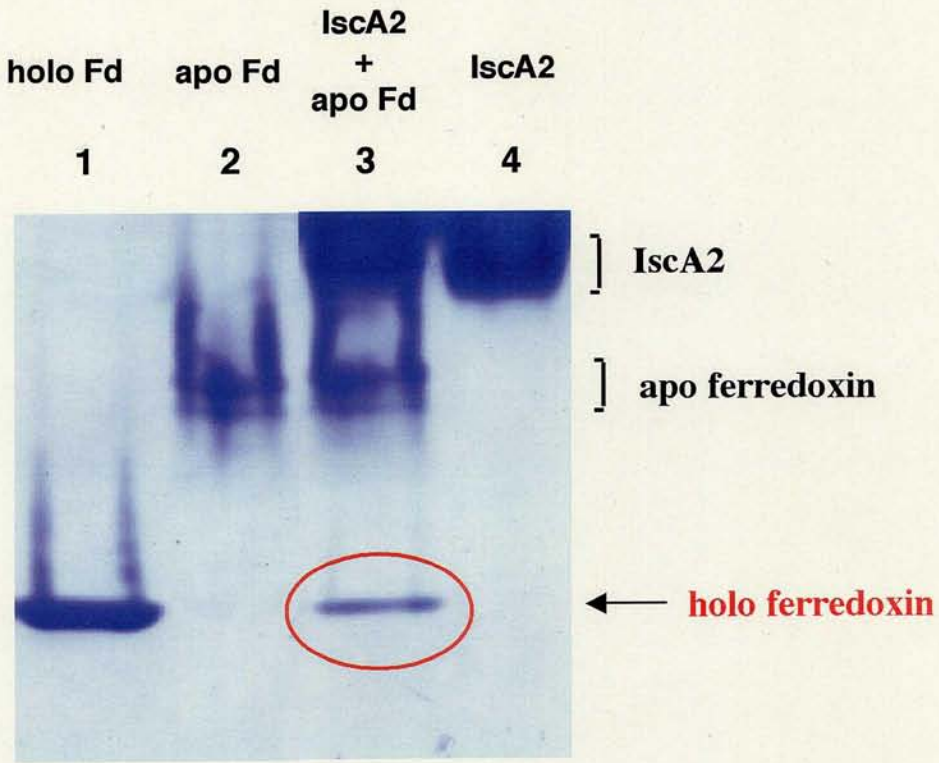

Fig.2-24 Iron-sulfur cluster transfer from holo IscA2 to apo ferredoxin.
For the iron-sulfur cluster transfer reaction, 20 μg apo ferredoxin (from *Spinach*) and 50 μg holo IscA2 were incubated in 40 μl of buffer containing 50 mM Tris-HCl pH7.5, 50 mM KCl, 5 mM DTT, and 1 mM EDTA for 1 h at 310 K. Analysis of the transfer reaction was performed by nondenaturing PAGE using 17.5 % polyacrylamide gel as described by Nishio et al.

Lane 1: holo ferredoxin.
Lane 2: apo ferredoxin.
Lane 3: incubation mixture of apo ferredoxin and holo IscA2.
Lane 4: holo IscA2.

Red circle indicates holo ferredoxin formed from apo ferredoxin by the reaction of the iron-sulfur cluster transfer from holo IscA2.

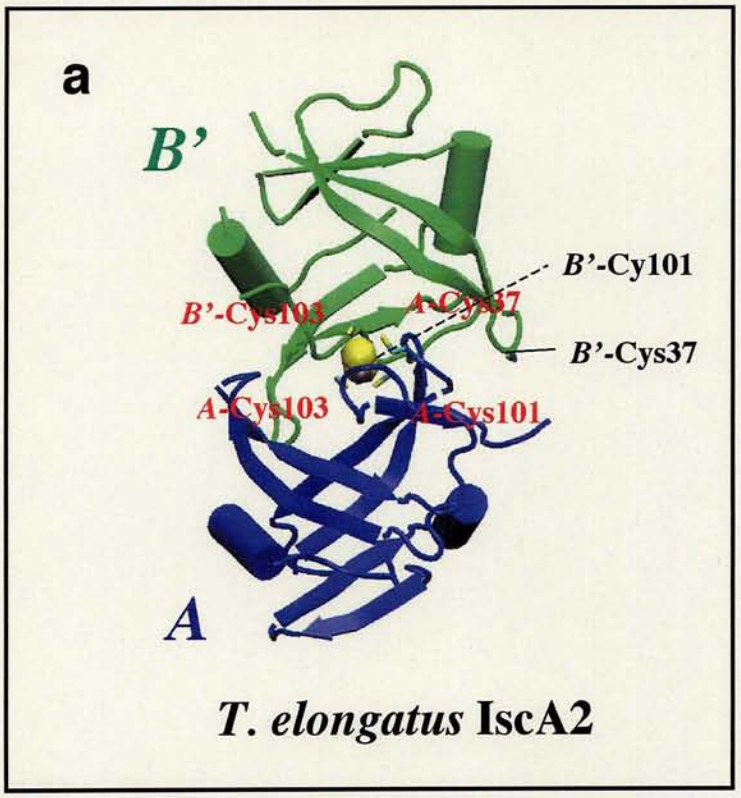

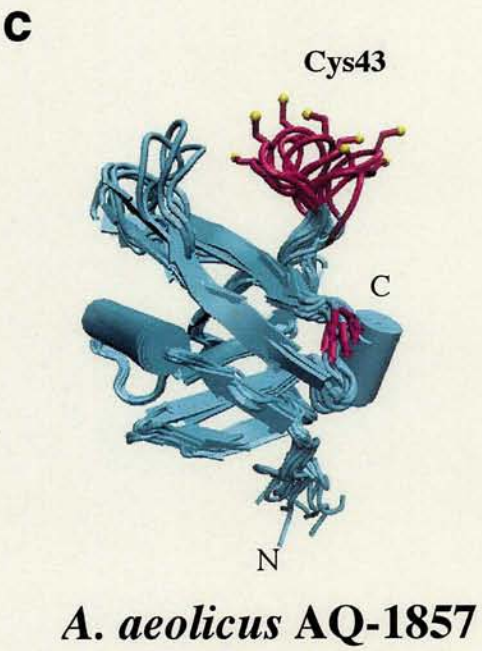

Fig. 2-25. Structural comparison of *T. elongatus* IscA2 with homologues from other organisms.
(a) Structure of holo *T. elongatus* IscA2 dimer proposed in this study.
(b) Crystal structure of *E. coli* IscA. One monomer is highlighted by orcher color.
(b) NMR structure of *A. aeolicus* AQ-1857 protein.
Evolutionally conserved cysteine residues are indicated by red letters (cluster ligands) or black letters (not cluster ligands).

REFERENCES

Agar, J. N., Krebs, C., Frazzon, J., Huynh, B. H. , Dean, D. R. , Johnson, M. K. (2000)
IscU as a scaffold for iron-sulfur cluster biosynthesis: sequential assembly of [2Fe-2S] and [4Fe-4S] clusters in IscU.
Biochemistry **39**, 7856-7862.

Andrade, M. A., Petosa, C., O'Donoghue, S. I., Muller, C. W., Bork, P. (2001)
Comparison of ARM and HEAT protein repeats.
J Mol Biol. **309**, 1-18.

Beinert, H., Holm, R. H., Münck, E. (1997)
Iron-sulfur clusters: nature's modular, multipurpose structures.
Science **277**, 653-659.

Beinert, H. (2000)
Iron-sulfur proteins: ancient structures, still full of surprises.
J. Biol. Inorg. Chem. **5**, 2-15.

Bennett, M. J., Schlunegger, M. P., Eisenberg, D. (1995)
3D domain swapping: a mechanism for oligomer assembly.
Protein Sci. **4**, 2455-2468.

Bilder, P. W., Ding, H., Newcomer, M. E. (2004)
Crystal structure of the ancient, Fe-S scaffold IscA reveals a novel protein fold.
Biochemistry. **43**, 133-139.

Corpet, F. (1988)
Multiple sequence alignment with hierarchical clustering.
Nucleic Acids Res. ***16, 10881-10890.***

Cupp-Vickery, J. R., Silberg, J. J., Ta, D. T., Vickery, L. E. (2004)

Crystal structure of IscA, an iron-sulfur cluster assembly protein from Escherichia coli.
J Mol Biol. **338**, 127-137.

Dean, D. R., Bolin, J. T., Zheng, L. (1993)
Nitrogenase metalloclusters: structures, organization, and synthesis.
J. Bacteriol. **175**, 6737-6744.

Fu, W., Jack, R. F., Morgan, T. V., Dean, D. R., Johonson, M. K. (1994)
*nif*U gene product from *Azotobacter vinelandii* is a homodimer that contains two identical [2Fe-2S] clusters.
Biochemistry **33**, 13455-13463.

Hermann, S., Ursula, B., Heinrich, A., Thomas, A. L., Gebhard, V. J. (1985)
Isolation and amino acid sequence of the smallest subunit of beef heart bc_1 complex.
FEBS Lett. **190**, 89-94.

Humphrey, W., Dalke, A., Schulten, K. (1996)
VMD: visual molecular dynamics.
J. Mol. Graph. **14**, 33-38.

Jacobson, M. R., Cash, V. L., Weiss, M. C., Laird, N. F., Newton, W. E., Dean, D. R. (1989)
Biochemical and genetic analysis of the *nif*USVWZM cluster from *Azotobacter vinelandii.*
Mol. Gen. Genet. **219**, 49-57.

Jensen, L. T., Culotta, V. C. (2000)
Role of *Saccharomyces cerevisiae* ISA1 and ISA2 in iron homeostasis.
Mol. Cell. Biol. **20**, 3918-3927.

Jones, T. A., Zou, J. Y., Cowan, S.W., Kjeldgaard, M. (1991)
Improved methods for building models in electron density maps and the location of errors in these models.

Acta Crystallogr A. **47**, 110-119.

Kaut, A., Lange, H., Diekert, K., Kispal, G., Lill, R. (2000)
Isa1p is a component of the mitochondrial machinery for maturation of cellular iron-sulfur proteins and requires conserved cysteine residues for function.
J. Biol. Chem. **275**, 15955-15961.

Krebs, C., Agar, J. N., Smith, A. D., Frazzon, J., Dean, D. R., Huynh, B. H., Johnson, M. K. (2001)
IscA, an alternate scaffold for Fe-S cluster biosynthesis.
Biochemistry **40**, 14069-14080.

Lill, R., Kispal, G. (2000)
Maturation of cellular Fe-S proteins: an essential function of mitochondria.
Trends Biochem. Sci. **25**, 352-356.

Liu, Y., Eisenberg, D. (2002)
3D domain swapping: as domains continue to swap.
Protein Sci. **11**, 1285-1299.

Morimoto, K., Nishio, K., Nakai, M. (2002)
Identification of a novel prokaryotic HEAT-repeats-containing protein which interacts with a cyanobacterial IscA homolog.
FEBS Lett. **519**, 123-127.

Morimoto, K., Sato, S., Tabata, S., Nakai, M. (2003)
A HEAT-repeats containing protein, IaiH, stabilizes the iron-sulfur cluster bound to the cyanobacterial IscA homologue, IscA2.
J. Biochem. **134**, 211-217.

Murshudov, G. N., Vagin, A. A., Dodson, E. J. (1997)
Refinement of macromolecular structures by maximum-likelihood method.
Acta Crystallogr D. **53**, 240-255.

Nakai, Y., Nakai, M., Hayashi, H., Kagamiyama, H. (2001)
Nuclear localization of yeast Nfs1p is required for cell survival.
J Biol Chem. **276**, 8314-8320.

Nakamura, Y., Kaneko, T., Hirosawa, M., Miyajima, N., Tabata, S. (1998)
CyanoBase, a www database containing the complete nucleotide sequence of the genome of *Synechocystis* sp. strain PCC6803.
Nucleic Acids Res. **26**, 63-67.

Neuwald, A. F., Hirano, T. (2000)
HEAT repeats associated with condensins, cohesins, and other complexes involved in chromosome-related functions.
Genome Res. **10**, 1445-52.

Nishio, K., Nakai, M. (2000)
Transfer of iron-sulfur cluster from NifU to apoferredoxin.
J. Biol. Chem. **275**, 22615-22618.

Nishio, K., Nakai, M., Hase, T. (1999)
Fe-S cluster formation of ferredoxin in chloroplast stroma in photosynthesis: Mechanisms and Effects.
(Garab, G., ed.) pp. 3155-3158, Kluwer Academic Publishers, Dordrecht

Ollagnier-de-Choudens, S., Mattioli, T., Takahashi, Y., Fontecave, M. (2001)
Iron-sulfur cluster assembly: characterization of IscA and evidence for a specific and functional complex with ferredoxin.
J. Biol. Chem. **276**, 22604-22607.

Ollagnier-de-Choudens, S., Sanakis, Y., Fontecave, M. (2004)
SufA/IscA: reactivity studies of a class of scaffold proteins involved in [Fe-S] cluster assembly.
J. Biol. Inorg. Chem. **9**, 828-838.

Pelzer, W., Mulenhoff, U., Diekert, K., Siegmund, K., Kispal, G., Lill, R. (2000)
Mitochondrial Isa2p plays a crucial role in the maturation of cellular iron-sulfur proteins.
FEBS Lett **476**, 134-139.

Schwartz, C. J., Giel, J. L., Patschkowski, T., Luther, C., Ruzicka, F. J., Beinert, H., Kiley, P. J. (2001)
IscR, an Fe-S cluster-containing transcription factor, represses expression of Escherichia coli genes encoding Fe-S cluster assembly proteins.
Proc. Natl. Acad. Sci. U. S. A. **98**, 14895-14900.

Schuck, P. (2000)
Size distribution of macromolecules by sedimentation velocity ultracentirifugation and Lamm equation modeling.
Biophys. J. **78**, 1606-1619.

Smith, A.D., Agar, J.N., Johnson, K.A., Frazzon, J., Amster, I.J., Dean, D.R., Johnson, M.K. (2001)
Sulfur transfer from IscS to IscU: the first step in iron-sulfur cluster biosynthesis.
J. Am. Chem. Soc. **123**, 11103-11104.

Tagawa, K., Arnon, D. I. (1968)
Oxidation-reduction potentials and stoichiometry of electron transfer in ferredoxins.
Biochim. Biophys. Acta **153**, 602-613.

Takahashi, Y., Nakamura, M. (1999)
Functional assignment of the ORF2-iscS-iscU-iscA-hscB-hscA-fdx-ORF3 gene cluster involved in the assembly of Fe-S clusters in Escherichia coli.
J. Biochem. **126**, 917-926.

Tokumoto, U., Takahashi, Y. (2001)
Genetic analysis of the *isc* operon in *Escherichia coli* involved in the biogenesis of

cellular iron-sulfur proteins.
J. Biochem. **130**, 63-71.

Tsukihara, T., Fukuyama, K., Mizushima, M., Harioka, T., Kusunoki, M., Katsube, Y., Hase, T., Matsubara, H. (1990)
Structure of the [2Fe-2S] ferredoxin I from the blue-green alga Aphanothece sacrum at 2.2 A resolution.
J. Mol. Biol. **216**, 399-410.

Wollenberg, M., Berndt, C., Bill, E., Schwenn, J. D., Seidler, A. (2003)
A dimer of the FeS cluster biosynthesis protein IscA from cyanobacteria binds a [2Fe2S] cluster between two protomers and transfers it to [2Fe2S] and [4Fe4S] apo proteins.
Eur. J. Biochem. **270**, 1662-1671.

Wu, G., Mansy, S. S., Hemann, C., Hille, R., Surerus, K. K., Cowan, J.A. (2002)
Iron-sulfur cluster biosynthesis: characterization of *Schizosaccharomyces pombe* Isa1.
J. Biol. Inorg. Chem. **7**, 526-532.

Wu, S. P., Cowan, J. A. (2003)
Iron-sulfur cluster biosynthesis. A comparative kinetic analysis of native and Cys-substituted ISA-mediated [2Fe-2S]2+ cluster transfer to an apoferredoxin target.
Biochemistry. **42**, 5784-5791.

Xu, D., Liu, G., Xiao, R., Acton, T., Goldsmith-Fischman, S., Honig, B., Montelione, G. T., Szyperski, T. (2004)
NMR structure of the hypothetical protein AQ-1857 encoded by the Y157 gene from Aquifex aeolicus reveals a novel protein fold.
Proteins. **54**, 794-796.

Yuvaniyama, P., Agar, J. N., Cash, V. L., Johnson, M. K., Dean, D. R. (2000)
NifS-directed assembly of a transient [2Fe-2S] cluster within the NifU protein.
Proc. Natl. Acad. Sci. U.S.A. **97**, 599-604.

Zheng, L., White, R. H., Cash, V. L., Jack, R. F., Dean, D. R. (1993)
Cysteine desulfurase activity indicates a role for NIFS in metallocluster biosynthesis.
Proc. Natl. Acad. Sci. U.S.A. **90**, 2754-2758.

Zheng, L., White, R. H., Cash, V. L., Jack, R. F., Dean, D. R. (1994)
Mechanism for the desulfurization of L-cysteine catalyzed by the *nif*S gene product.
Biochemistry **33**, 4714-4720.

Zheng, L., Cash, V. L., Flint, D. H., Dean, D. R. (1998)
Assembly of iron-sulfur clusters. Identification of an *isc*SUA-*hsc*BA-*fdx* gene cluster from *Azotobacter vinelandii*.
J. Biol. Chem. **273**, 13264-13272.

ACKNOWLEDGMENTS

This work was performed at Division of Enzymology, Institute for Protein Research, Osaka University.

I am greatly obligated to **Associate Prof. M. Nakai** (Institute for Protein Research, Osaka University, Japan) for his guidance and continuous encouragement throughout this work.

I am grateful to **Prof. T. Hase** (Institute for Protein Research, Osaka University, Japan) for variable discussions, and for giving me the opportunity and wonderful environment to do this work.

I am grateful to **Prof. T. Tsukihara** (Institute for Protein Research, Osaka University, Japan) for variable discussions, and for giving me helpful suggestions on the protein crystals.

I am grateful to co-workers.

Dr. S. J. Lee (MRC Laboratory of Molecular Biology, England) gave me helpful suggestions on the preparation of protein crystals.

Dr. E. Yamashita (Institute for Protein Research, Osaka University, Japan) did data collection and structure determination of protein crystals and gave me helpful suggestions.

Mr. Y. Kondo (Institute for Protein Research, Osaka University, Japan) helped me to refine the crystal structure and gave me helpful suggestions to analyze the protein structure.

Prof. A. Nakagawa (Institute for Protein Research, Osaka University, Japan) helped me to refine the crystal structure.

Prof. Humio Arisaka (Tokyo Institute of Technology, Japan) and **Ms. M. Sakai** did analytical ustracentrifugation studies.

Dr. K. Nishio (Matsusihta Corporation, Japan) prepared purified ferredoxin and especially contributed to my early works.

Dr. S. Sato and **Dr. S. Tabata** (Kazusa DNA Research Institute, Japan) did the initial yeast two-hybrid screening of the cyanobacterial proteins.

Dr. T. Kaneko (Kazusa DNA Research Institute, Japan) gave me genomic information of *T. elongatus*.

Prof. M. Ikeuchi (Tokyo University, Japan) and **Dr. H. Fukuzawa** (Kyoto University, Japan) provided the cyanobacterial strain.

Ms. Y. Yoshimura (Institute for Protein Research, Osaka University, Japan) did peptide sequencing.

Dr. Y. Satomi (Institute for Protein Research, Osaka University, Japan) helped me to do mass spectroscopy.

Dr. G. Hanke (Institute for Protein Research, Osaka University, Japan) helped me to do carboxymethylation and mass spectroscopy and checked this thesis.

Mr. S. Okutani (Institute for Protein Research, Osaka University, Japan) helped me to do carboxymethylation and mass spectroscopy.

Mr. T. Yabe (Institute for Protein Research, Osaka University, Japan) helped me to do in vitro experiment of cluster transfer from IscA2 to apo ferredoxin.

It is my pleasure for me to acknowledge the numerous cooperations and kindness of all members of our laboratory. Especially, I would like to thank **Ms. C. Uchida** and **Ms. R. Nakanishi** for technical and secretarial assistance, respectively.